

https://dspace.org/

The quantification of uncertainty attached to selected sampling protocols in a kimberlite using a discrete simulation method

Thurston, Malcolm Lawrence

1998
https://hdl.handle.net/10539/26850

Downloaded from a DSpace repository. https://dspace.org/

THE QUANTIFICATION OF UNCERTAINTY ATTACHED TO SELECTED SAMPLING PROTOCOLS IN A KIMBERLITE USING A DISCRETE SIMULATION METHOD

Malcolm Lawrence Thurston

THE QUANTIFICATION OF UNCERTAINTY ATTACHED TO SELECTED SAMPLING PROTOCOLS IN A KIMBERLITE USING A DISCRETE SIMULATION METHOD

Malcolm Lawrence Thurston

A thesis submitted to the Faculty of Engineering, University of the Witwatersrand, Johannesburg, in fulfilment of the requirements for the Doctor of Philosophy.

Johannesburg, 1998

DECLARATION

I declare that this thesis is my own, unaided work. It is being submitted for the Degree of Doctor of Philosophy in the University of the Witwatersrand, Johannesburg. It has not been submitted before for any degree or examination in any other University.

Malcolm Thurston

15th day of June 1998

ABSTRACT

The prime objective of this thesis is to understand, in a quantitative way, how the uncertainty in local and global grade estimates change with different sampling configurations, both in terms of the size of a sample and in terms of the number of samples taken.

A second objective, and necessary in order to achieve the first, is to practically apply a new simulation method that takes into account the statistical, spatial and discrete nature of the diamond distribution in a kimberlite.

A limited number of practical, sampling protocols were considered.

For global grade estimates, and for the situations tested, it was shown that the number of holes required to place the global estimate within 10% of the "true" global mean (at a lower 90% confidence interval) ranged from 12 holes for a high nugget effect semi-variogram model to 16 holes for a low nugget effect semi-variogram model.

For larger samples the results showed very little improvement in the global confidence limits for the low nugget semi-variogram model while the high nugget semi-variogram model improved significantly.

For local grade estimates, and for the situations tested, it was shown that 90% of the blocks estimated were within 25% of their true value for both the low and high nugget semi-variogram models. Moving to a larger sample size improved the confidence in the local estimates for the low and high nugget effect models.

The effect of bottom cutoff on local and global grade confidence limits was investigated and found to be, for the situations tested, minimal in the case of global grade estimates but played a role when local estimates were required.

The possibility of estimating diamond grade across part of the diamond size distribution was explored and shown to be a promising technique in circumstances where the full diamond size distribution is known. The advantage of this approach is that the grade of the restricted size range can be estimated using a smaller sample size.

To Lynne, Laura and Emma for their patience and support.

ACKNOWLEDGEMENTS

I am grateful to De Beers Consolidated Mines for the use of their equipment and data while compiling this thesis.

I wish to express my appreciation to Isobel Clark for her comments, encouragement and advice during the preparation of my thesis.

I would to thank Wynand Kleingeld for his encouragement in pursuing this thesis and his useful discussions on conceptual issues. A special thanks must go to Wynand for introducing me to the geostatistics of "discrete particles" and the many discussions we have had on insitu sampling.

This thesis would not have been possible without the support of all my colleagues and friends. In particular I must mention Christian Lantuéjoul, who wrote the Cox algorithm, and spent time patiently discussing simulation and geostatistical principles with me. Duncan Campbell, who was always willing to add insight to observations and problem areas. Chris Prins, who provided invaluable programming tips and who wrote the software used to create the simulation presented in Chapter 3. Margaret Armstrong, who encouraged the idea of a thesis many years ago and has taken a constant interest in its progress. Christina Dohm and Johan Ferreria who have offered continuous moral support.

In addition, a special thanks must go to Christina Dohm and Chris Prins for assistance in editing the final text.

Last but not least, my thanks to my wife Lynne and my children Laura and Emma, who have each supported my thesis in their own way. Your patience and sacrifice is very much appreciated.

CONTENTS PAGE

DECLARATION		ii
ABSTRACT		iii
DEDICATION		v
ACKNOWLEDGEMENTS		vi
CONTENTS		vii
LIST OF FIGURES		xiv
LIST OF TABLES		xix
1	**INTRODUCTION**	**1.1**
1.1	**Preamble**	1.1
1.2	**Problem statement**	1.2
1.3	**Aim of the thesis**	1.4
1.4	**The need for this research**	1.4
1.4.1	The sampling of kimberlites	1.4
1.4.2	The lack of research in this area	1.5
1.4.3	The importance of the research	1.7
1.4.4	Original aspects of the research	1.8
1.5	**What is not covered in this thesis**	1.8
1.6	**The organisation of the thesis**	1.9
2	**BACKGROUND TO THE SAMPLING AND EVALUATION OF KIMBERLITES**	**2.1**
2.1	**Introduction**	2.1
2.2	**Geology**	2.2
2.3	**The sampling of kimberlite**	2.5

CONTENTS PAGE

2.4	**Global estimation, local estimation and grade units**	**2.8**
2.5	**The diamond size distribution**	**2.10**
2.6	**The mining of kimberlite**	**2.12**
2.7	**The statistical modelling of diamond deposits**	**2.13**
2.7.1	The two parameter lognormal distribution	2.13
2.7.2	The Compound lognormal distribution	2.15
2.7.3	The mixing of stone populations	2.18
2.7.4	The Compound Poisson distribution	2.19
2.8	**Spatial models for the distribution of Diamonds**	**2.23**
2.8.1	The importance of simulation as a tool	2.24
2.8.2	Different types of geostatistical simulation	2.26
2.8.3	Simulation models created for discrete particles	2.33
2.8.4	Why the Cox model as a simulation method	2.37
2.9	**Chapter conclusion**	**2.41**
3	**AN EXPERIMENT TO SHOW HOW THE DISTRIBUTION STONES MAY EFFECT SAMPLING AND EVALUATION**	**3.1**
3.1	**Introduction**	**3.1**
3.2	**The simulation method**	**3.2**
3.3	**Results and discussion**	**3.4**
3.4	**Chapter conclusion**	**3.13**

CONTENTS PAGE

4	**THE SIMULATION OF STONES WITHIN A KIMBERLITE USING THE COX PROCESS**	**4.1**
4.1	**Introduction**	**4.1**
4.2	**The Cox simulation in a geological context**	**4.1**
4.3	**The Cox simulation**	**4.3**
4.4	**Statistical inference**	**4.5**
4.4.1	Distribution of the potential	4.6
4.4.2	Covariance of the potential	4.6
4.4.3	Model assumptions	4.6
4.4.4	Non-conditional simulation	4.7
4.5	**The practical estimation of simulation parameters for Deposit One**	**4.8**
4.5.1	Mean of the Potential	4.9
4.5.2	Variance of the Potential	4.9
4.5.3	Semi-variogram of the Potential	4.11
4.5.4	Parameters of the Gamma distribution of Potential	4.11
4.5.5	Estimation of the multi Gaussian covariance of the Potential	4.12
4.5.6	Size of the simulated area	4.13
4.5.7	Number of lines used for the Turning bands	4.13
4.5.8	Modelling of the semi-variogram to take into account the shape of the drill samples	4.13
4.5.9	A proposed solution	4.15
4.5.10	Texture of the simulated simulation	4.19

CONTENTS PAGE

4.6	**Chapter conclusion**	**4.22**
5	**THE EFFECT C : SAMPLE DENSITY AND SAMPLE SIZE ON GLOBAL ESTIMATION**	**5.1**
5.1	***Introduction***	**5.1**
5.2	**A high nugget effect model**	**5.2**
5.3	**The effect of sample density**	**5.5**
5.3.1	Method	5.5
5.3.2	Results	5.6
5.4	**The effect of increasing sample size**	**5.8**
5.4.1	Method	5.8
5.4.2	Results	5.10
5.4.3	Discussion	5.11
5.5	**The effect of decreasing sample size**	**5.12**
5.5.1	Method	5.12
5.5.2	Results	5.14
5.6	**Chapter conclusion**	**5.17**
6	**THE EFFECT OF SAMPLE SIZE ON LOCAL ESTIMATION**	**6.1**
6.1	**Introduction**	**6.1**
6.2	**Method**	**6.2**

CONTENTS PAGE

6.3	**The calculation of weights for each sample size**	**6.5**
6.3.1	Nugget effect	6.5
6.3.2	The range	6.7
6.3.3	Estimation of the semi-variogram total sill	6.8
6.3.4	Calculated semi-variogram parameters and sample weights	6.10
6.4	**Results**	**6.12**
6.5	**Discussion**	**6.15**
6.6	**"Cluster sampling"**	**6.19**
6.7	**Chapter conclusion**	**6.21**
7	**THE EFFECT OF BOTTOM CUTOFF ON LOCAL AND GLOBAL ESTIMATION**	**7.1**
7.1	**Introduction**	**7.1**
7.2	**General approach**	**7.2**
7.3	**The creation of a sample grade between 1.5mm and 2.4mm**	**7.3**
7.4	**The effect on global estimation**	**7.5**
7.4.1	Method	7.5
7.4.2	Results	7.6
7.4.3	Discussion	7.8
7.5	**The effect on local estimates**	**7.9**
7.5.1	Method	7.9
7.5.2	Results	7.10
7.5.3	Discussion	7.15

CONTENTS		PAGE
7.6	**Chapter conclusion**	**7.17**
8	**SUMMARY, CONCLUSIONS AND THE WAY FORWARD**	**8.1**
8.1	**Objectives of the thesis**	**8.1**
8.2	**Summary of the previous chapters**	**8.2**
8.3	**Sensitivity of the results to changes in the simulation parameters**	**8.6**
8.3.1	The diamond size distribution	8.7
8.3.2	The semi-variogram	8.11
8.3.3	The effect of grid size	8.14
8.3.4	The mean number of stones per sample	8.16
8.3.4	The large scale geological model	8.19
8.3.6	Conclusion	8.19
8.4	**The way forward**	**8.20**
8.5	**Chapter summary**	**8.23**
REFERENCES		**R1**

LIST OF FIGURES **PAGE**

1.1	Proportion of ore versus homogeneity (after King 1982)	1.6
2.1	Model of a kimberlite pipe modified after Hawthorne 1975.	2.3
2.2	The diamond size distribution of Deposit One on logarithmic probability paper.	2.11
2.3	Relationship between the Compound Lognormal model and the lognormal model (after Dohm 1995)	2.17
2.4	The axes of 2.3 arranged in the same way as the diamond size distribution plot shown in Figure 2.2	2.17
3.1	Random texture. Each circle represents a horizontal slice at 6m intervals through the simulation	3.5
3.2	Slightly clustered texture. Each circle represents a horizontal slice at 6m intervals through the simulation	3.6
3.3	Clustered texture. Each circle represents a horizontal slice at 6m intervals through the simulation	3.7
3.4	Random texture for 40m sampling	3.8
3.5	Slightly cluster texture for 40m data	3.8
3.6	Clustered texture for 40m sample data	3.8
3.7	Slightly clustered texture for the 50m grid samples	3.9
3.8	Clustered data for the 50m grid	3.9

LIST OF FIGURES **PAGE**

3.9	"True" values against kriged values for the 40m, slightly clustered data	3.12
3.10	"True" block values against kriged values for the clustered data	3.12
4.1	Histogram of stones per sample for Deposit One	4.10
4.2	Semi-variogram of Deposit One	4.10
4.3	Explanation of anisotropy due to sample shape	4.14
4.4	The regularised cube semi-variogram versus the usual semi-variogram	4.17
4.5	Texture of "stones per sample" for the low nugget semi-variogram model. The simulation area is 300m x 300m by one 12m bench	4.18
5.1	Texture of "stones per sample" for the high nugget semi-variogram model. The simulation area is 300m x 300m by one 12m bench	5.3
5.2	Comparison of low and high nugget semi-variogram models. The simulation area is 300m x 300m by one 12m bench	5.4
5.3	Low nugget semi-variogram model showing the central 80% confidence limits for different grids	5.7
5.4	High nugget semi-variogram model showing the central 80% confidence limits for different grids	5.7

LIST OF FIGURES **PAGE**

5.5	Low nugget semi-variogram model showing the central 80% confidence limits for different grids and different sample sizes	5.9
5.6	High nugget semi-variogram model showing the central 80% confidence limits for different grids and different sample sizes	5.9
5.7	High and low nugget models showing the central 80% confidence limits for a three, six and twelve inch diameter sample	5.15
5.8	High nugget model showing the central 80% confidence limits in SPM3 and CPM3 for a three, six and twelve inch diameter sample	5.16
5.9	Low nugget model showing the central 80% confidence limits in SPM3 and CPM3 for a three, six and twelve inch diameter sample	5.16
5.10	The probability of exceeding a cutoff for Samples of three, six and twelve inches for High and low nugget models. The cutoff is expressed as the ratio of the cutoff to the mean grade	5.17

LIST OF FIGURES **PAGE**

6.1	Plan view of the kriging neighbourhood	6.3
6.2	Section view of the kriging neighbourhood	6.3
6.3	Sample numbering for the three levels of The kriging neighbourhood	6.11
6.4	Variance of (Z*-Z) for the high and low nugget models against the area of the sample (0m² t	6.17
6.5	As for Figure 6 axis has been limited to 30 more detail	6.17
6.6	Variance of blocks based on 2, 4, 9 and 16 samples compared to the theoretical estimation variance of a 10m block for the high and low nugget semi-variogram models.	6.20
7.1	Comparison of the central 80% confidence limits for different numbers of samples. C2 is the 2mm grade, C1F is the 1mm grade Factored to 2mm and C3F is the 1.5mm to 2.4mm grade factored to 2mm	7.7
7.2	The same graph as 7.1 except that the X axis has been extended to 350 samples. C2 is the 2mm grade, C1F is the 1mm grade factored to 2mm and C3F is the 1.5mm to 2.4mm grade factored to 2mm	7.7
7.3	Simulated sample data at 1mm in SPM3	7.11
7.4	Simulated data at 2mm in SPM3	7.11
7.5	Simulated data at 1.5mm to 2.4mm in SPM3	7.11

7.6	Semi-variogram of the 1mm data used for The kriging	7.12
7.7	Semi-variogram of the 2mm sample data	7.12
7.8	Semi-variogram of the 1.5mm to 2.4mm sample data	7.13
7.9	"True" estimates versus the 1mm adjusted block ,nates	7.14
7.10	"True" block estimates versus the 2mm block estimates	7.14
7.11	"True" block estimates versus the 1.5mm to 2.4mm adjusted block estimates	7.14

LIST OF TABLES **PAGE**

3.1	Sample statistics for the three textures. SKEW=skewness, KURTO=kurtosis and CV=coefficient of variation	3.10
3.2	Statistics for "true" block values against estimated values	3.11
4.1	Example of the output from the modelling programme showing the reconstituted cube semi-variogram in the X direction. The approximate range is bolded	4.20
4.2	Example of the output from the modelling programme showing the reconstituted cube semi-variogram in the X direction. The approximate range is bolded	4.21
6.1	Semi-variogram ranges	6.9
6.2	Semi-variogram parameters (spherical model) for the high nugget semi-variogram	6.9
6.3	Semi-variogram parameters (spherical model) for the low nugget semi-variogram	6.12
6.4	Sample weights calculated for each sample size (high nugget semi-variogram model). The size is in unit samples of 0.3m by 0.3m by 0.3m	6.13
6.5	Sample weights calculated for each sample size (high nugget semi-variogram model). The size is in unit samples of 0.3m by 0.3m by 0.3m	6.14

6.6	Simulated values compared to kriging values for the high nugget semi-variogram model	6.16
6.7	Simulated values compared to kriging values for the high nugget semi-variogram model	6.16
6.8	The "90th" percentile of |Z*-Z|/Z indicates the relative difference below which 90% of the values lie	6.18
7.1	Sample statistics for "true" on estimated block values	7.15
8.1	Table of results for global estimation	8.12
8.2	Table of results for local estimation	8.15

CHAPTER 1

INTRODUCTION

A diamond is a sun ray condensed
in the ground and cooled by time; it
shows all the colours of the rainbow
but remains transparent as a drop
of water -
A Kuprin

In this chapter we will:

- Introduce the problem examined in the thesis
- The objectives of the thesis
- The need for research around this problem
- The organisation of the thesis

1.1 Preamble

The world's supply of natural diamonds is approximately 110 million carats per year worth about 6.4 billion US$ (Rombouts 1996). Of this approximately 82 million carats are recovered from kimberlites and one lamproite (worth about 3.7 billion US$) and the balance from secondary deposits. To maintain this demand, mining and exploration companies are engaged in a world wide search for diamonds estimated to cost US$ 300 million per year.

Once an exploration company has located a kimberlite, and initial sampling has been carried out, a decision is required on whether to carry on with further sampling or abandon the prospect. The initial samples that are

collected are used to estimate the grade for the deposit. The fact that only a portion of the mineral deposit is sampled, and not the total body, leads to the concept of uncertainty in the estimate. King (1982) states that

"*the general aim of evaluation is to make the result secure against the possibility of substantial surprises*".

For the exploration company a "*substantial surprise*" might be the abandonment of a prospect that turns out to be a profitable mine and, for a mining company, the opening of a mine that proves unprofitable. This leads naturally to the question of how to define the uncertainty attached to a given sampling protocol and, perhaps more importantly, how to sample sufficiently such that the result will only produce "surprises" within defined bounds. For the exploration and mining companies this decision is taken against the background of a valuable mineral that is low in concentration and heterogeneous in spatial distribution.

This thesis looks at sampling protocols in kimberlites. The aim is to understand, in a quantitative way, how the uncertainty in the grade estimate changes with different sampling configurations, both in terms of size of sample and the number of samples taken.

1.2 Problem statement

The development of a newly discovered prospect into an operating mine involves a number of stages. At each stage sampling information is collected and analysed with the objective of making a decision. In the early stages of prospect development the decision to be made is whether to "walk away" from a prospect or to continue spending money on further sampling. At the feasibility stage of the project it may be whether to open a mine and

in the later stages of the mine life what blocks of ore to mine to reduce the variability of the mineral reporting to the treatment plant. The decisions made at each stage of development are based on the sample information available at the time and not on a complete knowledge of the deposit. **The estimates made are therefore subject to uncertainty.**

In an ideal situation each sampling campaign should have a specific management objective. For instance, the decision to move onto a further phase of sampling is taken if the chance of meeting or exceeding a given grade is greater than 80%. In such a situation the sampling protocol should be optimised such that the level of uncertainty required is met with the minimum amount of sampling. Similarly, at the feasibility stage of development, the decision to develop a mine may require a maximum monthly fluctuation of 15% in the amount of mineral extracted. This monthly variation can be influenced by several factors of which uncertainty in the grade estimates is one.

In the cases above what is required is an understanding of the uncertainty in the estimate associated with a given sampling protocol. In other words, how well is a given estimate known or, in a pro-active situation, how much information should be collected in order to achieve the desired management objective.

The problem examined in this thesis is the quantification of the uncertainty attached to sampling protocols used in the evaluation of kimberlite deposits.

1.3 Aim of the thesis

The research presented has been done with two objectives in mind. The prime objective **is to gain a quantitative understanding of the variability of sampling protocols used to evaluate kimberlites.**

This is achieved by simulating a number of different sample protocols using a simulation method that takes into account the statistical and spatial characteristics of the diamond distribution in the kimberlite.

The different sampling protocols are examined in terms of global estimation, where the estimation method was the average of available sample values, and local estimation, where the estimation method was ordinary kriging. In both cases the uncertainty associated with the sampling protocol is quantified.

The second objective, and necessary in order to achieve the first, **is to practically apply a new simulation approach for simulating discrete particles in space.**

1.4 THE NEED FOR THIS RESEARCH

1.4.1 The sampling of kimberlites

The sampling of a kimberlite is no trivial matter. Although the geological model of a kimberlite is well understood (at least at a large scale) the mineralisation occurs in economic concentrations as low as 40 parts per billion and has an irregular spatial distribution. This combination of low concentration and heterogeneity makes the evaluation of kimberlites more difficult than most other deposits. In addition, **only one in every two hundred kimberlites have commercial grades** (Duval 1996, p20).

King (1982) attributed the uncertainty associated with a grade estimate to four factors: the drilling density (including sample size), the grade of the valuable constituent, the "*spottiness*" or heterogeneity of the mineralisation and the estimation procedure. Generally the confidence in the grade estimate becomes less as the sampling becomes sparser, the lower the grade of the deposit and the less continuous the mineralisation.

King (1982) combines the *"proportion of valuable constituent"* and *"spottiness (or heterogeneity)"* of a deposit into a graph that pictorially expresses the difficulty of estimation of a given mineral (see Figure 1.1). In this figure a kimberlite is considered less difficult to estimate than a placer deposit of gold or diamonds but more difficult than stratiform gold.

Sampling a deposit, where the mineralisation is irregularly distributed or "spotty", presents a number of unique sampling problems (Kleingeld and Lantuéjoul 1992). The first is a geometric problem. If the patches are not intersected often enough during the sampling process then a sampling bias may occur as all the patches are extracted during the mining process. To overcome the geometric problem many drill holes are required. The second problem is that the mineral within the patches is highly variable. Kleingeld and Lantuéjoul note that the impact of the second factor can be reduced if a sample of the same size as the "patch" is taken. The combination of these two factors accounts for the observed natural variability of grade in the deposit.

1.4.2 The lack of research in this area

The need to estimate what is in the ground based on a few samples has probably been around as long as Man has been excavating useful minerals from the ground (at least 10 000 years). Over the past 100 years extensive research has been carried out into **broken ore sampling.**

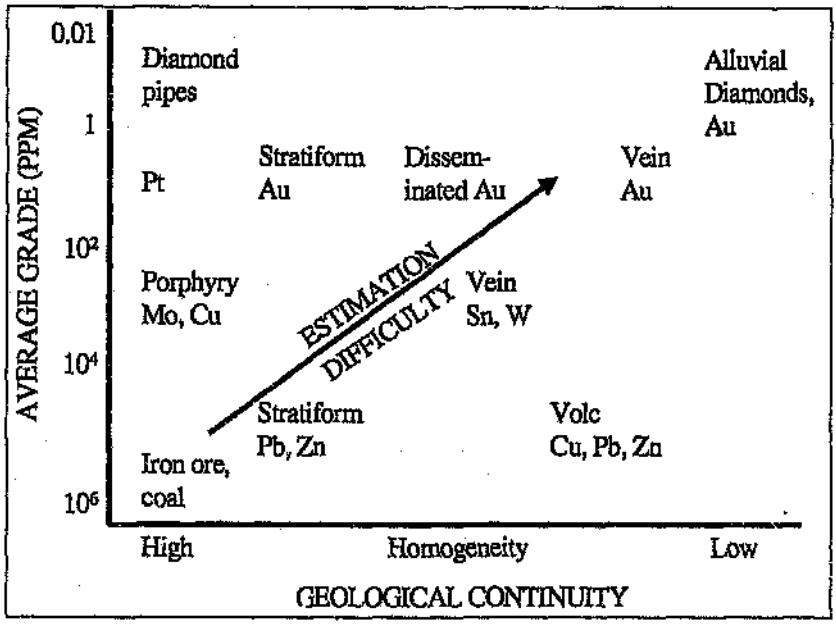


Figure 1.1: Proportion of ore mineral versus homogeneity (after King 1982)

Much of this work has been unified in the ideas and theory developed by P Gy (1979).

The "sampling theory" developed by P Gy relates to the sampling of broken ore. In other words, how much material must be taken from a mass of broken rock or mineral to be representative of the original mass ? In recent times various authors have placed this work in a geostatistical perspective (François-Bongarçon 1991). In this research the effect of sample variability in space and the impact of this variability on global and local estimation is studied. This is distinct and different from the broken ore theory described by P Gy.

Relatively little work has been published on the uncertainty attached to sampling protocols used for kimberlites. However research has been carried

out by Kleingeld (1987) into the sampling of mineralisation that consisted of "discrete particles". This work was developed further in a publication by Kleingeld and Lantuejoul in 1992 and further papers in 1994 (Kleingeld et al) and 1996 (Kleingeld et al) where the simulation technique used in this thesis was presented (see also section 2.7). In addition, Caers (1996) presents a number of tools for the estimation of confidence limits in diamond deposits.

1.4.3 Importance of the research

From a company perspective the most important reason for understanding the uncertainty attached to a sampling protocol is financial. In particular;

- **More accurate and precise "walk away" strategies**. An exploration company does not want to "walk away" from an economic prospect but nor does it want to carry out too much sampling before abandoning an uneconomic find. An understanding of the uncertainty attached to the sampling protocol will enhance a correct decision.

- **More cost effective sampling campaigns.** The cost of sampling a moderate sized pipe is US $1.3 million. Understanding the uncertainty in the sampling protocol, and a clear management objective, will allow the sampling to be more cost effective.

- **Clearer definition of the sampling uncertainty at the pre-feasibility and feasibility stages.** In defining the technical and financial risk associated with the pre-feasibility or feasibility study, a clear indication of the confidence in the estimate is required.

  The cost of opening a surface mine to work kimberlite is in the order of US $100 million. This assumes a moderate pipe, moderate infrastructure and "appropriate" technology. The cost of going

underground would be greater.

The risk of a mining failure is not as small as might be thought. Lassonde (1990) lists 50 mining failures (admittedly all non kimberlite) in North America. A failure was classified by Harquial as a project that failed to recover its original capital. More than half of the projects failed as a result of poor grade prediction or over optimistic reserve estimates.

- **Classification of the mineral resource.** An understanding of the uncertainty in the sampling protocol will allow the resource to be classified into measured, indicated or inferred resources.

1.4.4 Original aspects of the research

Firstly the quantification of confidence limits, for local and global estimates of grade, associated with various sampling protocols used in practice on kimberlites (chapters 5, 6 and 7). To the best of the author's knowledge this has not been done before. Secondly, the practical application of a new approach to simulation that takes into account the spatial character and discrete nature of the mineralisation within the kimberlite (chapter 4). This new simulation approach has been developed by Dr Ch Lantuéjoul at the Centre de Géostatistique in Fontainebleau, France (Kleingeld and Lantuéjoul 1992).

1.5 What is not covered in this thesis

The evaluation of kimberlite pipes involves the consideration of many aspects. **Only the topics directly relevant to the research in this thesis have been discussed.** Topics which are not discussed include :

- The types of samples required for the collection of information other than for grade. This includes information for geological modelling, diamond value and assortment, geotechnical and metallurgical information.
- Evaluation techniques for the estimation of global or local estimates other than the arithmetic mean and ordinary kriging.
- Adjustments to the sampling resource for diamond breakage, sample plant inefficiencies or poor data collection.
- Upgrading the resource to a reserve. In particular the allowance of differences in diamond liberation between the sampling process and the mining process.
- The use of micro diamond techniques for grade estimation[1].
- The estimation of diamond value

1.6 Organisation of the thesis

This thesis consists of 8 chapters. The first chapter brings into focus the need for the thesis and emphasizes the research elements. The second chapter provides some necessary background to the evaluation of kimberlites and sets the scene against which the research is carried out. Chapter 3 illustrates the need to understand the spatial distribution of stones in a kimberlite. Chapter 4 presents the Cox simulation while chapters 5 and 6 apply the Cox simulation to the definition of uncertainty in practical sampling protocols used to evaluate kimberlites. Chapter 7 answers a specific question relating to "bottom cutoff" in the evaluation process. Finally, chapter 8 collates the findings in the thesis, examines how general the findings are and looks at the way ahead.

---

1 These are diamonds less than 0.5mm in size that are used to make predictions of grades above 0.5mm.

CHAPTER 2

THE GEOLOGY, SAMPLING AND MINING OF KIMBERLITES

In this chapter we will review:

- The geology, sampling and mining of kimberlite pipes
- Grade units and diamond size distribution
- Statistical and spatial models for kimberlite pipes

2.1 INTRODUCTION

The objective of this chapter is to provide the reader with a practical background to kimberlites. This was thought necessary as, with the exception of one recent paper (Rombouts 1995), there has been relatively little information published on the evaluation of kimberlite pipes.

This chapter discusses the formation of kimberlites, the sampling methods and philosophy of sampling, the grade units commonly associated with kimberlites, the stone density distribution and the diamond size distribution.

The final section reviews the statistical models that are available for the modelling of diamond distributions and sets the scene for the Cox simulation presented in chapter 4.

2.2 Geology

Kimberlites are ultra-basic, igneous rocks which occur as vertical diatremes, dykes and, rarely, sills. A kimberlite starts with the upward migration of the kimberlite melt from 2 to 3 km below the paleo-surface. Upward migration takes place by hydraulic fracturing, wedging, marginal stoping and intrusive brecciation and is terminated at a depth of 0.5 km or less by an explosive eruption to surface and subsequent formation of the diatreme zone and volcanic crater.

Three broad textural varieties of kimberlite have been identified: The crater facies, the diatreme zone and the root zone (see Figure 2.1).

1 Crater facies kimberlite consists of pyroclastic and epiclastic rocks occurring at the surface of the erupting kimberlite. Epiclastic rocks are produced by the reworking of pyroclastic rocks by sedimentological processes and are typically very variable in character.

2 The diatreme zone is characterised by a steep (80 degrees), inclined, cone like body consisting of tuffisitic kimberlite breccia (TKB) and occasional rafts of country rock. It represents the rocks associated with the explosive eruption of the kimberlite to surface.

3 The root zone has irregular pipe contacts, complex internal geology and distinct intrusions. The root zone typically contains hypabyssal and kimberlite breccia and represents the remains of embryonic pipes preserved at the base of the diatreme.

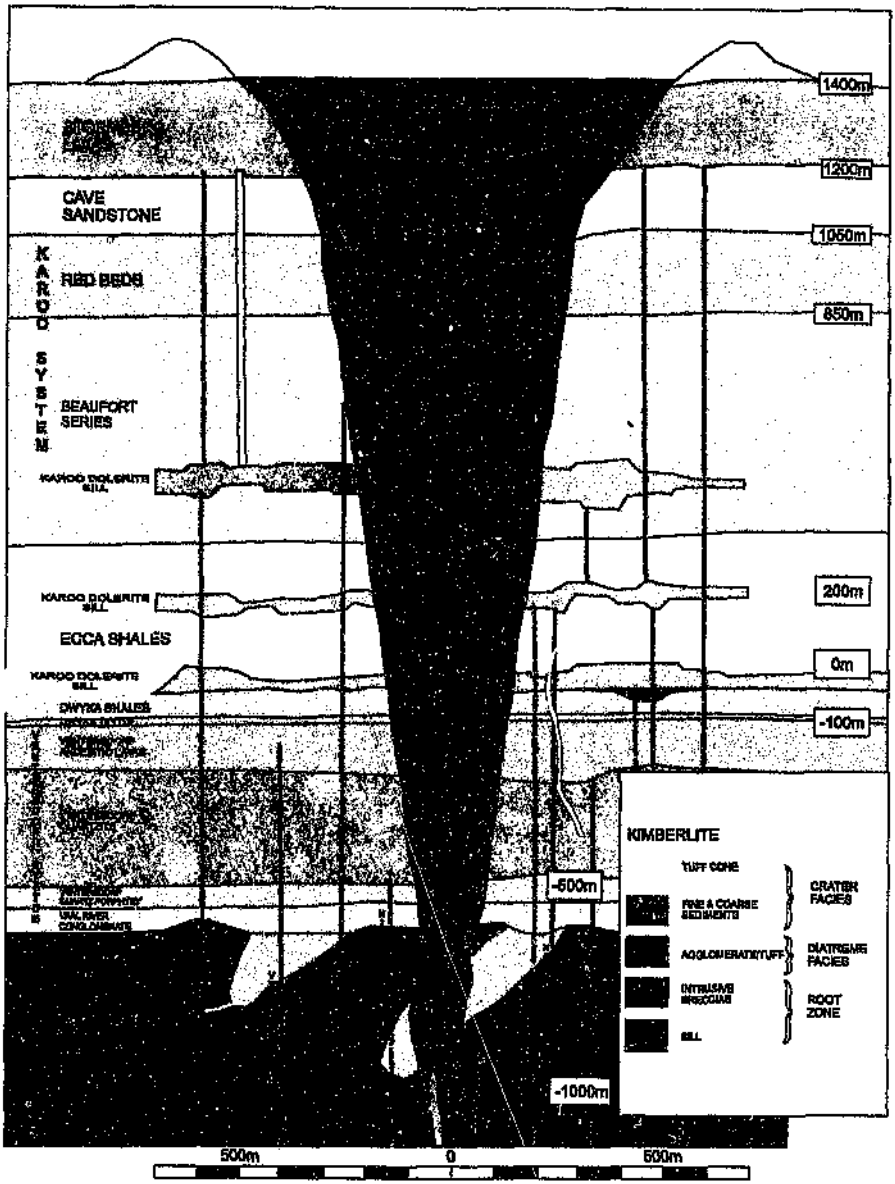


Figure 2.1: Model of kimberlite pipe (modified after Hawthorne 1975) showing the crater facies, the diatreme facies and the root zone. The sampling data used in this thesis has been taken from the diatreme facies of the pipe.

Large kimberlite pipes may show repeated periods of intrusion and eruption resulting in a complex sequence of volcanic and sub-volcanic structures.

The present understanding of the distribution of diamonds in a kimberlite is aptly summarised by Clement (1988):

"*With the exception (and to some degree) of crater zones where, in epiclastic facies material, diamond distributions are at least in part governed by accepted and broadly understood sedimentological controls, our knowledge of diamond distributions in kimberlite is rudimentary*".

At a mining scale (50m by 50m by 12m blocks) the grade of the crater facies can be extremely variable. Such grade variations are seen, for example, at Orapa mine in Botswana. Such grade variations, although not fully understood, have been explained in terms of various sedimentological processes eg: Talus slope formation on the side of the crater.

The diatreme facies is less variable in grade. This reflects, according to Clement (1988), the mixing that took place during fluidisation. The distribution of diamonds at a local scale (say the scale that would influence the grade of a borehole) is not known.

Grades in the root zone of the kimberlite can be erratic, vary systematically with depth or reflect a similar grade distribution to the diatreme kimberlite.

Clement (1988) advances two mechanisms to explain the distribution of grade in a kimberlite. These are :

- ☐ The mechanical distribution of diamonds during emplacement
- ☐ The differential sampling of diamond rich upper mantle rocks

Some of the mechanical processes proposed by Clement (1988) include : gravity settling, flowage differentiation, convection, volatile streaming and elutriation.

The second process suggests that grade variations within the pipe are the result of "sampling effectiveness". In other words, separate pulses of kimberlite, to be intruded into the same pipe, have sampled diamond rich mantle with different degrees of success or have sampled different sources with varying concentrations of diamonds.

A further cause of grade difference within and between intrusions is undoubtedly the dilution of the kimberlite by xenolithic material on a micro to macro scale. Xenolith dilution is affected by the mechanical processes mentioned above. Even if the diamonds were well mixed, an uneven distribution of xenolithic material would result in grade variation. Major changes in grade between two intrusions may reflect differences in the content of xenolithic material

2.3 The sampling of kimberlites

The following is required when evaluating a kimberlite pipe:

- Geological information
- Diamond grade
- Diamond size
- Diamond value and assortment
- Geotechnical information
- Metallurgical information

This information is collected using a phased approach moving from relatively little information at the early stages of exploration to detailed information that may include local block estimates at the later stages. The phased approach allows a decision to abandon or continue with the project to be taken after each phase helping to minimise the cost of sampling.

The reconnaissance stage : The objective of this early phase is to obtain an overall indication of grade, diamond value and the potential size of body.

Due to the limited amount of data available the confidence limits around estimates at this stage are wide.

The exploratory phase : The objective of this phase is to obtain a global indication of grade within specified confidence limits together with estimates of diamond assortment and value. The kimberlite would be sampled to a depth sufficient to sustain a mining operation for a number of years.

The results of this phase are used for a pre-feasibility study. If the sampling produces a favourable result the project will move forward to the detailed sampling phase.

The detailed sampling phase : The objective of this phase is to obtain

sufficient information to allow the estimation of grades per mining block. Typical mining blocks would be 50m x 50m by 10m high and would form the basis for detailed mine scheduling.

The information from the detailed sampling phase would form the basis of a feasibility study on which a new mine would be opened.

The typical tools used to sample a Kimberlite are surface pits, trenches, shaft and tunnel information and large diameter drilling.

Large diameter drilling is the only method of providing a three dimensional picture of grade within the pipe. Modern drill rigs, using reverse circulation technology, are used to drill the kimberlite to depths of 400m. Drilling is carried out using one hole per grid node or, if larger volumes of sample are required, "clusters" of holes.

The large diameter drilling can be solid core or percussion drilling using down the hole hammers, drag bits or tri-cone bits. The core diameters of percussion drill rigs vary in size from 6" to 1m. The use of 6" percussion drilling for pipe evaluation is rare but may occur if the drill rig has to be flown into a remote site. The diameter of solid drill core (observed by the author) can be 40cm with rare holes up to 1m in diameter.

The sample data used in later chapters is taken from large diameter percussion drill holes, 12" in diameter.

The samples collected from the sampling program are treated through a sampling plant to liberate and recover diamonds from the kimberlite. The samples are crushed and the screened product, between a defined bottom

and top cutoff, is fed to a heavy media separator that separates the liberated diamonds and the heavy minerals in the kimberlite from the "waste[1]". The diamonds are separated from the concentrate using recovery techniques based on X-ray fluorescence or hand sorting.

The plant design to achieve the above can vary considerably. Some plants may have a re-crush circuit that allows the "waste" to be re-circulated and crushed for a second time. Such a plant will liberate more diamonds than a plant with only a primary crush. Older plants made use of "pans" and grease to recover diamonds. Such plants would have a different recovery efficiency to plants with dense media separators and X-ray technology.

In order to place the grade of a kimberlite in perspective the plant used to treat the kimberlite samples must be understood.

2.4 Global estimation, local estimation and grade units

Grade estimates can be either in a global or local sense. A global estimate consists of a single grade per geological facies. No attempt is made to differentiate grade within a given geology. A local estimate consists of a grade estimate per mining block. Such estimates give an indication of grade variation horizontally and vertically within a geological facies. Global estimates are most commonly used at the pre-feasibility stage of an evaluation and local estimates at a feasibility stage.

---

1 The "waste" described here contains a high proportion of uncrushed kimberlite.

A kimberlite grade is usually described in carats per ton (CPT) or carats per hundred tons (CPHT). The grade variable CPHT is made up of a carats per cubic metre (CPM3) and density. CPM3 is in turn made up of stones per cubic metre (SPM3) and stone size expressed in carats per stone.

$$CPHT = CPM3 * \frac{1}{density} = SPM3 * \frac{carats}{stone} * \frac{1}{density}$$

The variable SPM3 is usually less variable than CPM3 at the scale of a mining block and shows a stronger spatial relationship. If the number of stones per sample is high and the variable carats per stone does not vary within the deposit, then the estimation could be carried out using CPM3 directly. If the stone size varies within the kimberlite it may be necessary to estimate SPM3 first and then estimate "carats per stone" separately.

The distribution (histogram) of the variable SPM3 is referred to as the stone density distribution. The distribution (histogram) of carats per stone is referred to as the diamond size distribution. A statistical model for the stone density distribution is discussed in section 2.7.4.

When sampling a kimberlite the degree of diamond liberation, and hence the grade of the sample, is a combined function of the physical nature of the kimberlite, the method of sampling and the flow sheet of the sample treatment plant. This can result in differences in grade between pit sampling and large diameter drilling despite both methods having sampled the same kimberlite.

Diamonds can vary in size from microscopic sizes (10^{-6} of a carat) to hundreds of carats. Commercial plants usually recover stones larger than

1mm in size (approximately 0.02 carat per stone). The grade of a kimberlite is dependant on the bottom cutoff chosen at the sample plant. In other words the grade of a kimberlite at 1mm will be different to that quoted at 2mm. This is because, at 2mm, the diamonds between 1mm and 2mm have been excluded. The bottom cutoff on a production plant is based on the value of the stones in these small sizes. As this is not usually known at the time of the evaluation most sampling campaigns are carried out at a 0.5mm or 1mm bottom cutoff.

The grade estimates at one cutoff can be adjusted to another cutoff using the diamond size distribution (discussed in section 2.5).

2.5 The diamond size distribution

As stated above, the size of diamonds in a kimberlite can vary from microscopic sizes (10^{-5} of a carat) to hundreds of carats. The top size of diamond extracted is a function of the natural diamond size distribution in the kimberlite and the crushing regime used in the plant.

The distribution of diamond sizes in a pipe, called the diamond size distribution, has been shown to follow a two parameter lognormal distribution (Sichel 1971) if the stones are taken from a single geological environment. When plotted on logarithmic probability paper (see Figure 2.2) the diamond size distribution usually plots as a straight line.

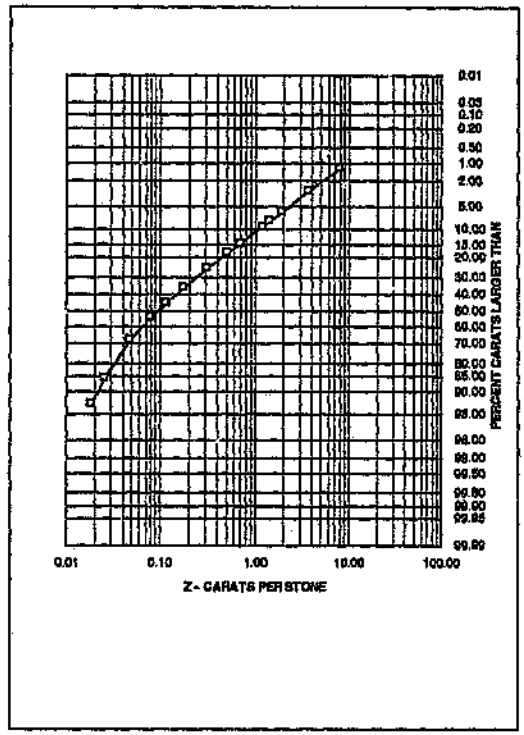


Figure 2.2: The diamond size distribution of deposit one on logarithmic probability paper. The reversed probability scale is by convention.

Exceptions to this would be :

- Sample plant inefficiencies which have caused the loss of stones from the diamond size distribution. For instance, such plots often bend down towards the bottom cutoff of the sample plant reflecting the loss of smaller stones in the plant due to sieving inefficiencies.
- The distribution may not plot as a straight line if the stone population has sampled more than one geological environment resulting in a

mixture of Lognormal populations. This situation is discussed in section 2.7.4.

The diamond size distribution is used to make adjustments to the grade estimate of a sample or deposit to allow for a different bottom cutoff. For example, if the sampling was carried out at a bottom cutoff of 0.5mm but the production plant required an estimate at a bottom cutoff of 1.0mm, the diamond size distribution could be used to adjust the 0.5mm grades to a 1.0mm cutoff. This is done by excluding the carats below 1.0mm in the diamond size distribution and recalculating the grade.

2.6 The mining of kimberlite

The mining and treatment of kimberlite are relatively simple processes. Most kimberlites start off as open cast operations. Near surface, weathered Kimberlite (up to 50m in depth) is usually soft enough to be ripped. Harder "blue ground" is blasted. Loading is done with electric shovels into diesel 50 ton, 75 ton or 100 ton trucks.

Once open pitting becomes uneconomic the mining continues underground using mining techniques such as block caving or vertical crater retreat.

The treatment of the kimberlite is similar to that described in section 2.3 for the sample plant, the major difference being the size of the operation.

2.7 Statistical models for diamond deposits

In this section a review is given of the statistical models that have been applied to diamond size and grade distributions.

2.7.1 The two parameter lognormal distribution

The earliest statistical models were applied to the diamond size distribution by Sichel (Sichel 1973). Sichel noted that a two parameter lognormal distribution could be used to model the diamond size distribution where the samples were taken from a single geological zone.

The two parameter lognormal distribution is defined as

$$f(z) = \frac{1}{\sqrt{2\pi}\,\sigma^2}\, e^{(-(\ln z-\xi)^2 / 2\sigma^2)} \qquad (2.1)$$

Where z is the diamond size in carats, ξ the logarithmic mean and σ^2 the logarithmic variance.

The lognormal nature of the diamond size distribution can be seen by plotting the size distribution on logarithmic probability paper. The X-axis in Figure 2.1 consists of the diamond size expressed in carats per stone. The Y-axis consists of a probability scale giving the percentage of carats greater than a given stone size z. In practice the weight of the individual stones are not plotted but rather the average weight of diamonds per sieve class.

In practice the sieving close to the bottom cutoff of the plant is inefficient and the line will often bend downwards as it approaches the bottom cutoff indicating a relative loss of smaller stones.

The diamond size distribution expressed as the weight per size class can be converted to the number of stones per sieve class using the expressions :

$$\text{Mean of the stone size distribution} = \xi - \sigma^2$$
$$\text{Variance of the stone size distribution} = \sigma^2$$

where ξ = the mean of the weight distribution and σ^2 = the variance of the weight distribution.

Rombouts (1995) explains the lognormal nature of the diamond size distribution by suggesting that the diamond growth is the result of a proportional effect. He states :

"Kapteyn (1903) quoted extensively in Aitchinson and Brown (1957), introduced the proportional effect as a mechanism for creating lognormal distributions. The addition of a large number of small independent effects in a random normal variable. If the small independent effects are represented by $\delta x/x$, rather than by x, the resulting normal variate will be $\ln x = \int \delta x/x$ and x will be a lognormal variable. The growth of diamond crystals proportional to $\delta x/x$ seems plausible as it is analogous to the mass action law, where the change in concentration of a chemical reagent is proportional to $\delta x/x$."

The two parameter distribution is acceptable where the size distribution is taken from a single geological population. Where the diamond size distribution represents a mixture of different geological environments, each

with its own lognormal distribution, then the resulting distribution is no longer lognormal but compound lognormal (Sichel 1973).

2.7.2 The Compound lognormal distribution

Sichel (1973) carried out his research on the diamond bearing beach deposits adjacent to the Namibian coast. Sampling that took place across different geological environments (different beaches), each with their own ξ and σ^2 parameters, would result in a mixing of lognormal distributions. To allow for such a mixing Sichel (1973) proposed the Compound lognormal distribution.

The Compound lognormal model is discussed at length in Sichel 1973, Assibey-Bonsu 1991 and Dohm 1995.

The beach deposits investigated by Sichel (1973) are believed to have entered the sea from the Orange river mouth and then to have been worked northwards along the Namibian coast line by the prevailing long shore currents. The continuous reworking by the sea led to a natural sorting where the coarser stones were trapped close to the Orange river mouth and the finer stones travelled northwards. Sichel (1973)argued that the situation would result in the parameters ξ and σ^2 being related inversely to the distance d from the Orange river mouth and directly to each other. He formalised this relationship as

$$\xi = a + b\sigma^2 \qquad (2.2)$$

By substituting this value for ξ in equation 4.1, making x=ln(z) and assuming the mixing distribution of the logarithmic variance to follow a Pearson Type III (gamma) function of the form

$$\delta(\sigma^2) = \frac{\rho^\tau}{\Gamma(\tau)} (\sigma^2)^{\tau-1} \exp(-\rho\,\sigma^2) \qquad (2.3)$$

he obtained the compound lognormal distribution

$$f(x) = \frac{s\,(1-c)^{\nu+½}}{2^\nu\sqrt{\pi}\;\Gamma(\nu+½)} e^{(\sqrt{c}\,s(x-a))} k_\nu(s|x-a|) \qquad (2.4)$$

for $-\infty < x < \infty$.

The parameters of the compound lognormal distribution are as follows

$k_\upsilon(.)$ is the auxiliary modified Bessel function of the second kind
a is the location parameter where $-\infty < a < \infty$
s is the scale parameter where $s > 0$ and is given by $s = (2\rho + b^2)^{½}$
c is the skewness parameter where $0 \le c < 1$ where $c = b^2/(2\rho + b^2)$
υ is the Kurtosis parameter where $\upsilon > -½$ and is given by $\upsilon = \tau - ½$

The relationship of the compound lognormal distribution to the 2 parameter lognormal distribution is shown in Figure 2.3 (after Dohm 1995, p. 3.7) and Figure 2.4.

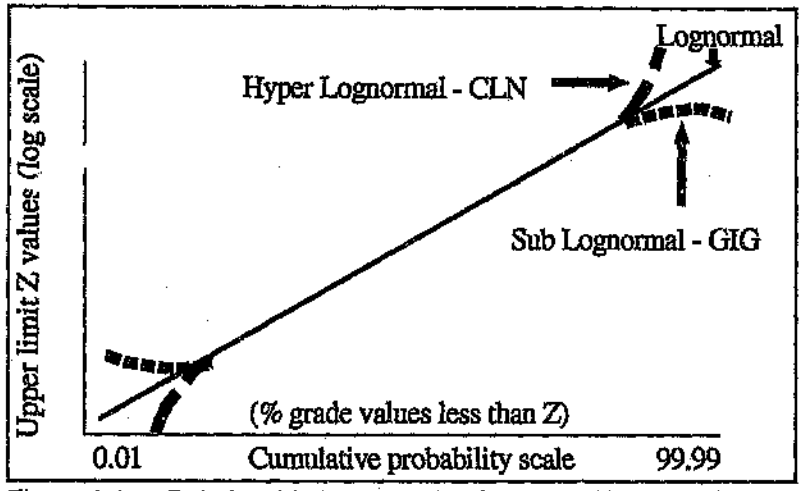


Figure 2.3: Relationship between the Compound lognormal model and the lognormal model (after Dohm 1995).

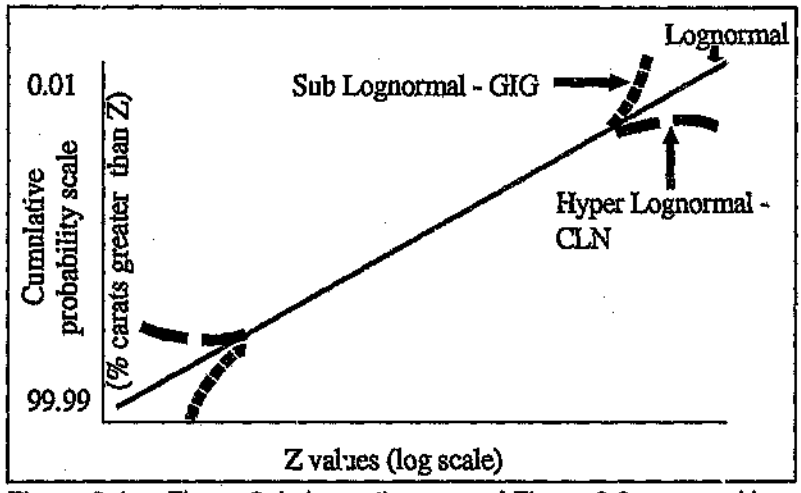


Figure 2.4: Figure 2.4 shows the axes of Figure 2.3 arranged in the same way as the diamond size distribution plot shown in Figure 2.2.

On logarithmic probability paper the compound lognormal distribution shows a bending downwards of the line at the coarser stone sizes indicating more large stones than for the 2 parameter lognormal distribution.

2.7.3 The mixing of stone populations in kimberlites

When considering the crater zone of a kimberlite it is likely that, if different stone populations existed, a mixing of stone populations could have occurred during successive kimberlite eruptions or later as various sedimentological processes acted upon the kimberlite within the crater itself.

In section 2.2 two mechanisms were proposed to explain the grade distribution within the diatreme zone of the pipe. These were:

- The mechanical distribution of diamonds during the formation of the diatreme
- The differential sampling of the diamond rich upper mantle rocks

It is not inconceivable that both processes could have resulted in the mixing of stone populations, each with their own ξ and σ^2 parameters, within a single kimberlite facies.

Unfortunately, very little work has been carried out on the fitting of the Compound lognormal model to diamond size distributions in kimberlites. This is partially because the mining does not preserve the source of the kimberlite mined (several facies can be mixed in varying proportions) and secondly that the diamond size distribution that results from the treatment of the kimberlite is partially a function of the treatment process itself.

2.7.4 The Compound Poisson distribution

In the same paper Sichel (1973) developed a unique distribution to explain the stone density distribution of diamonds along the Namibian coast. This was the Compound Poisson distribution.

Sample results from the Namibian beaches typically consisted of stone counts in the order of 0,1, 2, 3 etc. Typically, a large number of samples would be zero with a rare sample containing several thousand stones. The distribution created by these samples was a reversed J shaped distribution with a very long upper tail. Conventional discrete distributions, such as the negative binomial distribution, failed to fit these distributions due to the number of zero samples and the long tail.

The results of the sampling can be understood if one considers the trapping mechanism along the Namibian coast. The diamonds washed north of the Orange river are trapped in natural bedrock irregularities along the coast or in gravel beds being deposited on beaches. The trench samples taken are small in size and the majority of the time fail to intersect a trap site. The results of the sampling therefore produces a large number of zero or low stone count samples. On a rare occasion the sampling will encounter a trap site or part of a trap site. Depending on the quality of the trap site the sample may collect several thousand stones.

Considering the rarity of the trap sites one might expect that the Poisson distribution would provide a reasonable fit to the stone density distribution. In trying to model the stone density distribution of the Gbenko deposits in Guinea (west Africa) Rombouts (1984) noted that the Poisson distribution

provided a poor fit to the stone density distribution. The explanation he proposed was that diamonds do not occur at random in a deposit. In the case of the Gbenko deposit he states

"Geological control on a local scale makes them (diamonds) cluster around boulders, in small depressions, at confluences, etc"

Kleingeld (1987) notes that the statistical model used to describe the stone density distribution

"must take into consideration the distribution of the particles in a trap site as well as the distributional characteristics of the trap sites"

This suggests a conceptual model of the type

$$\Phi(r) = \int_0^\infty P(r|\lambda)\, f(\lambda)\, d\lambda \qquad (2.5)$$

Where $\Phi(r)$ is the number of stones per sample, $P(r|\lambda)$ is the conditional probability of a particle given a trap site and $f(\lambda)$ is a flexible mixing distribution function describing the distribution of the trap sites.

If $P(r|\lambda)$ is a Poisson distribution

$$P(r|\lambda) = \frac{e^{-\lambda}\lambda^r}{r!} \qquad (2.6)$$

and the mixing distribution is the Pearson III gamma distribution

$$f(\lambda) = \frac{1}{\Gamma(\lambda)}\left(\frac{1-\theta}{\theta}\right)\lambda^{(\gamma-1)}e^{\left(-\frac{(1-\theta)}{\theta}\lambda\right)} \qquad (2.7)$$

then Φ (r) is a Negative binomial distribution for $Y \leq 0$

$$\Phi(r) = \frac{(1-\theta)^{\gamma}\,\Gamma(r+\gamma)\,\theta^{r}}{\Gamma(\gamma)\,r!} \qquad (2.8)$$

As already said the Negative Binomial distribution is unable to model the J shaped distribution observed from the sampling so Sichel (1973) proposed a more flexible mixing distribution

$$f(\lambda) = \tfrac{1}{2}\frac{2\sqrt{1-\theta}}{\alpha\theta}\,\frac{1}{K_{\gamma}(\alpha\sqrt{1-\theta})}\,\lambda^{(\gamma-1)}\,e^{\left(-(\frac{1}{\theta}-1)\lambda-\frac{\alpha^2\theta}{4\lambda}\right)} \qquad (2.9)$$

where $-\infty < \gamma < \infty$, $0 < \theta < 1$ and $\alpha > 0$ are the three parameters. This mixing distribution is intermediate to Pearson's type III and type V distributions. $K_{\gamma}(.)$ is the modified Bessel function of order γ.

Substitution of equations 2.6 and 2.9 into equation2. 5 gives a new family of discrete distributions

$$\theta(r) = \frac{(\sqrt{1-\theta})^{\gamma}}{K_{\gamma}(\alpha\sqrt{1-\theta})}\,\frac{(\alpha\theta/2)^{r}}{r!}\,K_{r+\gamma}(\alpha) \qquad (2.10)$$

where r = 0,1 2 3 .... ∞.

This family of distributions was published by Sichel (1971) and encompasses most of the better known discrete distributions such as the Poisson, negative binomial distribution, geometric, Fisher's logarithmic, Yule, Good, Waring and Riemann distributions (Sichel 1973).

If, in equation 2.10, γ is made negative then a new set of discrete distributions are generated of the type

$$\theta(r) = \frac{1}{(\sqrt{1-\theta^{\gamma}})\ K_{\gamma}(\alpha\sqrt{1-\theta})} \frac{(\alpha\theta/2)^{r}}{r!} K_{r-\gamma}(\alpha) \qquad (2.11)$$

where $0 \leq \theta \leq 1$, r= 0,1,2 3 ....∞

Sichel discusses the special case of $\gamma = -1/2$. In such a case equation 2.10 becomes

$$\theta(r) = \sqrt{\frac{2\alpha}{\pi}}\ e^{(\alpha\sqrt{1-\theta})}\ \frac{(\alpha\theta/2)^{r}}{r!} K_{r-\frac{1}{2}}(\alpha) \qquad (2.12)$$

This distribution has two parameters which have to be estimated from the sample data. These are α where $\alpha > 0$ and θ where $0 < \theta < 1$ or $\alpha > 0$ and $\beta > 0$.

The θ parameter characterises the tail of the distribution and represents the degree of clustering in the deposit. For θ=0 there is no clustering of diamonds, the tail of the distribution becomes short and the stone density distribution follows a Poisson distribution.

The significance of the Compound Poisson distribution to this research is that it recognised, for the first time, the need for a two step model to explain the distribution of diamonds and suggested the idea of a mixture of Poisson distributions with different means per cluster. **The simulation used in this thesis can be interpreted as a spatial version of the compound Poisson distribution suggested by Sichel.**

The Sichel distribution assumes that the trap sites are distributed according to a Poisson distribution and that the trap sites have a punctual support (Kleingeld 1987). Matheron (1981) developed the Sichel model further by proposing a generalised family of distributions dependant on three parameters (not two as for the Sichel model) that allowed for the modelling of a change of support in the parameters α and θ.

Kleingeld (1987) made use of these new distributions by Matheron and the special statistical properties of the Sichel distribution to develop a simulation model for discrete particles where the simulation had a defined spatial structure and the histogram was either a Sichel model or Negative Binomial model.

2.8 Spatial models for the distribution of diamonds

The results presented in this thesis make use of a stochastic simulation based on a particular model. In this section the concept of simulation is introduced, different simulation techniques are reviewed and the work leading up to the development of the Cox simulation is described.

2.8.1 The importance of simulation as a tool

As mentioned in section 1.1 only a portion of the mineral deposit is sampled. This leads to the concept of uncertainty in the estimation process. At the points in the deposit which were not sampled there will be a difference between the true value and the estimated value. Kriging estimators are designed to minimise this difference but in the process of doing so often result in estimated values that are **less variable** than the real ones (Journel 1978, p479).

In many cases it may be sufficient to provide a "best"[2] estimate of the block value. However, if the exercise involves assessing the variability of a given parameter, using the estimated values can be misleading.

To answer the questions posed in chapter one it is necessary to have a complete model of the deposit under discussion and, ideally, many such deposits in order to estimate the confidence in a given sampling method.

Simulation offers a means of generating many realisations of a mineralisation according to statistical parameters obtained from the sampling. This way many kimberlites can be generated and sampled. The sampling from each simulation can be used to estimate a local or global grade and the estimated grade can be compared to the "true" grade calculated from the simulation. If sufficient simulations are carried out then a confidence interval can be established for each deposit.

---

2 Best is the minimum estimation error for the kriging method applied.

If the simulation reproduces the statistical and spatial character of the deposit but the simulated values at each sample location are different from the actual sample values at that point, the simulation is called a non-conditional simulation.

If the simulation reproduces the statistical and spatial character of the deposit and the simulated values at each sample location coincide with the actual sample values at that point, the simulation is called a conditional simulation.

Conditional simulations allow the outcome generated to be conditioned to the available sample data. Such conditioning is important where, for instance, the variability associated with a mine plan is required. As the mine plan is fixed in space, it is important that the simulated grades reflect, as closely as possible, sampling results in the same area.

Conditional simulations are usually less variable than non-conditional simulations as the differences between possible outcomes are smaller due the conditioning influence of the sample data. The more sample points available to condition the data the more similarity is seen between possible outcomes. Conversely, a conditional simulation based on relatively few data will give results similar to a non-condition simulation.

If an understanding of the variability between possible outcomes is required then a non-conditional simulation may be sufficient. For instance, a non-conditional simulation can be used to test the efficiency of different sampling campaigns.

In this study a number of non-conditional simulations are carried out. These are used to visualise a complete model of the mineralisation, compare the efficiency of different sampling campaigns and assign a confidence interval to global and local block estimates.

2.8.2 Different types of geostatistical simulation

There are several geostatistical simulation methods available in practice. These include the Turning bands (Matheron 1973, Journel 1974, Mantoglou and Wilson 1982, Mantoglou 1987). LU decomposition (Alabert 1987, Dowd 1992, Dowd 1994), Sequential simulation (Journel and Alabert 1989, Deutsch and Journel 1992, Dowd 1992 and Gomez-Hernandez and Cassiraga 1994), and more recently Truncated Plurigaussian simulation, an extension of Truncated Gaussian simulation (Le Loc'h and Galli 1996).

The simulation approach used in this thesis has been especially developed to model discrete particles in space and makes use of the Turning bands method in a two step simulation process. For completeness and in order to add substance to the discussion on a choice of simulation model, a brief discussion of each method is given below.

The Turning bands

The Turning bands method is the most widely known method of geostatistical simulation and has been extensively described in the literature (Matheron 1973 p. 461, Journel 1974, Mantoglou and Wilson 1982, Mantoglou 1987).

In the Turning bands method a one dimensional random function is generated along lines evenly distributed in space. The one dimensional simulations are then projected onto defined points in 2 or 3 dimensions where they are summed to give the required simulated value. The approach takes advantage of the simplicity of simulations in one dimension.

Several criticisms have been levelled at the original Turning bands method although Dowd (1992), noted that these criticisms reflect the algorithm used to implement the Turning bands rather than the theory itself. These criticisms include :

1 The generation of lines or stripes on simulations.
2 The Turning bands method is limited to certain forms of the covariance function.
3 The introduction of geometric or zonal anisotropy is not straight forward as the Turning bands method assumes an isotropic covariance function.
4 The Turning bands method requires a separate kriging step in order to condition it.

Most of these criticisms refer to the original algorithm used to create the Turning bands (see, for instance, Zimmerman and Wilson 1990 for an example of an early algorithm).

The Turning bands method requires an even distribution of lines. In the original version of the Turning bands the number of lines in 3 dimensions was limited to 15, this being the group of lines that join the mid points of opposite edges of a regular Icosahedron. This limitation would often result

in lines or stripes when the simulation was visualised. Lantuéjoul (1994) shows that many lines can be generated in 3 dimensions using a method developed by Freulon (Freulon 1991 and 1992 cited in Lantuéjoul 1994).

The limitation of the Turning bands method to certain covariance forms has been investigated by several authors. These include the work by Mantoglou and Wilson (1982) and Mantoglou (1987) who make use of a spectral approach to generalise the Turning bands method. The use of spectral methods allowed the use of more varied covariance functions and made the introduction of anisotropy easier. Lantuéjoul (1994) noted that the unidimensional covariance function can be generated using a spectral method, a dilation method (the traditional approach) or particular methods suited to the covariance function to be generated.

To introduce geometric anisotropy the 3 dimensional grid is "stretched" to allow an anisotropic simulation. Once complete, the grid is "shrunk" back to its original form. In the case of zonal anisotropy the covariance function is modelled as the sum of each model. Turning bands simulates each of the component models separately and then adds the resulting realisations at each grid node. Modelling anisotropy in the "modern" turning bands is not more difficult than any other simulation method.

To condition the Turning bands a separate conditioning step is required. This is in contrast to Sequential methods or LU decomposition.

The modified method of Turning bands is applied in this thesis.

LU decomposition

The Lower - Upper (LU) decomposition method (Alabert 1987, Journel and Deutsch 1992, Dowd 1992, Dowd 1994) is based on the triangular decomposition of the matrix of covariances between the data points and the grid nodes to be simulated. The method can be used to produce non-conditional and conditional simulations. Its advantages are that it is fast and simple to use, performs conditioning as it simulates, is not restricted to particular covariance forms and can handle anisotropies.

The main disadvantage of LU is that the method requires all the conditioning data and grid nodes be considered in a single matrix. The method is therefore limited by computer memory requirements to a few hundred points in 3 dimensions. To over come this limitation Alabert (1987) suggested a moving window and Dowd (1994) has suggested a method of ring decomposition. The advantage of Dowd's approach is that a moving window is not required, maintaining the simplicity of the LU approach and avoiding possible artefacts that result during the simulation when using the moving window.

Sequential Gaussian simulation (SGS) and Sequential indicator simulation (SIS)

Sequential simulation methods are described in many papers including Journel and Alabert 1989, Deutsch and Journel 1992, Dowd 1992 and Gomez-Hernandez and Cassiraga 1994.

Sequential methods are based on an application of Bayes' theorem in which it is stated that n dependant events, A_i, i=1,...n can be sequentially simulated using the expression (Dowd 1992) :

$$P(A_1,.....A_n) = P(A_n \mid A_1,.....A_{n-1}) \cdot P(A_n\text{-}1 \mid A_1,... A_{n-2}) ..$$
$$..P(A_2 \mid A_1) \cdot P(A_1) \quad (2.13)$$

The simulation algorithm for SGS is as follows :

1 Transform the data to a standard Gaussian distribution and model the semi-variogram.

2 Define a random walk through all grid nodes to be simulated.

3 At each node krige a value using all values (simulated and actual) in the kriging neighbourhood. The conditioning data is increased as the simulation continues since the simulated points become part of the conditioning data set.

4 Using the kriged value and estimation variance, draw a value at random from this distribution and add this value to the simulated values.

5 Repeat steps 3 and 4 until all nodes requiring simulation have been visited.

6 Transform the Gaussian values back to original space.

The advantages of this method are that the conditioning of the simulation is carried out as part of the simulation, anisotropies are handled easily, it can be applied to any covariance function and the method is simple as all that is required is a kriging algorithm and the random selection rule.

In SIS the conditional probability distribution is estimated directly from the indicator variables defined at different cut offs.

The simulation algorithm for SIS is as follows :

1 Approximate the range of values taken by the variable by K discrete cut off values.
2 Code each conditioning value into a vector of K indicator values.
3 Model the semi-variograms of each indicator cutoff.
4 Define a random path through all grid nodes to be simulated.
5 At each node obtain a kriged value of each indicator at each cutoff. Each of the K indicator estimates is regarded as an estimate of :

$$Pr\ (Z \leq z_k) \qquad (2.14)$$

6 Choose a value at random from the pseudo-distribution obtained in 5 and add this value to the simulated values.
7 Add the simulated value in 6 to the set of conditioning values, code it into the vector of K indicator values and go to step 5. Repeat until all grid nodes have been visited.

The advantages of SIS are the same as for SGS with the following additional points: No assumption is made about the distribution required and qualitative or "soft" information can be included in the simulation.

Truncated Plurigaussian simulation

Truncated Plurigaussian simulation is an extension of truncated Gaussian simulation (Galli et al 1994, Le Loc'h and Galli 1996, Armstrong 1997).

The object of Plurigaussian simulation is to simulate different geological facies of the same rock type or different rock types in one simulation. This is done by simulating indicator random functions for each facies or rock type. A Gaussian model is chosen because of the convenient mathematical properties of the Gaussian distribution. In particular, Gaussian random functions make it possible to set up mathematically consistent models for the indicator random functions used.

Four steps are required to create a Plurigaussian simulation (Armstrong 1997). These are :

1 Choose a model type.

The relationship between the different facies can take different forms. The facies can be, for instance, sequential, reflecting an underlying sedimentary model or mixed. It may be permissible for facies to be in contact with another or not. In the first step the relationship between the different facies is identified and an approach is chosen from a family of methods.

2 Estimate the key parameters.

The proportions of the various facies are estimated. This allows the cutoffs between the Gaussian values to be determined for each facies. Once known the semi-variogram and cross semi-variograms are calculated for each of the facies indicators. The semi-variograms of the underlying Gaussian variables are linked to those of the facies indicators by a set of equations.

3 Create Gaussian values for the Conditioning data

The conditioning data at each sample location is in the form of a rock or facies type and not a Gaussian value. In this stage the conditioning data are given a Gaussian value falling in the appropriate interval.

4 Simulate the deposit

The simulation is carried out using a Turning bands method (although SGS could also be used). Once complete the thresholds are used to back transform the Gaussian values to the geological or facies types simulated.

The advantage of the method is it's mathematical consistency and its ability to produce a wide range of images for simulation purposes. Its main disadvantage, in the author's opinion, is its complexity.

2.8.3 Simulation models created for discrete particles

Two stochastic models have been proposed to simulate diamond deposits. These are a variant of the Neyman-Scott process used by Kleingeld (1987) and Caers (1996) and the Cox process used in this thesis (Kleingeld et al 1994 and 1996). Both models are based on spatial point processes.

The mathematical background to point processes is well described in the literature. An overview of point process theory (and the point processes above) is given in Cressie (1993).

It is not the intention of the author to repeat the details described in these works but rather to present the concepts required to understand the point processes used in the Kleingeld (1987) and the Cox model.

Cressie (1993) describes a point process as "*a stochastic model governing the location of events $\{S_i\}$ in some set X*".

For a spatial point process (our interest here), and in an informal manner, we can view a spatial point process as a means of defining X, Y or Z points in two or three dimensional space according to a defined stochastic process. The points defined may be the location of individual stones or the location of cluster centres.

A Poisson point process is an example of spatial point process. Cressie (1993) defines an homogeneous Poisson process as follows :

1 For a given bounded region A the number of events in A have a Poisson distribution with mean

$$\lambda * |V_A| \qquad (2.15)$$

where $|V_A|$ is the volume of region A and λ is the intensity of the Poisson process.

2 Given n events in A, the n events are independent and form a random sample from a uniform distribution on A

To give this a physical meaning consider the two dimensional simulation of the process :

1 Define a two dimensional region A with extent 0 to A_x and 0 to A_y where $A_x * A_y = A$.

2 Draw an X co-ordinate from a uniform distribution where X is $0 < X < A_x$.

3 Draw a Y co-ordinate from a uniform distribution where Y is $0 < Y < A_y$.

4 Carry out the draw N times where N is the number of events defined by a Poisson distribution of mean $\lambda * |V_A|$.

In the homogenous Poisson process the intensity of the Poisson process is constant. In the "inhomogeneous[3]" Poisson process (Cressie 1993) the intensity of the Poisson process becomes a function of spatial location. **The idea of spatially varying the intensity of the Poisson process leads directly to the Cox point process named after D R Cox (1955).** Cressie (1993) defines the Cox point process as an "inhomogeneous" Poisson process where the mean measure is randomised.

The use of the Cox point process to model diamond deposits was first proposed by Kleingeld and Lantuéjoul (1992). In this publication the intensity of the Poisson point process was modelled as a regionalised random function called the potential. The stones in such a simulation are then spatially distributed according to a Poisson distribution with a random

---

3 As stated by Cressie 1993. Perhaps a better word, from the English language point of view, would be heterogeneous.

intensity equal to the potential. **It is this spatial point model that has been adopted in this research for the simulation work on the kimberlites.**

This simulation method is discussed in detail in chapter 4.

A alternative spatial point model was introduc ' by Kleingeld (1987) to model diamond deposits. The model adopted is a variant of the Neyman-Scott point process.

This Neyman-Scott point process was introduced by Neyman (1939), Cressie (1993) defines the Neyman-Scott process as follows :

1 Parent processes are generated from a Poisson process with a mean μ .
2 Each parent produces a random number of K offspring, realised independently and identically for each parent according to a discrete probability distribution model.
3 The positions of the offspring, relative to their parent process, are distributed according to a two dimensional probability density function.
4 Only the offspring are considered in the final process.

A variant of this simulation was used by Kleingeld (1987) and Caers (1996) to model diamond deposits The simulation is summarised as follows :

1 A domain, A, is divided into regions of constant cluster density.
2 The number of clusters in a region, X_i , is drawn from a gamma distribution.
3 The X_i cluster centres are placed in the polygon according to an homogeneous Poisson process

4 The number of stones associated with each cluster is drawn from a density distribution $\gamma(s)$, this being the Poisson pocket density defined in Kleingeld 1987.

5 Finally the stones are seeded around the cluster centre according to a two dimensional probability density function.

The method of simulation is described fully in Kleingeld (1987) and Caers (1996).

2.8.4 Why the Cox model as a simulation method

Relatively little work has been done comparing the different simulation methods. Dowd (1992 p.1484) quotes work carried out by P. J. Ravenscroft showing a greater variation in the simulations produced by Turning bands when compared to SGS. This greater variation was particularly evident in the histogram of block values created by averaging the simulated point data into 12m by 12m blocks. Dowd (1992) suggests that the reason for this is that, as the number of conditioning points increases in the kriging neighbourhood, the kriging variance decreases and so the range of the conditional distribution from which the value can be drawn is smaller.

Gotway and Rutherford (1994) compared different simulation methods including Turning bands, Sequential methods, LU decomposition and Truncated Gaussian Random functions.

Gotway et al used several exhaustive data sets for the comparison and carried out both non-conditional and conditional simulations. The results of her comparisons indicated :

1 That the Gaussian simulation methods were more accurate than the Sequential Indicator methods.

2 Conditioning the data reduces the variability of the uncertainty distributions.

3 LU and Turning bands methods produced similar results.

4 There are notable visual differences in the realisations produced by the Turning bands and LU when compared to the Sequential simulation algorithms. The realisations produced by the Sequential simulation methods tend to result in a greater clustering of similar values. Gotway proposes that the clustering is an artefact of the kriging process used in the Sequential methods. Clustering was particularly pronounced in simulations produced by SIS.

What was evident from the paper was that different methods of simulating a random field can result in different uncertainty distributions even though the simulations make use of the same histogram and covariance functions.

It is clear from this paper, and the discussion that followed the paper (Armstrong and Dowd 1994), **that the choice of model used to create the simulation must be compatible to the data and the variable you wish to study.**

In considering a model with which to simulate diamonds it should be kept in mind that diamonds are distributed as discrete particles. The discrete nature of stone counts per sample cannot be directly simulated by methods such as Turning bands, LU or Sequential methods.

In addition, the work carried out by Sichel (1973) and Kleingeld (1987) strongly suggested that the simulation model of a diamond deposit must take

into account the distribution of the particles in a trap site as well as the trap site distribution. This implies a distribution model for the stones as follows Kleingeld 1987)

$$\varphi(r) = \int_0^\infty P(r|\lambda)\, f(\lambda)\, d\lambda \qquad (2.16)$$

Where $P(r|\lambda)$ is the conditional probability for a particle given a trap site and $f(\lambda)$ is a flexible mixing distribution describing the distribution function of the trap sites.

In simpler terms this states that the number of diamonds at a specific location is the **combined result** of diamonds being present (i.e. there is a source of diamonds available for concentration) and the presence of a trap site within which the diamonds can be concentrated.

Apart from the two spatial point processes none of the simulation models discussed above encompass this two stage model.

In considering the two point processes, it can be shown that under certain conditions the Cox and Neyman-Scott point processes are similar[4] (Kleingeld and Lantuéjoul 1992, Cressie 1993 and Caers 1996).

Caers (1996) in his thesis argues that the Neyman-Scott point process is more flexible then the Cox point process in that it allows a higher degree of

---

4 Cressie (1993) notes that the two processes are equivalent if the number of offspring in the Neyman-Scott process are Poisson distributed around their parent events where the parent events are the result of an inhomogeneous Poisson process.

clustering and allows the stones to be distributed very close to the cluster centres. This, he argues, is difficult to achieve with the Cox simulation.

It is possible that the Neyman-Scott process is better suited to deposits where diamonds are confined to very specific and focussed bedrock traps and where few, if any, diamonds are found between such traps. Apart from the beach deposits discussed by Schel (1973) this model may also apply to certain alluvial deposits where bedrock irregularities may be small and highly focussed.

Although the distribution of diamonds in kimberlites is not well understood it is unlikely, based on sampling seen to date, that the diamonds in kimberlites are clustered to the same extent as the Namibian beach deposits. Unlike the beach deposits, stone count distributions are usually modelled using a negative binomial distribution. The Cox model should suit the work carried out in this research on kimberlites and, for that matter, deposits where the stone counts can be readily modelled with a negative binomial distribution. It is also simpler to apply than the Neyman-Scott process.

Finally, two historical points that perhaps support the Cox process in favour of the Neyman-Scott point process. Firstly, one of the reasons that the Cox simulation model was developed was that the simulation produced by Kleingeld (1987) did not always result in an acceptable visualisation. This was due to the mosaic appearance of the simulation area. The search for an alternative point model lead to the development of a model based on the more general Cox point process.

Secondly, the Cox model was able to model the"trap site" effect observed by Kleingeld (1987). Usually, as the sample size increases, the error

associated with the estimation of a mining block **decreases**. The "trap site" effect is a marked slowing in this rate of decrease. Kleingeld and Lantuéjoul (1992) explained the "trap site" effect as follows: While the sample size remains **smaller** than the "trap site" the sample variability is dominated by the within "trap site" variance, and there is no appreciable fall in the estimation error. Once the sample size is **larger** than the "trap site" then the variability between "trap sites" becomes more important and the estimation error continues to fall as would be expected.

The Cox model appears a conceptually appropriate model with which to model diamonds in a kimberlite, building on the models developed by Sichel (1973) and the experience of Kleingeld (1987).

2.9 Chapter conclusion

This chapter has presented various practical aspects of kimberlites as background to the research presented in chapters 3 to 7. This was considered necessary as relatively little has been published on kimberlite evaluation.

Finally, a review of the statistical models available for the modelling of diamonds are presented. Again, not all models are reviewed, but only those that give a useful background to the research carried out in the thesis.

In the next chapter some early research work is presented to illustrate that the way diamonds are distributed in a pipe can influence the statistical results obtained from a sampling campaign.

CHAPTER 3

An experiment to show how the distribution of stones may effect sampling and evaluation

Completely homogeneous materials
are so rare that they can be
considered non-consistent
I O Ingamells.

In this chapter we will:

- Describe a method to place stones in place according to a Poisson point process
- Distribute stones in space with three different spatial patterns
- Illustrate that, different spatial patterns can result in different statistics for the same sampling configuration

3.1 Introduction

In this chapter the results of an experiment are presented in which stones are placed randomly in space using a Poisson point process.

The objective of the experiment is to illustrate that the way diamonds are distributed in space can lead to **different statistical results** from the **same sampling campaign.**

3.2 The simulation method

The simulation described here was an early attempt at simulating diamonds in space. It has been superseded by the more sophisticated Cox simulation that is used in subsequent chapters of this thesis.

The Poisson point process used to place the stones in space is described in Chapter two, section 2.8.3.

In the simulation that follows three scenarios were envisaged. The first is a situation where the stones are randomly distributed throughout the pipe. This follows the belief by some geologists that the "Kenwood mixer" effect during diatreme emplacement (see section 2.2) would have thoroughly mixed the diamonds into the kimberlite melt resulting in a random distribution of stones in the pipe.

The second scenario is one where clusters, or concentrations of diamonds, are superimposed on a random background of diamonds. One interesting aspect of this model is that, although both the background and cluster centres are seeded in space using a Poisson point process, the combined effect results in a semi-variogram where the range of the semi-variogram is related to the dimensions and frequency of the clusters.

The third scenario is an extension of the second, where the clusters were made smaller and given a higher grade.

The three scenarios explore the possibility of a random (even) distribution of stones, a kimberlite where the stones are slightly clustered and a kimberlite where the stones are clustered.

To ea · · of these scenarios a drilling configuration was applied and the results used to compare sampling statistics between the different textures.

The simulation was generated as follows :

1 Define the three dimensional space within which the simulation is to be generated.
2 Define the number of stones in the pipe. Use this as the mean input to a Poisson distribution and draw the number of stones to be simulated.
3 Divide this number of stones into a background and clustered component.
4 Place a uniform background of stones in the pipe.
5 Define the size and shape of stone clusters in the pipe.
6 Generate an X, Y and Z cluster centre. Seed stones around this centre to form a stone cluster.
7 Average the stones generated into blocks for later comparison with local block estimates.

The random, slightly clustered and clustered textures generated by the simulation above were sampled using a 40m grid with samples taken every 12m down the drill hole to a maximum depth of 60m depth. In addition, the slightly clustered and clustered textures were sampled using a 50m grid with samples taken every 12m down the hole to a maximum depth of 60m.

3.3 Results and discussion

The three textures generated are shown in Figures 3.1 to 3.3. In each case the simulation has been cut at 6m intervals to indicate the texture of the simulation both horizontally and with depth. The diameter of each circle is 150m. Each dot on the plot represents a stone in space. It should be noted that Figures 3.1 to 3.3 represent a diluted version of reality as the actual stone density is too high for each stone to be represented individually.

The histograms of the 40m sampling are shown in figures 3.4 to 3.6.The histograms of the 50m sampling are shown in Figures 3.7 and 3.8. The sample statistics for each sampling is summarised in Table 3.1.

For the example given (a high grade pipe with 225 samples) the global grade of 66 SPM3 used to simulate the deposit has been well reproduced in all three textures with the possible exception of the clustered sampling where the mean value was slightly overestimated[1].

It is clear from Table 3.1 and Figures 3.4 to 3.6 that, as the texture moves from random to clustered, there is an increase in the skewness of the sample histogram and an increase in the sample variance. The 50m sampling results show a similar pattern to the 40m sampling with slightly higher sample variances.

---

1 This is not surprising as the sample information from the 40m grid represents 45 holes from a relatively high grade pipe. Global estimation is usually carried out with 12 or fewer holes.

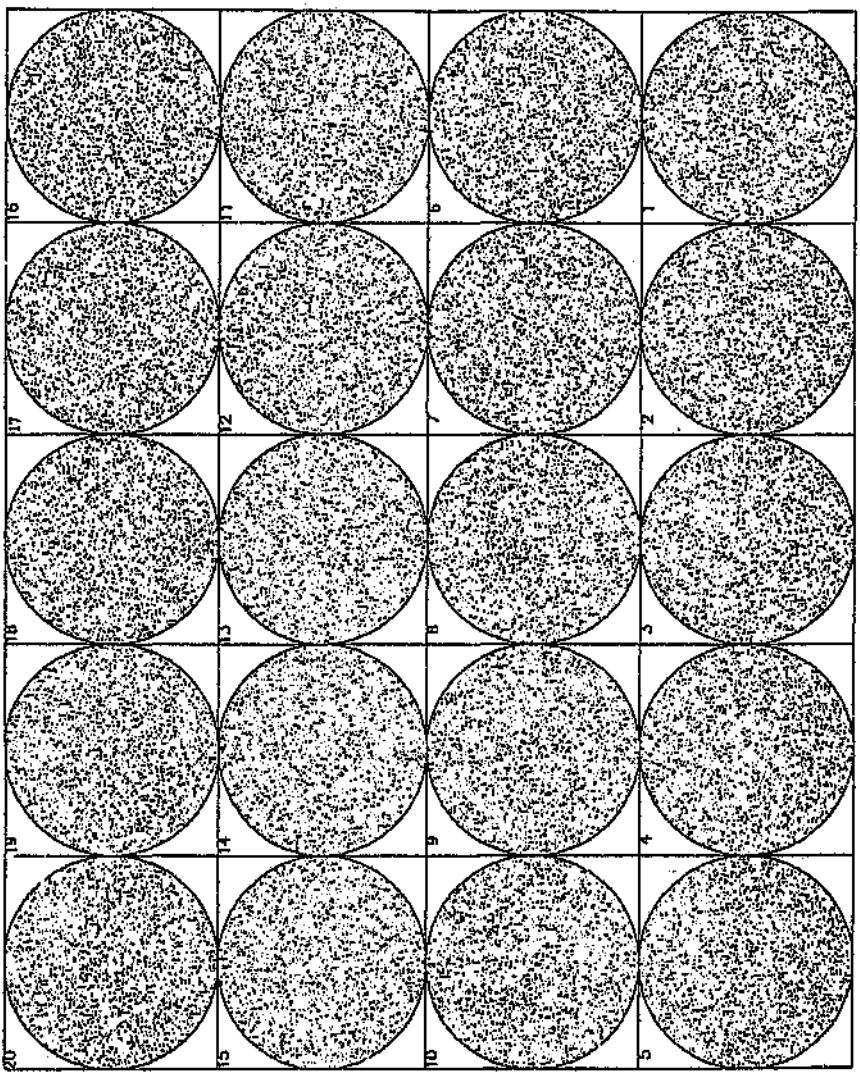


Figure 3.1 Uniform, random texture. Each circle represents a horizontal slice at 6m intervals through the simulation

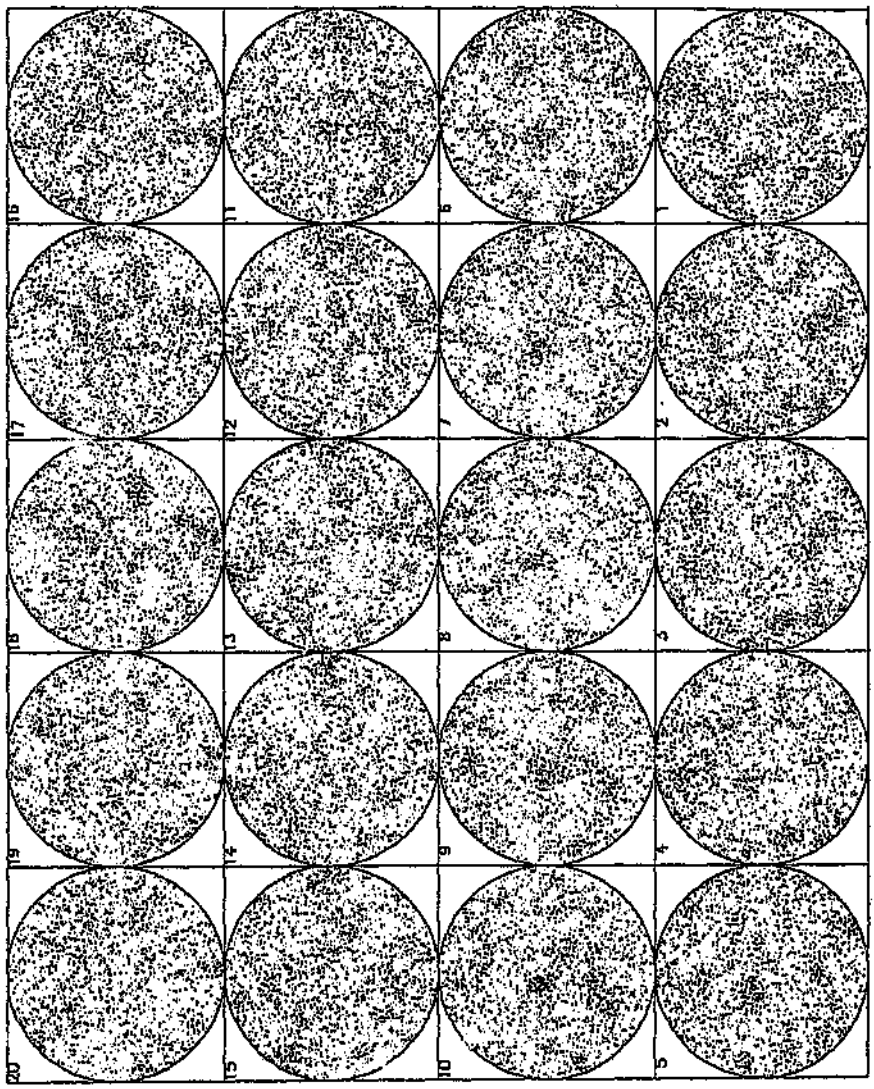


Figure 3.2 Slightly clustered texture. Each circle represents a horizontal slice at 6m intervals through the simulation.

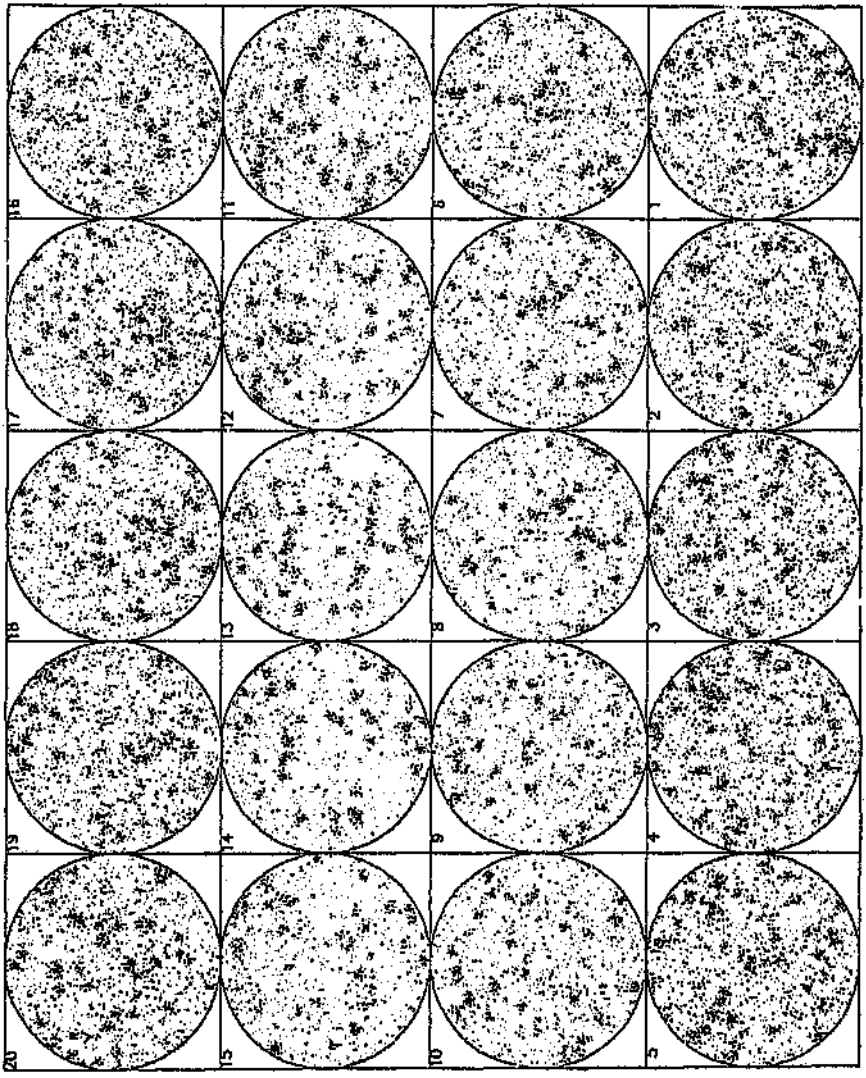


Figure 3.3 Clustered texture. Each circle represents a horizontal slice at 6m intervals through the simulation.

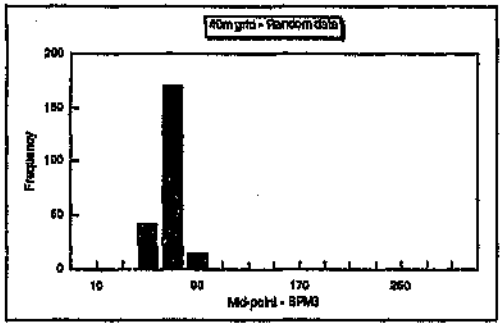


Figure 3.4: Random texture for 40m sample data

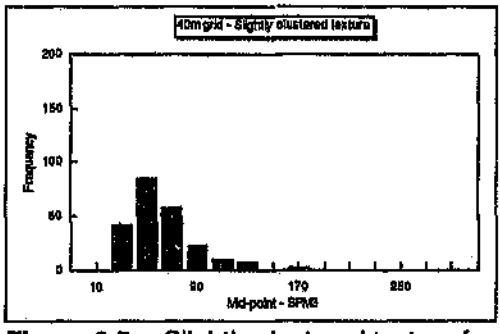


Figure 3.5: Slightly clustered texture for 40m sample data

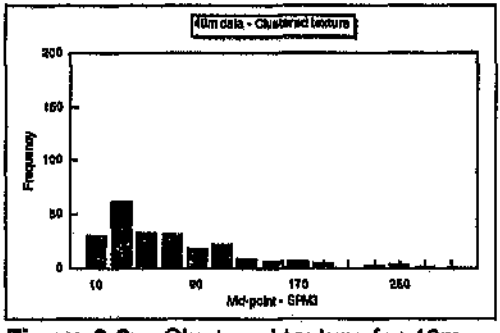


Figure 3.6: Clustered texture for 40m sample data

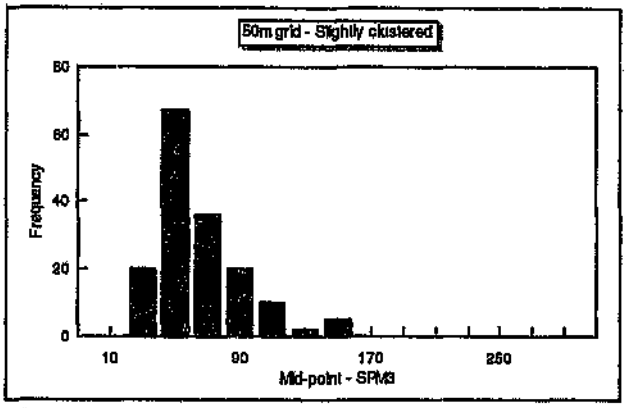


Figure 3.7: Slightly clustered texture for the 50m grid samples

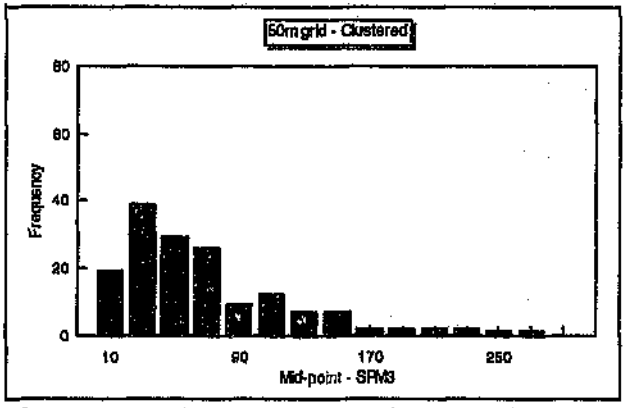


Figure 3.8: Clustered data for the 50m grid sampling

In general, the more skew a sample histogram the more difficult global and local estimation becomes. For the example given, the confidence limits surrounding the global and local estimates from the random data would be narrower than for the clustered texture. In other words, to achieve a defined confidence interval, more sample data would be required in the case of a clustered texture than in the case of a random texture.

Description	Statistics	Texture		
		Random	Hint of cluster	Clustered
Diameter of 311mm A 40m grid The number of samples is 225	MEAN	66	62	70
	VARIANCE	57	619	3658
	SKEWNESS	0.14	1.33	2.05
	KURTOSIS	0.33	2.25	6.11
	CV	0.11	0.40	0.86
Diameter of 311mm A 50m grid The number of samples is 160	MEAN		65	74
	VARIANCE		722	5646
	SKEWNESS		1.18	3.78
	KURTOSIS		1.08	22.38
	CV		0.41	1.01
Diameter of 500mm A 50m grid The number of samples is 160	MEAN		66	
	VARIANCE		751	
	SKEWNESS		1.20	
	KURTOSIS		4.50	
	CV		0.17	
Diameter of 90mm A 50m grid The number of samples is 160	MEAN		68	
	VARIANCE		1583	
	SKEWNESS		1.00	
	KURTOSIS		4.00	
	CV		0.34	

Table 3.1: Sample statistics for the three textures. CV = coefficient of variation.

Variography, for kriging purposes, was carried out on all three textures using the 40m sampling data.

A pure nugget effect was modelled for the random texture. The slightly clustered and clustered textures were modelled with spherical semi-variograms with the following structures:

Slightly clustered:	Spherical (range=56m, sill=561SPM3^2, nugget=59.5 SPM3^2).
Clustered:	Spherical (range=42m, sill=2900SPM3^2, nugget=500 SPM3^2

The 40m sampling data from the slightly clustered and clustered data were kriged into 40m x 40m x 12m blocks using Ordinary kriging and a rectangular kriging neighbourhood of 3 x 3 x 3 blocks. The estimated block values were then compared to the "true" block grades calculated from the simulation. The results of the comparison are shown in Figures 3.9 and 3.10.

Description	R squared	Slope	Residual variance
Slightly clustered	0.52	0.88	12.11
Clustered	0.00	-0.01	17.54

Table 3.2: Statistics for "true" block values against estimated values.

The quality of the local estimates can be summarised using the slope of regression of the "true" values on the estimated values (indicating the degree of conditional bias), the coefficient of correlation between the "true" and

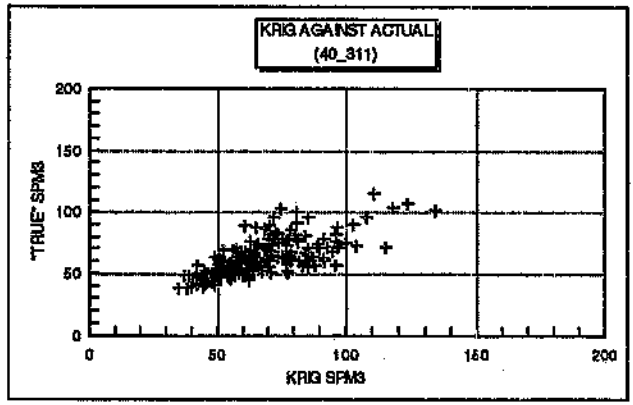


Figure 3.9: "True" values against kriged values for the 40m, slightly clustered data

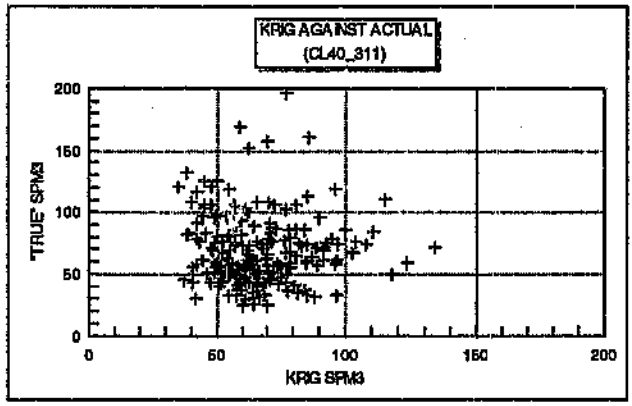


Figure 3.10: "True" block values against kriged values for the clustered data

estimated values and the variation in "true" values for all estimated grades given by the residual variance. These parameters are summarised in Table 3.2.

Ideally one would like the conditional bias close to one and the residual

variance as small as possible. The results in Table 3.2 and figures 3.10 and 3.11 demonstrate that the quality of local estimation deteriorates as the texture moves from a slightly clustered to a clustered texture.

3.4 Chapter conclusion

The results of sampling the three textures indicate **that the way diamonds are distributed in space can lead to different statistical results even if the same sampling configuration was used.**

A serious draw back of the simulation method used in this chapter is that only the mean is reproduced in the simulation. The histogram and semi-variogram of the deposit cannot be reproduced (at least not easily). To continue with the research it was necessary to use a simulation method that was capable of simulating diamonds in space with the correct histogram and semi-variogram.

Chapter 4 introduces the Cox simulation and presents the conceptual and statistical background to the simulation method. In the chapters that follow the Cox simulation is used to simulate diamonds in a kimberlite with a given histogram and spatial distribution.

CHAPTER 4

The simulation of stones within a kimberlite using the Cox process

In this chapter we will:

- Present the theory behind the Cox simulation
- Discuss the practical implementation of the simulation
- Give an example of the simulation

4.1 Introduction

The objective of this chapter is to describe the simulation used in this research. This chapter will discuss the need for simulation, the geological and statistical concepts behind the simulation method used and show how the parameters of the simulation can be estimated from the original data.

4.2 The Cox simulation in a geological context

In order to gain an intuitive feeling for the Cox simulation it is convenient to use the example of discrete particles in a marine placer. Such particles could be gold grains, heavy minerals or diamonds. In such an environment the concentration processes are well understood and readily visualised.

The distribution of diamonds in a marine placer is affected by factors such as the diamond source, local geography and footwall lithology. The concentration (or absence) of diamonds cannot be attributed to any one

factor alone as the individual factors are not independent. To describe the combined influence of the different factors, a regionalised concept called potential is introduced. The potential associated with a region of the deposit represents the propensity of that region to be rich. The greater the potential the greater the chance the region will contain many particles.

In a marine placer it is possible to imagine a beach consisting on the one side of schist and on the other side of granitic basement. Sea action has eroded the schist flat whereas the granite has become gullied and pot holed. The capacity of the schist to trap particles, washed ashore by long shore drift, is minimal and therefore its potential is low. On the other hand, the gullied granitic bedrock can readily trap particles, in other words its potential is high.

In practice, although an area of beach is gullied and therefore represents an area of high potential, it is possible to have gullies that are low in particles or even barren. Perhaps the sea energy was too high or the source of the particles was inadequate at that point of the beach. In the model presented here this is accommodated by making the hypothesis that the number of particles in a gully follows a Poisson distribution with a mean value equal to the potential of that gully. More generally, the number of particles within any region is assumed to follow a Poisson distribution with a mean value equal to the potential of that region.

The processes, likely to cause the clustering or irregular grouping of diamonds in a kimberlite, are more difficult to discuss or visualise because the exact distribution of diamonds in a kimberlite is not known. As mentioned in Chapter 2 the mechanisms responsible for the distribution of diamonds in a kimberlite include processes such as gravity settling, flowage differentiation, convection, volatile streaming, elutriation or differential

sampling of diamond rich rocks in the upper mantle. In a kimberlite the potential of the Cox simulation can be interpreted as the end result of an interaction between these processes.

Features that are common to both a diamond placer and a kimberlite are:

- The diamonds are distributed as discrete particles.
- Processes have acted upon the diamonds such that they are irregularly distributed.

Some important differences between the two are:

- The concentration processes in a kimberlite may result in different sized clusters or concentrations of diamonds.
- The number of stones per sample is much larger than for an alluvial deposit[1] with the result that there are very few zero samples.

4.3 The Cox simulation

The statistical development of the Cox simulation was carried out by Dr Ch Lantuéjoul between 1992 and 1996. A description of the process is given here but the reader is referred to the papers Kleingeld et al 1992, 1994 and 1996 for further details. The author of this thesis was a co-author of the 1994 and 1996 papers.

To construct a statistical model for the simulation the potential is considered as a regionalised variable. This implies that, for a given region, there will be areas richer in potential than others. In terms of the geological discussion

---

1 Perhaps 40 stones per sample in a kimberlite versus 0.3 stones per sample in an alluvial deposit.

given above, areas with the ability to concentrate diamonds will have a higher potential for grade than areas which can not.

For the simulation to succeed we have to infer the statistical parameters of the potential from the information that is experimentally available[2]. To do this a statistical model is required. Statistical inference and degree of generality within a model are often on opposite sides of the seesaw. The more general the model the harder statistical inference becomes and vice versa. The choice of a model carries implications and therefore must be chosen with care : **the quality of the information obtained from the simulation will depend directly on how well the model reflects reality.** The choice of the Cox process in this simulation offers a degree of flexibility in the simulation textures that can be generated while allowing statistical inference to take place.

In a formal manner the Cox process can be described as an implantation of discrete particles according to a Poisson point process for which the regionalised intensity is a random function.

Suppose initially we know the value of the potential in any region of the deposit. Then, applying our assumption that the number of particles are distributed according to a Poisson process with a regionalised potential, we have :

$$P\{N_x = n\} = e^{\{-Z_x\}} \frac{Z_x^n}{n!} \qquad (4.1)$$

Where N_x is the number of particles contained in the domain v and Z_x the potential attached to v.

---

2 The histogram and semi-variogram of the number of stones per sample.

In practice the potential is not known. If we consider the potential of a sample to be a realisation of a stationary random function, it follows that the number of particles contained in a region follows a Poisson distribution with a random mean.

$$P\{N_x = n\} = E\left\{\exp(-Z_x)\frac{Z_x^n}{n!}\right\} \tag{4.2}$$

Where the potential of a sample at point x is Z_x and the number of particles in a sample at x is N_x where $Z_x=Z(v_x)$ and $N_x=N(v_x)$.

This implies that the potential and the number of stones have the same mean.

$$E\{N_x\} = E\{Z_x\} \tag{4.3}$$

It can also be shown that the variance can be expressed as the sum of two terms :

$$Var\{N_x\} = Var\{Z_x\} + E\{Z_x\} \tag{4.4}$$

The first term takes into account the statistical fluctuations of the potential while the second, the Poisson implantation of the particles.

4.4 Statistical Inference

The spatial law of the Cox process is entirely specified by the spatial law of the potential.

4.4.1 Distribution of the potential

The distribution of the potential Z_x can be derived from the equation (2) using an inversion formula (see Kleingeld et al 1996, pp. 690-692). It can be shown that if N_x follows a negative binomial distribution then Z_x follows a gamma distribution (Feller, 1968) and similarly if N_x follows a Sichel distribution then Z_x follows an inverse Gaussian distribution (Sichel, 1973).

4.4.2 Covariance of the potential

Concerning the covariance of the potential we have:

$$\mathrm{Cov}\left\{Z_x, Z_{x+h}\right\} = \mathrm{Cov}\left\{N_x, N_{x+h}\right\} - \mathrm{E}\left\{N(v_x \cap v_{x+h})\right\} \qquad (4.5)$$

The covariance function of the potential coincides with that of the number of stones per sample with the exception of the term $\mathrm{E}\{N(v_x \cap v_{x+h})\}$. This term is zero if the two terms v_x and v_{x+h} are disjoint and is empirically seen as the nugget effect.

4.4.3 Model assumptions

Knowing the distribution of Z_x and its semi-variogram is not sufficient to define the spatial law of Z unless Z is an anamorphosed multigaussian random function (since the spatial law of a multigaussian random function is completely specified by its covariance function). This is the case considered for the Cox simulation used in the thesis. This assumption is not restrictive as many different forms of the potential are possible (Kleingeld et al 1994, p.30).

The potential Z is transformed to an anamorphosed, multigaussian function where Y is a standard, stationary, multigaussian, random function.

$$Z_x = \varphi(Y_x) \tag{4.6}$$

If φ is expanded in terms of Hermite polynomials we have

$$\varphi(y) = \sum_{n=0}^{+\infty} \frac{\varphi_n}{n!} H_n(y) \tag{4.7}$$

In addition the covariance of the potential satisfies

$$\mathrm{Cov}\{Z_x, Z_{x+h}\} = \sum_{n=1}^{+\infty} \frac{\varphi_n^2}{n!} \rho^n(h) \tag{4.8}$$

where ρ is the correlation function of Y.

Knowing the anamorphosis[1] and the covariance of the potential[2], equation (6) allows us to obtain the multigaussian covariance of the model specified.

4.4.4 Non-conditional simulation

Consider the simulation field D to be composed of a union of small, disjoint domains v_i of identical size and shape to those of the samples.

---

1 Which can be derived from the distribution of of Z_x

2 Which can be deduced from the number of stones per sample particle count (see equation (4.3)),

$$D = \bigcup_{|s|} v_i \qquad (4.9)$$

The simulation is carried out in three steps :

1 Simulation of the potential.

2 Simulation of the number of particles in each sample. In the sample v_i the number of particles follows a Poisson distribution with mean z_i.

3 Simulation and seeding of the number of particles in each sample. The seeding of the stones is not always carried out, as what is usually required is the number of particles per sample rather than the individual particles. If required, the individual particles are distributed uniformly into each sample.

4.5 The practical estimation of simulation parameters for Deposit One

In this section the practical steps involved in estimating the statistical parameters for the Cox simulation are given for a kimberlite referred to as Deposit One.

The sample data is taken from the diatreme facies of Deposit One and consists of six, 12.25" diameter holes drilled on a 50 m grid. Samples were taken every 12 m down each hole to a depth of 350 m.

The average number of stones per sample was 41 with a variance of 417 stones per sample^2 (SPS^2). The histogram of the stones per sample (SPS) is shown in Figure 4.1. A spherical semi-variogram was calculated with a nugget effect of 77, a sill of 340 and a vertical range of 89 m (see Figure

4.2). The horizontal structure was poorly defined and an isotropic spatial structure was assumed.

The simulation requires knowledge of the mean, variance, gamma distribution and semi-variogram of the potential as well as the size of the sample to be simulated.

4.5.1 Mean of the potential

It is shown in section 4.5 (equation 3) that the potential and number of stones per sample have the same mean. Hence, for Deposit One, we have:

Mean number of stones per sample (m) = mean of the potential = 41.

4.5.2 Variance of the potential

The variance of the potential is given by:

$$\sigma^2_{potential} = \sigma^2_{number\ of\ stones} - m \qquad (4.10)$$

Where m is the average number of stones per sample.

For Deposit One we have:

Variance of the potential = 417 - 41 = 376.

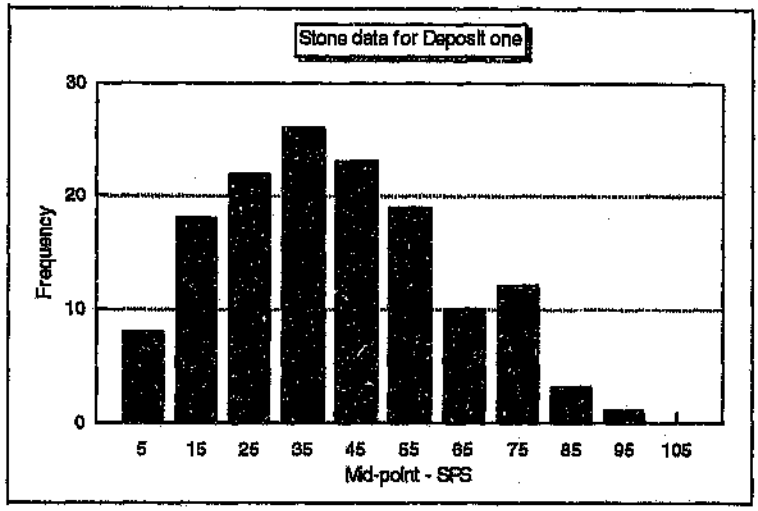


Figure 4.1: Histogram of stones per sample for Deposit one

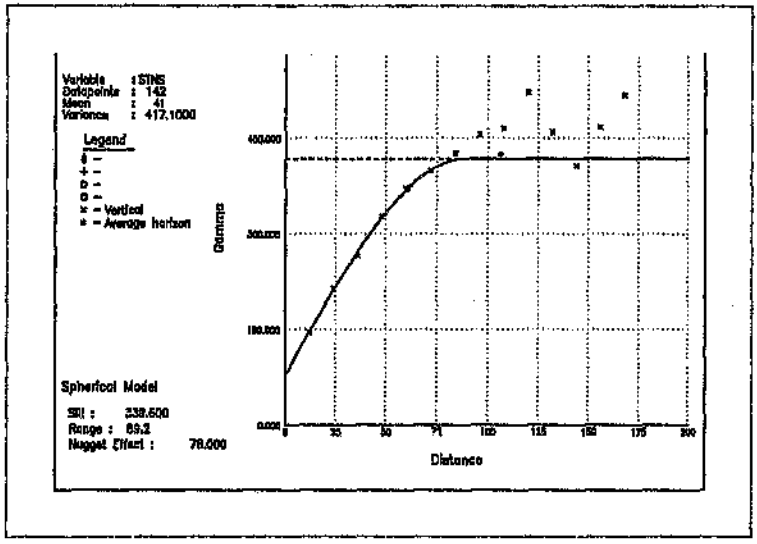


Figure 4.2: Semi-variogram of Deposit one.

4.5.3 Semi-variogram of the potential

The semi-variogram of the potential is given by:

$$\gamma_{potential}(h) = \gamma_{stones\ per\ sample}(h) - m \qquad (4.11)$$

For Deposit One we have:

Variogram of the potential = spherical (range=89m, sill = 340 SPS^2, nugget=36 SPS^2).

4.5.4 Parameters of the Gamma distribution of the potential

The distribution of the potential follows a gamma distribution if the distribution of number of stones per sample follows a negative binomial distribution.

The gamma distribution can be represented as follows:

$$f(x) = \frac{\beta^{\alpha}}{\Gamma(\alpha)} x^{\alpha-1} e^{-\beta x} \qquad (4.12)$$

Where x is a random variable following a gamma distribution defined by parameters α and β. It can be shown (Johnson and Kotze p99 - 101) that the mean (m) of a gamma distribution is given by α/β and variance (σ^2) by α/β^2.

Hence we have:

$$\alpha = \frac{m^2}{\sigma^2} \quad \text{and} \quad \beta = \frac{m}{\sigma^2} \qquad (4.13)$$

Applying this to Deposit One we have:

$$\alpha = 4.470745 \qquad \text{and} \qquad \beta = 0.109043.$$

4.5.5 Estimation of the multi Gaussian covariance of the potential

Knowing the distribution of the potential and its semi-variogram is not sufficient to define the spatial law of the potential unless the potential is an anamorphosed multi Gaussian random function (since the spatial law of a multi Gaussian random function is completely specified by its covariance function). Knowing the anamorphosis it is possible to obtain the multi Gaussian covariance by successive approximations. This step is carried out using a specially written program.

Using the α and β values of the Gamma distribution. A Gaussian anamorphosis is performed using Hermite polynomials and the mean and variance of the back transformed data are given to check the overall fit of the transformation. The program prompts for a lag distance and a guess for the Gaussian γ value at this distance. This γ value is back transformed to a γ value for the potential. This value can be compared to the calculated γ value at the specified distance. If the back calculated value does not match the calculated γ value of the potential the process is repeated until a satisfactory comparison is obtained.

The process is repeated for each lag up to the range of the semi-variogram. Once the program is terminated the Gaussian γ values are written to a file and modelled using a semi-variogram fitting program.

The following Gaussian semi-variogram was fitted to Deposit One:

Multi Gaussian semi-variogram of the potential = spherical (range=89m, sill=0.912, nugget=0.088).

4.5.6 Size of the simulated sample

For the purposes of the simulation the area of the sample is transformed to an equivalent square area. The length of the sample is left unchanged.

The surface area of a single Deposit One sample is 0.0760m^2. For the purposes of the simulation an equivalent square surface area of 0.3m x 0.3m was simulated.

4.5.7 Number of lines used for the turning bands

This has been set at 2000.

4.5.8 Modelling of the semi-variogram to take into account the shape of the drill samples

The cross sectional area of a drill hole is usually small when compared to its length. In the case of Deposit One the length of the hole is approximately 40 times the diameter of the hole.

In an isotropic deposit the semi-variogram value of two cubes lying adjacent to one another at a distance h and h + 0.3m will be identical to the semi-variogram value of two cubes lying vertically above one another at a distance h and h + 0.3m. However, if the sample shape becomes elongated then the semi-variogram values will not be the same. **even if the deposit is isotropic.** The greater the degree of elongation the greater the differer that can be expected between the semi-variogram values in the two

directions. In such a case, and in order to achieve a valid simulation, the deposit cannot be considered as isotropic.

One way to understand this is to consider the Deposit One drill samples as a string of 40 cubes, 0.3m x 0.3m x 0.3m, stacked vertically one above the other (see Figure 4.3). The vertical range has been defined as 89m. In practice this is the range from the mid point of the sample to the midpoint of the next vertical sample. If the distance between the centre of the last cube in the top sample and the first cube in the bottom sample is considered then

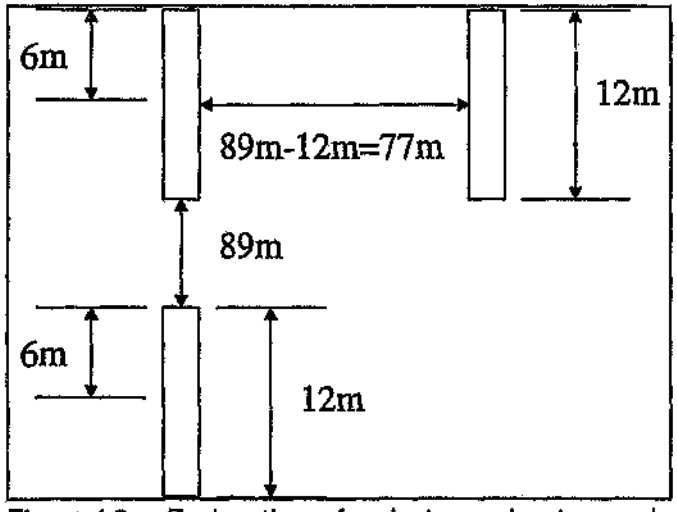


Figure 4.3: Explanation of anisotropy due to sample shape

the distance is 77m. In the horizontal direction two cubes are independent from one another at a distance of 77m.

A practical rule of thumb (Journel and Huijbregts 1978, p.90), in the case of a spherical semi-variogram, is to take the range between two cubes in the horizontal direction and add the length of the sample. In the case of Deposit

One we have a vertical range so the rule of thumb becomes vertical range less the length of a sample.

One practical way to remove the effect of sample shape would be to reduce the sample semi-variogram to a semi-variogram based on a very small support. This semi-variogram could then be used to generate a number of points that are added together to make up samples corresponding to the original sample size and shape.

Semi-variograms based on very small sample volumes are referred as "point" semi-variograms in the geostatistical literature.

The estimation of a "point" semi-variogram from a semi-variogram based on a given support size is described in Journel and Huijbregts (1978, pp.90-91) and Clark (1982, pp.49-53). In these cases, and in other literature, the emphasis is on a semi-variogram based on grade and not stones per sample.

If grade is considered then the sill of a grade semi-variogram decreases with increasing size of sample support, as does the nugget effect. In the case of stones per sample the sill of the semi-variogram **increases** with increasing sample size as does the nugget effect. A further difference when dealing with grade is that the mean grade of the samples does not change as the sample size changes. In the case of stones per sample the mean number of stones per sample increases or decreases as the sample support increases or decreases.

4.5.9 A proposed solution

In this section a solution to the shape problem is proposed and implemented for the Deposit One pipe. Two steps are envisaged; first to calculate a "point"

semi-variogram based on the vertical semi-variogram of the potential. Then to use this semi-variogram to calculate empirically the range in the horizontal direction. The shape problem is then solved by introducing an artificial anisotropy into the simulation to accommodate the elongated nature of the samples.

To calculate the "point" semi-variogram for Deposit one, each 12m long sample was considered as the union of vertically arranged cubes 0.3m x 0.3m x 0.3m. The semi-variogram of these cubes is taken as an approximation of the "point" semi-variogram and used to calculate the semi-variogram of 12m samples in the vertical and horizontal directions. These semi-variograms are modelled and used to calculate the anisotropy required for the simulation.

In practice the cube semi-variogram is not known and must be estimated from the 0.3m x 0.3m x 12m sample data. This is done using a specially written program. The steps of the procedure are as follows:

1 Calculate the stones per sample semi-variogram from the 12m drill hole data.
2 Calculate the semi-variogram of the potential.
3 Estimate the semi-variogram of the cubes.

The cube semi-variogram is estimated as follows:

1. A guess is made at the semi-variogram model for the 0.3m x 0.3m x 0.3m cubes.
2. The program uses this guess to calculate a theoretical 0.3m x 0.3m x 12m semi-variogram

3. This theoretical 12m semi-variogram is compared to the actual semi-variogram calculated from the 0.3m x 0.3m x 12m sample data.
4. Once a reasonable comparison is achieved the model of the cube semi-variogram is accepted. If the comparison is unacceptable than steps 1 to 4 are repeated.
5. Once the cube semi-variogram has been satisfactorily estimated, it is used to calculate the range of 0.3m x 0.3m x 12m samples in the vertical and horizontal directions.

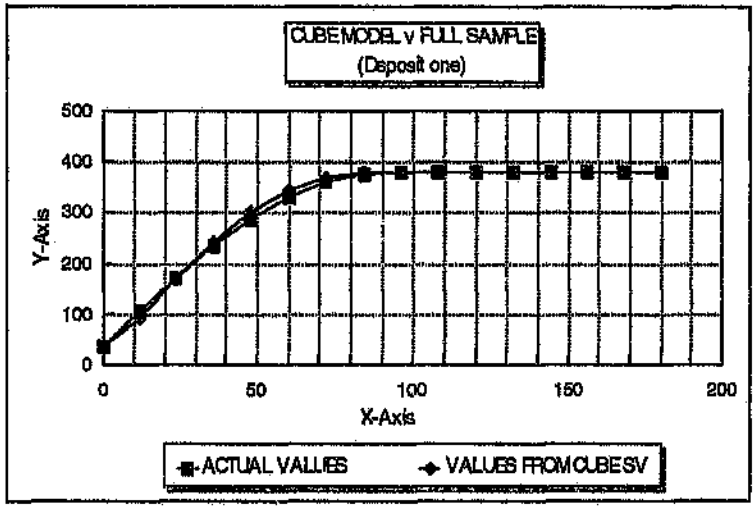


Figure 4.4: The 12m theoretical semi-variogram, estimated from the cube semi-variogram ("values from cube SV") compared to the real 12m semi-variogram ("actual values").

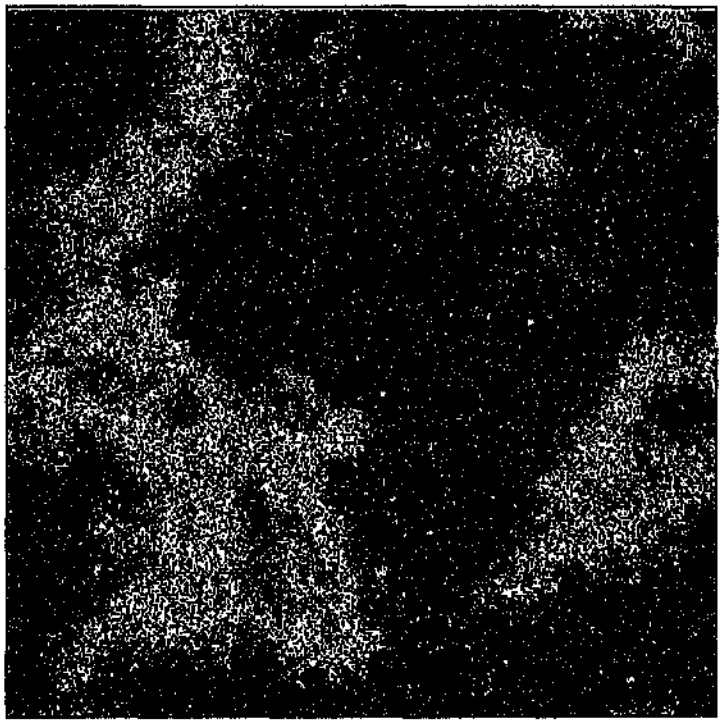


Figure 4.5: Texture of stones per sample for the low nugget semi-varlogram model. The simulation area is 300m x 300m x one 12m bench. The colours are distributed equally from low grade (blue) to high grade (red).

A cube semi-variogram was estimate, for Deposit one, as follows:

Spherical(range = 80m, sill = 0.22968, nugget = 0.925)

In Figure 4.4 the actual semi-variogram values of the potential are compared with the full sample semi-variogram values based on the cube semi-variogram.

Tables 4.1 and 4.2 show the full sample semi-variogram values, calculated from the cube semi-variogram, for various lags in the horizontal and vertical directions. A range of approximately 80m is indicated for the horizontal direction and a range of approximately 90m for the vertical direction.

4.5.10 Texture of the simulated simulation

The usual checks in assessing the quality of a non-conditional simulation is to check the statistics and semi-variogram of the simulated data against the simulation parameters. This is usually done by exhaustively sampling the simulation. A further useful, and very important check, is to examine the physical appearance of the simulation once it is plotted out. In particular, to check that the simulation **visually** reflects the grade changes that are expected.

Figure 4.5 shows the texture of the Deposit One simulation. The simulation area plotted is approximately 300m x 300m x a single 12m level. The colours are distributed equally from low grade (blue) to high grade (red). The plot shows large continuous areas of similar colour reflecting the long range (relative to the 300m square plotted) and low nugget to sill ratio of the semi-variogram model.

DIST X	DIST Y	DIST Z	GAMMA
0.00	0.00	0.00	37.00
3.00	0.00	0.00	45.97
6.00	0.00	0.00	61.47
9.00	0.00	0.00	79.16
12.00	0.00	0.00	97.75
15.00	0.00	0.00	116.66
18.00	0.00	0.00	135.62
21.00	0.00	0.00	154.43
24.00	0.00	0.00	172.97
27.00	0.00	0.00	191.14
30.00	0.00	0.00	208.86
33.00	0.00	0.00	226.04
36.00	0.00	0.00	242.63
39.00	0.00	0.00	258.55
42.00	0.00	0.00	273.73
45.00	0.00	0.00	288.12
48.00	0.00	0.00	301.66
51.00	0.00	0.00	314.27
54.00	0.00	0.00	325.91
57.00	0.00	0.00	336.51
60.00	0.00	0.00	346.02
63.00	0.00	0.00	354.37
66.00	0.00	0.00	361.50
69.00	0.00	0.00	367.36
72.00	0.00	0.00	371.89
75.00	0.00	0.00	375.03
78.00	**0.00**	**0.00**	**376.71**
81.00	**0.00**	**0.00**	**377.01**
84.00	0.00	0.00	377.01
87.00	0.00	0.00	377.01
90.00	0.00	0.00	377.01
93.00	0.00	0.00	377.01

Table 4.1: Example of output from the cube modelling program showing the reconstituted cube semi-variogram values in the X direction. The approximate range in the X direction is in bold and lies between 78m and 81m.

DIST X	DIST Y	DIST Z	GAMMA
0.00	0.00	0.00	37.00
0.00	0.00	3.00	41.70
0.00	0.00	6.00	54.06
0.00	0.00	9.00	71.46
0.00	0.00	12.00	91.27
0.00	0.00	15.00	111.28
0.00	0.00	18.00	130.99
0.00	0.00	21.00	150.35
0.00	0.00	24.00	169.31
0.00	0.00	27.00	187.80
0.00	0.00	30.00	205.77
0.00	0.00	33.00	223.15
0.00	0.00	36.00	239.90
0.00	0.00	39.00	255.95
0.00	0.00	42.00	271.24
0.00	0.00	45.00	285.72
0.00	0.00	48.00	299.33
0.00	0.00	51.00	312.01
0.00	0.00	54.00	323.69
0.00	0.00	57.00	334.34
0.00	0.00	60.00	343.88
0.00	0.00	63.00	352.25
0.00	0.00	66.00	359.40
0.00	0.00	69.00	365.28
0.00	0.00	72.00	369.83
0.00	0.00	75.00	373.08
0.00	0.00	78.00	375.16
0.00	0.00	81.00	376.30
0.00	0.00	84.00	376.81
0.00	**0.00**	**87.00**	**376.97**
0.00	**0.00**	**90.00**	**377.00**
0.00	0.00	93.00	377.01

Table 4.2: Example of output from the cube modelling program showing the reconstituted cube semi-variogram values in the Y direction. The approximate range in the Y direction is in bold and lies between 87m and 90m.

4.6 Chapter conclusion

In this chapter the background to the Cox simulation was presented and importantly, how the parameters for the simulation could be estimated from observed sample data.

The problem of sample shape in the simulation was discussed and a solution proposed based on introducing anisotropy into the simulation. A visual example of the simulation was generated.

In the next chapter the Cox simulation is used to simulate different sampling protocols for the estimation of global grade. Many realisations of each sampling protocol are carried out allowing the quantification of confidence limits for the sampling configurations investigated.

CHAPTER 5

THE EFFECT OF SAMPLE DENSITY AND SAMPLE SIZE ON GLOBAL ESTIMATION

In this chapter we will :

- Examine the effect of **numbers** of samples on the confidence interval around the global mean
- Examine the effect of the **size** of samples on the confidence interval around the global mean

5.1 Introduction

There are two ways of increasing the confidence in the estimate of the global mean. The first is to increase the number of samples on which the estimate is based and the second is to keep the number of samples the same but increase the size of the samples. In this chapter we examine the effect of numbers of samples and size of samples on the confidence interval around the global mean.

To indicate the sensitivity of the confidence interval to the degree of randomness in the spatial structure, a high nugget semi-variogram was created from the Deposit One semi-variogram. The experiments are carried out using the Deposit One semi-variogram (the low nugget semi-variogram model) and the high nugget semi-variogram model.

5.2 A high nugget effect semi-variogram model.

A low nugget effect semi-variogram model was obtained from the data analysed from the Deposit One kimberlite. To indicate the sensitivity of these and future experiments to the degree of randomness in the spatial structure, a high nugget semi-variogram model was created by increasing the nugget effect for Deposit One from 20% of the total sill to 80% of the total sill.

The simulation parameters used for the high nugget semi-variogram model are:

- "High" nugget semi-variogram of stones per sample = spherical (range=89m, sill=83 stones per sample^2 , nugget=334 stones per sample^2).
- Mean of the potential = 41 stones per sample.
- Variance of the potential = 376 stones per sample^2
- Semi-variogram of the potential = spherical (range=89m, sill=83 stones per sample^2 , nugget effect=293 stones per sample^2)
- Alpha = 4.470745 and beta = 0.109043
- Multi-Gaussian semi-variogram of the potential = spherical (range=89m, sill=0.23, nugget effect=0.77)

The texture of the high nugget semi-variogram model, for one 12m bench, is shown in Figure 5.1. The simulation area is 300m by 300m.

Figure 5.2 compares the low and high nugget semi-variogram textures.

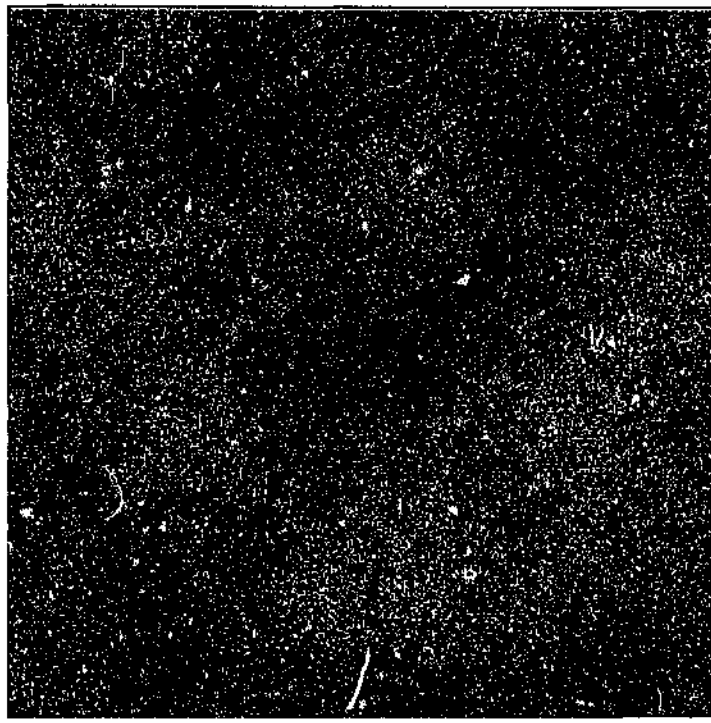


Figure 5.1: Texture of the stones per sample for the high nugget semi-variogram model. The simulation area is 300m by 300m by one 12m bench. The colours distributed equally from low grade (blue) to high grade (red).

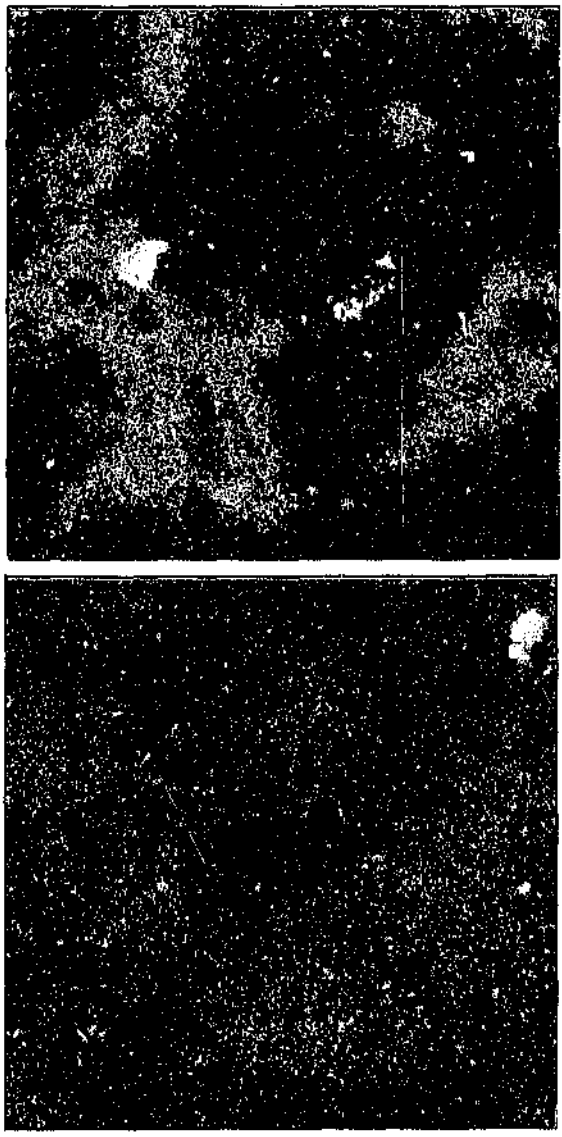


Figure 5.2: Comparison of the low and high nugget semi-variogram models. The simulation areas are 300m x 300m x one 12m bench. The colours are distributed evenly from low grade (blue) to high grade (red).

5.3 The effect of the number of samples

5.3.1 Method

In this exercises that follow the Cox simulation is used to simulate grades at the nodes of a sample grid. These simulated grades are used to calculate an average value per drill hole and the average of the drill holes is used to estimate a global mean for the pipe. The simulation is repeated 100 times generating one hundred mean values. The 100 mean values are ranked and the upper and lower 90% confidence intervals are taken as the 10th and 90th mean value in the ranked data.

The simulation exercises were based on the following sample configurations:

- Five sample grids were considered. Each grid consisted of holes equally spaced in a 300m x 300m square area.
- The grids prepared for the exercises were:
  - 4 holes on a regular 2 x 2 grid with holes 150m apart.
  - 9 holes on a regular 3 x 3 grid with holes 100m apart.
  - 16 holes on a regular 4 x 4 grid with holes 75m apart.
  - 25 holes on a regular 5 x 5 grid with holes 60m apart.
  - 36 holes on a regular 6 x 6 grid with holes 50m apart.
- Each drill hole consisted of 10, 12m samples giving a total depth per hole of 120m.

The sample area of 300m by 300m is a medium sized diamond pipe corresponding to an equivalent circular area of 9 hectares. The depth of 120m would be typical of a follow up program intended to identify a mine life of 5 to 15 years for a small mining operation.

The Cox simulations were created in three steps:

1 The simulation was used to generate the number of stones per sample at each node in the sample grid. This simulation was repeated for each sample grid and for the high and low nugget semi-variogram models.

2 Once a simulation was complete, the simulated stones per sample at each grid node was converted to carats per sample. This was carried out by allocating a stone size, in carats per stone, to each stone simulated. The allocation is based on the appropriate stone size distribution.

3 The simulated carats per sample at each grid node were converted to a grade in carats per cubic metre, by dividing the number of carats per sample by the sample volume.

5.3.2 Results

In Figures 5.3 (low nugget model) and 5.4 (high nugget model) the central 80% confidence limits around the global mean are presented for each grid. The upper and lower limits are plotted relative to the average of the 100 simulations run for each grid. The simulation results in stones per sample (SPS) and carats per sample (CPS) have been normalised to grade in stones per cubic metre (SPM3) and carats per cubic metre (CPM3) by dividing each sample result by the sample volume (0.3m by 0.3m by 12m).

Figure 5.3 presents the results when using the low nugget semi-variogram. The results indicate that 12 holes, on a regular grid and consisting of 10,

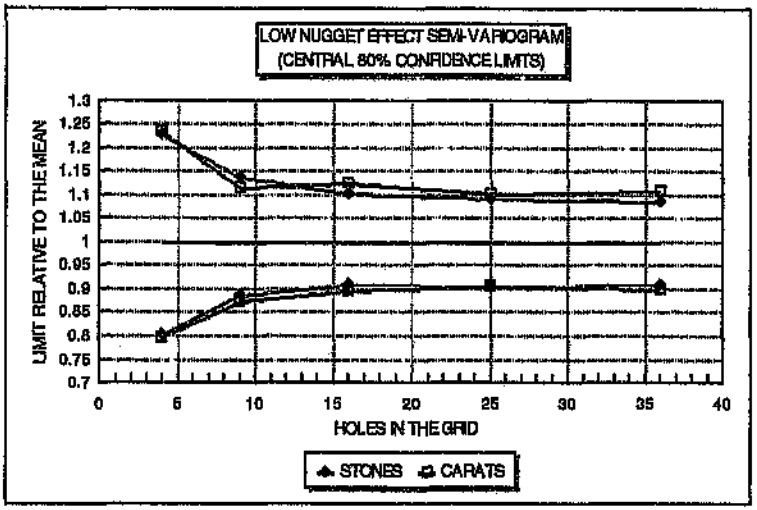


Figure 5.3: Low nugget semi-variogram model showing the central 80% confidence limits for different grids for SPM3 (stones) and CPM3 (carats).

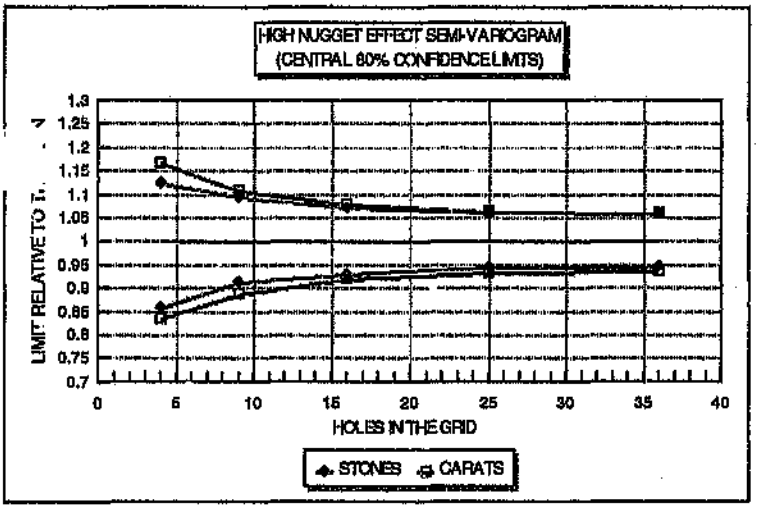


Figure 5.4: High nugget semi-variogram model showing the central 80% confidence limits for different grids

12m samples each, are required to achieve a lower 90% confidence limit within 10% of the "true" global mean (SPM3). Alternatively, with 12 holes in the grid, the sample grade in SPM3 will be 8 out of 10 times within 10% of the "true" global mean of the body sampled.

If the results of the simulation are converted to CPM3 then the number of holes required, for the same level of confidence, is increased to 16.

As the results of the evaluation will be regarded in terms of CPM3 or carats per hundred tons (CPHT) then the higher figure of 16 holes should be regarded as the minimum number of holes for the 10% level of confidence required.

Figure 5.4 shows the results for the high nugget semi-variogram. The results indicate that as few as 8 holes are required to achieve a lower 90% confidence limit within 10% of the "true" global mean (SPM3). If the results of the simulation are converted to CPM3 then the number of holes required is increased to 12.

5.4 The effect of increasing sample size

This section examines the effect of sample size on the confidence in the global mean.

5.4.1 Method

In this section large samples are generated at the nodes of a sample grid by generating groups of unit samples. For example a 0.9m x 0.9m x 12m sample is generated by simulating 3 by 3 unit samples adjacent to one another at the nodes of the sample grid.

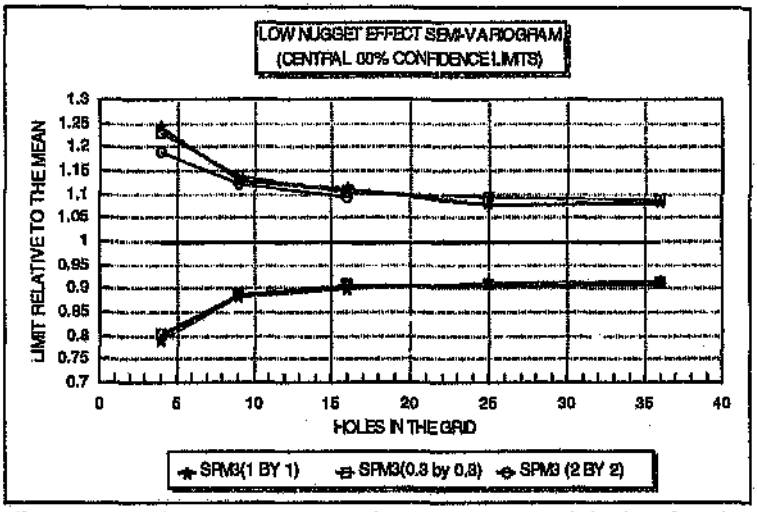


Figure 5.5: Low nugget semi-variogram model showing the central 80% confidence limits for different grids and different sample sizes

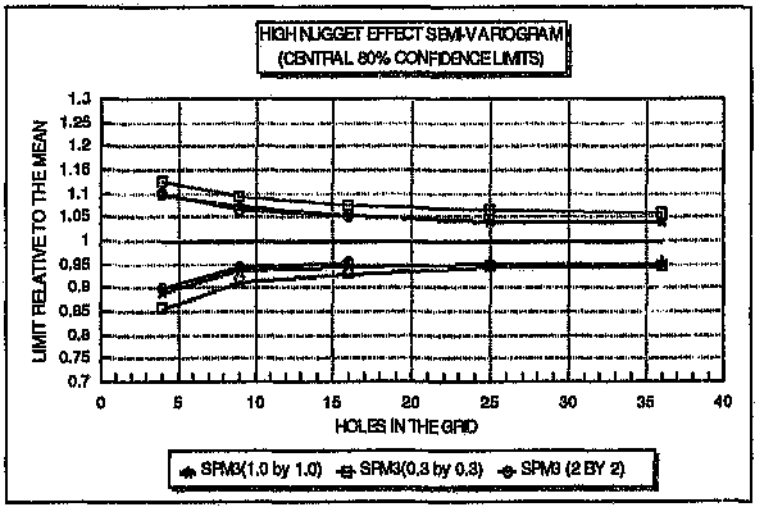


Figure 5.6: High nugget semi-variogram model showing the central 80% confidence limits for different grid and different sample sizes

Two larger sample sizes were generated: 0.9m x 0.9m x 12m, consisting of 3 by 3 unit samples and 2.1m x 2.1m x 12m, consisting of 7 by 7 unit samples.

These larger samples were generated for the 2 x 2 grid (holes 150m apart), the 3 x 3 grid (holes 100m apart) and the 4 x 4 grid (holes 75m apart), described in section 5.3.

For each simulation a global grade, in SPM3, is calculated by averaging all samples in the grid. The simulation is repeated 100 times generating one hundred mean values. The 100 mean values are ranked and the upper and lower 90% confidence intervals are taken as the 10th and 90th m[illegible] value in the ranked data. This process is repeated for the high and [illegible] semi-variogram models.

5.4.2 Results

In Figures 5.5 and 5.6 the central 80% confidence limits around the global mean are presented for each grid and for three sample sizes. As before the upper and lower limits are plotted relative to the average of the 100 simulations run for each grid. The simulation results in stones per sample (SPS) and carats per sample (CPS) have been normalised to grade in stones per cubic metre (SPM3) and carats per cubic metre (CPM3) by dividing each sample result by the sample volume.

Figure 5.5 presents the low nugget semi-variogram. The increase in size of sample has not reduced the upper and lower confidence limits to any practical degree. In contrast, moving to a larger sample size with the high nugget semi-variogram (Figure 5.6) has reduced the confidence limits. For the 10% confidence interval discussed the number of holes required for a

0.9m x 0.9m sample is 4 holes compared to 8 holes for the unit sample of 0.3m x 0.3m. If the sample size is increased to 2.1m x 2.1m in size there appears to be no practical decrease in confidence limits when compared to the 0.9m x 0.9m sample.

5.4.3 Discussion

Despite the 0.9m x 0.9m sample being 9 times greater than a single sample there is no practical improvement in the confidence of the global mean for the low nugget semi-variogram. This appears incorre t as the variability of large samples would normally be less than the variability of small samples.

To explain the small change in limits consider Krige's relation (David 1982, p.97):

$$VAR(v/D) = VAR(v/V) + VAR(V/D)$$

Where v is a drill hole, D is the deposit and V is a large sample.

From this relation the low nugget semi-variogram result is only possible if VAR(v/V) is small relative to VAR(V/D).

To test this 100, 0.9m x 0.9m x 12m samples were simulated on a regular 50m grid. Each large sample consisted of 9, 0.3m x 0.3m x 12m samples. Analysis of the simulation for each of the terms in Kriges relation gave:

$$354 \approx 57 + 298$$

Where VAR(v/G) is the mean variance of the 9, 100 sample sets generated in the simulation and VAR(v/V) is the mean variance of 100, 9 sample sets

and VAR(V/G) is the variance of the 100 samples, 0.9m x 0.9m x 12m in size. All variances relate to the grade variable SPM3. The analysis indicates that, as suggested, the term VAR(v/V) is small relative to VAR(V/G).

The low value for the VAR(v/V) term is the result of the high degree of correlation between samples at small distances.

If the same simulation is carried out for the high nugget semi-variogram we have:

$$337 \approx 228 + 115$$

In this case the VAR(D/C) term is large relative to VAR(C/G).

5.5 The effect of decreasing sample size

5.5.1 Method

In the experiments that follow we sample a simulation with the spatial and statistical parameters of the high and low nugget semi-variogram models used earlier in this chapter.

As the Cox simulation is based on simulating samples equivalent in size to the evaluation programme, in this case 0.3m by 0.3m by 12m, a direct simulation of smaller samples cannot be carried out.

To over come this it was necessary to develop an indirect approach to the sampling problem. The method adopted was as follows:

1 For this experiment the grid consisted of 12 holes on a 50m grid with 10 samples per hole. Each vertical sample was 12m in length.

The grid of 12 holes and 10 samples will provide a global estimate with the central 80% confidence limits within 10% of the "true" mean (see section 5.3.2).

2 The Cox simulation provides the number of stones at each sample location and the X, Y and Z of the sample centre.

These stones were distributed randomly within the 0.3m x 0.3m x 12m sample. For example, a sample consisting of 30 stones was transformed into 30 individual, randomly placed, X, Y and Z points each with a value of 1 stone.

The stones are distributed randomly within the sample as no information is available on how the stones are distributed at a scale smaller than the sample size.

3 Once stage two is complete the simulation was sampled at a scale smaller than the unit sample. This is done by searching for stones within the required sample size.

Sampling was carried out for hole diameters of 12", 6" and 3".The sample length of 12m was kept constant.

4 In the final stage a carat weight was added to each stone sampled using a Monte Carlo algorithm and the stone size distribution appropriate to the deposit.

Using the above, one hundred simulations were carried out for each of the three sample sizes and the process was repeated for the high and low semi-variogram models.

5.5.2 Results

The results were converted from SPS to SPM3 and from CPS to CPM3 for further analysis.

Figure 5.7 shows the central 80% confidence limits for 3", 6" and 12" samples from the high nugget and low nugget effect semi-variogram models.

The central 80% confidence limits increase from 10% to almost 50% as the sample size decreases in size from 12" to 3" in diameter. The greatest change occurs as the sample moves from 6" to 3".

The low nugget effect semi-variogram, as seen before, has wider confidence limits than the high nugget effect semi-variogram.

Figures 5.8 and 5.9 the compare the SPM3 results with the corresponding CPM3 results. For the high nugget semi-variogram (Figure 5.8) the effect of adding a stone weight to each stone increases the upper confidence limit slightly but made little difference to the lower limit.

For the low nugget semi-variogram (Figure 5.9) both the upper and lower limits were increased.

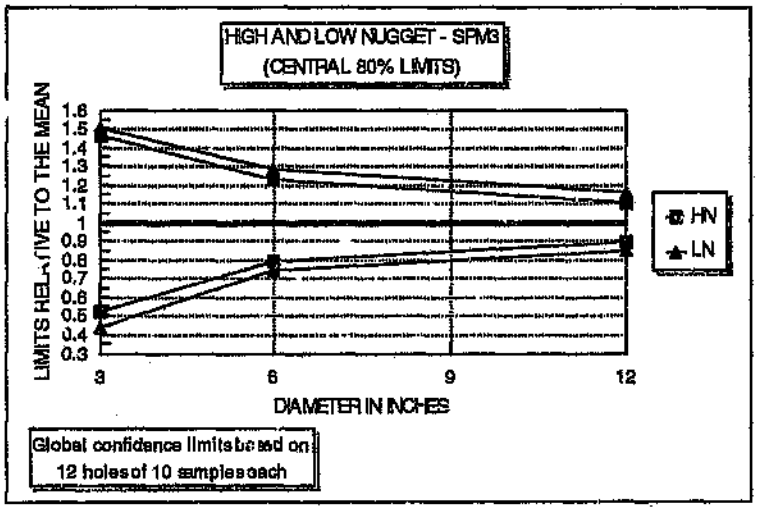


Figure 5.7: High and low nugget effect models showing the central 80% confidence limits for a three, six and twelve inch diameter sample. All samples are 12m in length.

Another way to interpret the results is to examine the probability of exceeding a given economic cutoff.

Figure 5.10 plots, for the simulation carried out, the ratio of the economic cutoff to global mean on the X axis and the probability of exceeding the economic cutoff on the Y axis for the 3", 6" and 12" sampling.

If it was necessary to be at least 95% sure that the economic cutoff was exceeded then, for this particular deposit and for a ratio of 0.6, 12 **six inch diameter holes** would have been sufficient. However, if the ratio is 0.8, then only the 12" diameter drilling would be acceptable. If the ratio is reduced to 0.9 then none of the drilling would match the desired level of confidence. In such a case a denser drill grid would be required or larger samples with the same grid.

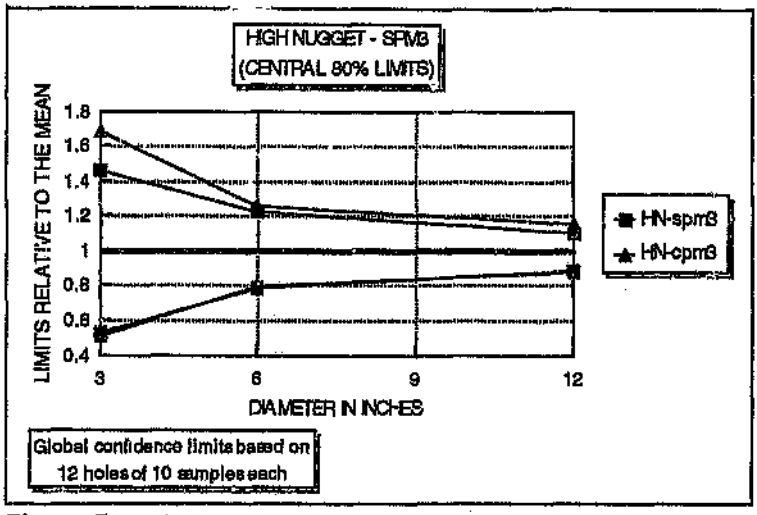


Figure 5.8: High nugget effect model showing the central 80% confidence limits in SPM3 and CPM3 for a three, size and twelve inch diameter sample. All samples are 12m in length.

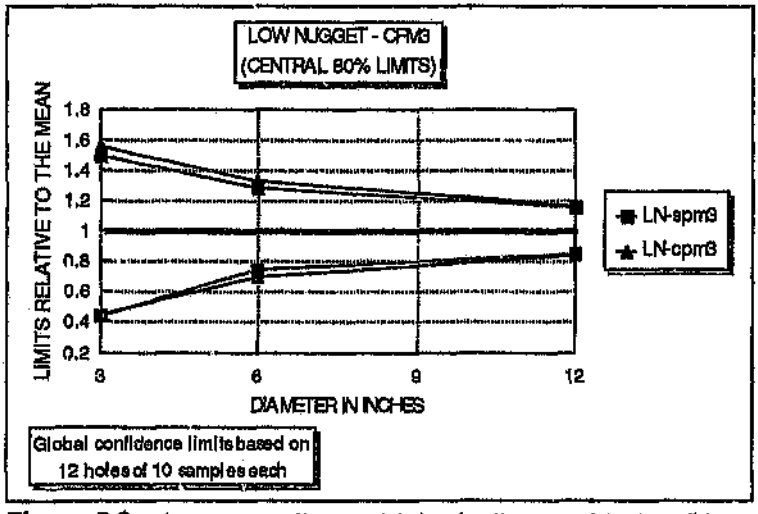


Figure 5.9: Low nugget effect model showing the central 80% confidence limits in SPM3 and CPM3 for a three, size and twelve inch diameter sample. All samples are 12m in length.

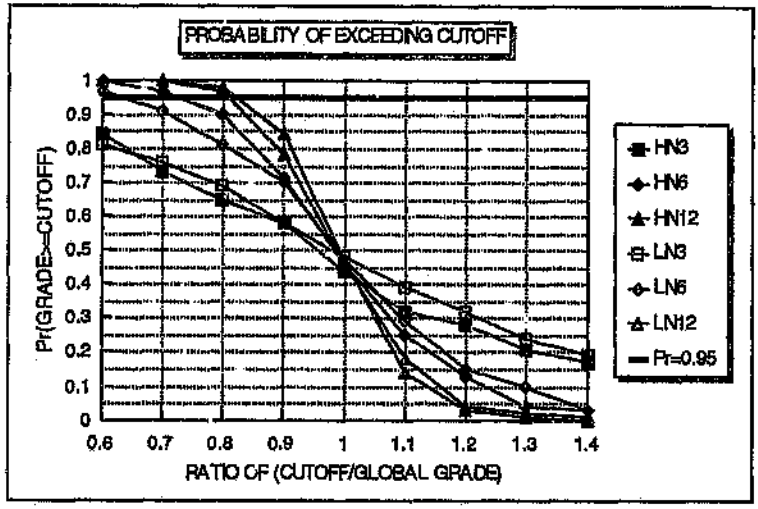


Figure 5.10: The probability of exceeding a cutoff for samples of three, six and twelve inches for the high and low nugget effect models. The cutoff is expressed as the ratio of the cutoff to the mean grade.

5.6 Chapter conclusion

The following points have emerged from this chapter:

- The high nugget semi-variogram model results in a narrower confidence limit than the low nugget semi-variogram model
- For the low nugget model at least 12 holes are required to allow a lower 90% confidence limit within 10% of the "true" global mean value. This is for a grade unit in SPM3. If the grade unit is in CPM3, as is more usually the case, then the number of holes required is 15.
- For the low nugget model the number of holes required are 8 and 12 respectively.
- Increasing the sample size up to 9 times the original sample volume had little effect on the confidence limits for the low nugget semi-variogram model. This is the result of the high degree of correlation between samples at small distances.

- In contrast, there was a significant narrowing of the confidence limits when the high nugget model was used. In the case tested the number of holes could be halved while achieving the same degree of confidence (8 holes could be reduced to 4).
- As might be expected, a smaller sample size results in wider confidence limits.
- In considering the design of the sampling protocol the ratio of the mean value of the deposit to the "pay limit" could be considered. For instance, it may be sufficient to be 95% sure that the "pay limit" is met or exceeded rather than have the global mean of the deposit estimated to within 15%.

This chapter has used the Cox simulation method to investigate the variability associated with the global estimation. In the next chapter the same low and high nugget effect models are used to investigate the effect on local estimation.

CHAPTER 6

THE EFFECT OF SAMPLE SIZE ON LOCAL ESTIMATION

The only way to save yourself from
the pain of lost illusions is to have
none
C Marriott

In this chapter we will :

- Examine the effect of **sample size** on the confidence interval around a defined mining block

6.1 Introduction

In the previous chapter the effect of sample density and sample size on global grade estimation was examined. In this chapter the exercise is extended to local estimates of grade. Local estimates of grade are required in the pre-feasibility or feasibility studies of an evaluation for detailed pit designs and estimates of the carat recovery. In an existing mine such estimates are used to schedule carats recovered in monthly, yearly or five yearly plans. To date there has been very little investigation of the degree of confidence that can be attached to local estimates (see Kleingeld 1987).

6.2 Method

The Cox simulation is used to estimate the confidence limits for local block estimates assuming a given sample configuration and ordinary kriging.

Samples larger than the unit sample size are constructed by si. 'ating samples adjacent to one another. For example, a 1m square sample is generated by simulating 9 samples in a 3 x 3 matrix centred on the X, Y and Z location of the sample.

The simulated values are used to calculate the variance of the error (Z* - Z) for a block, where Z* is the local block estimate using ordinary kriging and Z is the true grade of the block. The distribution of (Z* - Z) is used to estimate the confidence interval for the block.

Confidence limits were estimated for a 50m x 50m x 12m mining block. The grade of the block, Z*, was estimated using ordinary kriging. The true grade of the block, Z, was taken as the average of 100 samples equally spaced within the mining block.

The estimate of Z* was carried out using 27 samples located on a 50m x 50m x 12m sample grid. The mining block to be estimated is situated at the centre of the 27 samples with one sample lying at the centre of the mining block (see Figures 6.1 and 6.2).

This size of mining block and this sample configuration is similar to that used by diamond mines visited by the author[1] and was selected so that the results would be of interest to existing operations and feasibility studies.

---

1 Venetia, Orapa, Letlhakane and Jwaneng diamond mines.

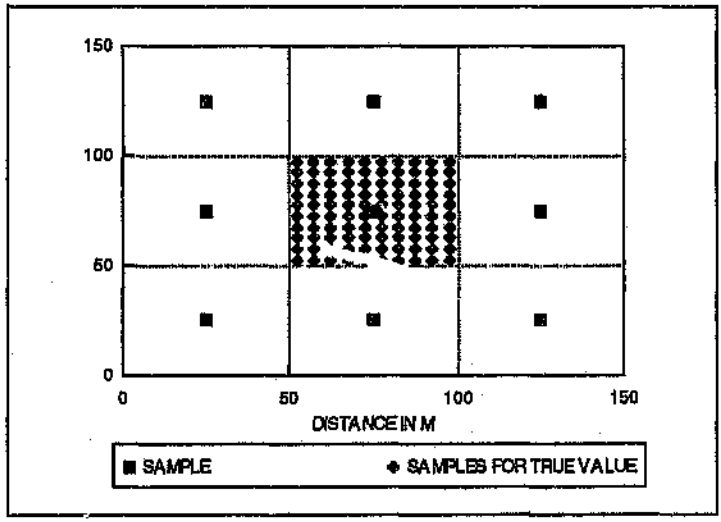


Figure 6.1: Plan view of the kriging neighbourhood showing the sample points surrounding the block to be kriged and the samples used to estimate the "true" value of the block to be kriged.

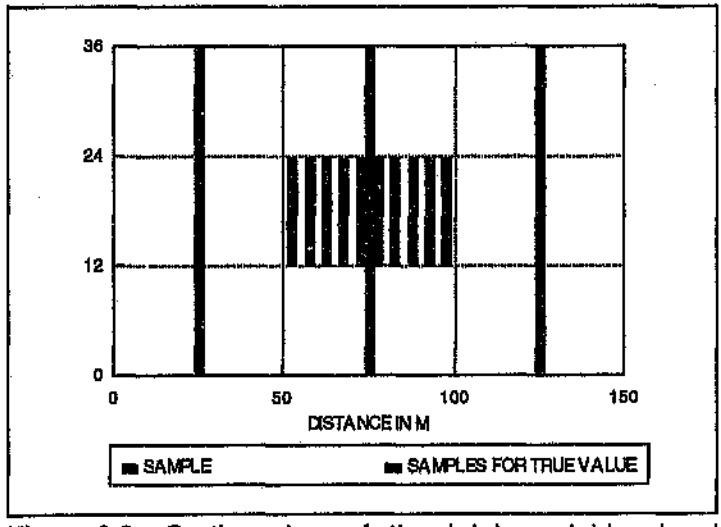


Figure 6.2: Section view of the kriging neighbourhood showing the samples surrounding the block to be kriged and the samples used to estimate the "true" value of the kriged block.

To obtain the confidence interval of (Z*-Z) the mining block and surrounding samples were simulated 500 times. For each realisation the difference (Z*-Z) was calculated generating 500, (Z*-Z) values. These differences were ranked and the 10th and 90th percentile values used to estimate central 80% confidence limits.

The steps of the simulation were as follows:

1 The X, Y and Z grid nodes were prepared for the 27 points in the kriging neighbourhood and the 100 points representing the block to be kriged.

A single point at each grid node was used to represent a single 0.3m x 0.3m x 12m sample. Larger samples were represented by grouping the required number of unit samples around the X, Y and Z grid nodes. For example, a $0.8m^2$ sample is generated by simulating 9 unit samples in a 3 by 3 matrix centred on the X, Y, and Z location of each sample grid node.

Six different sample sizes were simulated, namely: $0.09m^2$ represented by a single unit sample, $0.8m^2$ represented by 3 x 3 unit samples, $4.4m^2$ represented by 7 x 7 unit samples, $10.9m^2$ represented by 11 x 11 unit samples, $26m^2$ represented by 17 x 17 unit samples and $98m^2$ represented by 33 x 33 unit samples.

2 As the number of samples in the kriging neighbourhood are fixed the kriging weights to be applied to each sample were pre-calculated, for the semi-variogram appropriate to each sample size, and added to the X, Y and Z node information.

The semi-variogram of the 0.3m x 0.3m x 12m sample data was regularised to take into account the increased size of the samples, and appropriate weights calculated. This calculation is described below.

3 The simulation was repeated 500 times using the high and low nugget effect semi-variogram models.

6.3 The calculation of weights for each sample size

In order that Z^* can be calculated in the simulation a weight appropriate to each sample location must be calculated. The weight is dependant on the semi-variogram at the correct support size, the sample to sample relationship, the sample to block relationship and the size and shape of the block to be estimated.

The semi-variogram at each support size was estimated using the cube semi-variogram (see 4.7.10). For instance, the semi-variogram of a sample support consisting of 3 by 3 unit samples was estimated by regularising the cube semi-variogram to this sized support. A special program was written to achieve this regularisation.

This section describes the estimation of nugget effect, the estimation of range, the method of calculation and the semi-variogram parameters for each sample size.

6.3.1 Nugget effect

Using the "white noise" model for the nugget effect it can be shown (Journel and Huijbregts 1978, pp.152-157) that the nugget effect of a grade variable with support v is given by:

$$\theta(v) = A/v \qquad (6.1)$$

Where A is the nugget constant. Similarly the nugget effect of a grade variable with support V is given by:

$$\theta(V) = A/\sqrt{V} \qquad (6.2)$$

Combining (6.1) and (6.2) we arrive at :

$$\theta(V) = \theta(v) * v/V \qquad (6.3)$$

Where $\theta(V)$ is the unknown nugget effect at a support V and $\theta(v)$ is the known nugget effect at a smaller support v.

The regularisation of the nugget effect for the variable stones per sample can be considered as follows.

Lets suppose that the grade is reduced to a pure nugget effect. Then the variance of the grade, at a support v, is given by:

$$VAR(Z(v)) = A/v \qquad (6.4)$$

The relation between grade, Z(v), and the number of stones per sample, N(v), is:

$$N(v) = v * Z(v) \qquad (6.5)$$

Using (6.4) and (6.5) we can then draw the relationship:

$$\begin{aligned} VAR(N(v)) &= VAR(v * Z(v)) \\ &= v^2 * A/v \\ &= A * v \end{aligned} \qquad (6.6)$$

Applying the same logic as for grade we arrive at:

$$\theta(V) = \theta(v) * V/v \qquad (6.7)$$

As the sample size increases the nugget effect increases by the factor V/v. Conversely if the sample size decreases the nugget effect decreases.

6.3.2 The range

As the support size increases so allowance must be made for changes in the range of the semi-variogram. The method adopted here is based on the method described in Journel and Huijbregts (1978, P84) in which the range of a regularised core sample changes according to the relation:

$$A = OA + L \qquad (6.8)$$

Where A is the new range, OA is the range of the unit sample semi-variogram model and L is the length of the regularised core.

The length of the samples (12m in the case of Deposit One) does not change so no correction was made to the vertical ranges calculated. However, as the sample expands laterally the horizontal range will change.

A sample size measuring 10m by 10m by 12m will have a range of 80m in the horizontal direction compared to the present 90m estimated for the unit sample of 0.3m by 0.3m by 12m from the vertical semi-variogram. The range

was calculated by assuming that independence between two samples in the horizontal plane is achieved at 80m. As the sample size is 10m across then applying the formula above we have:

$$A = 80 + 10 = 90 \qquad \textbf{(6.9)}$$

This methodology was applied to the sample supports used in the experiment. The ranges used to calculate the weights are shown in Table 6.1

Note that these ranges were only used in the Kriging process. The original ranges were used in the simulation program as large samples are made up by simulating unit samples of 0.3m x 0.3m x 12m.

6.3.3 Estimation of the total sill of the semi-variogram

A program was especially written to estimate the semi-variogram models for rectangular samples of any size.

The regularisation of a grade variable is described in Journel and Huijbregts (1978, pp.77- 78) and is given by:

$$G_v(H) = G(v,v_h) - G(v,v) \qquad \textbf{(6.10)}$$

Where $G_v(H)$ is the stones per sample semi-variogram at the larger support, $G(v,v_h)$ is the **average** semi-variogram value at the smaller support and $G(v,v)$ is the **average** semi-variogram value within the block.

SIZE IN 0.3m BY 0.3m UNITS	VERTICAL RANGE IN M	HORIZONTAL RANGE IN M
1,1	89.00	80.00
3,3	89.00	80.90
7,7	89.00	82.10
11,11	89.00	83.30
17,17	89.00	85.10
33,33	89.00	89.90

Table 6.1: Semi-variogram ranges

SIZE IN 0.3m BY 0.3m UNITS	NUGGET EFFECT	SILL	TOTAL SILL
1,1	286.40	73.56	359.96
3,3	31.85	73.48	105.33
7,7	5.86	73.16	79.02
11,11	2.38	72.71	75.09
17,17	1.00	71.86	72.86
33,33	0.27	69.11	69.38

Table 6.2: Semi-variogram parameters (spherical model) for th[illegible]h nugget semi-variogram model

A similar relation can be derived for the variable stones per sample:

$$S_v(H) = S(v,v_h) - S(v,v) \qquad \textbf{(6.11)}$$

Where $S_v(H)$ is the stones per sample semi-variogram at the larger support, $S(v,v_h)$ is the **summed** semi-variogram value at the smaller support and $S(v,v)$ is the **summed** semi-variogram value within the block.

The steps required to estimate the total sill are as follows:

1 The stones per sample semi-variogram is used to obtain the cube semi-variogram.

2 The cube semi-variogram is used to obtain the nugget effect and total sill of supports of differing sizes. This can be done in both stones per sample and stones per cubic metre.

The conversion from stones per sample to stones per cubic metre is obtained by multiplying the stones per sample variance by $1/v^2$.

3 The semi-variogram parameters, block size and sample locations are used to obtain a kriging weight for each of the 27 samples used.

6.3.4 Calculated semi-variogram parameters and sample weights

The semi-variogram values for differing sizes are given in Tables 6.2 and 6.3 for the low and high nugget semi-variograms respectively.

The kriged weights per sample are summarised in Tables 6.4 and 6.5.

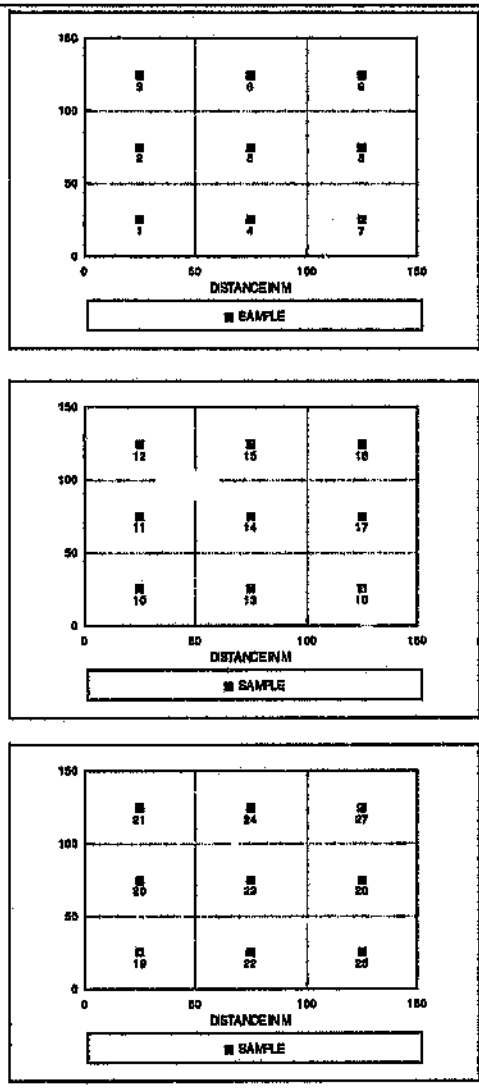


Figure 6.3: Sample numbering for the three levels of the kriging neighbourhood. The lowest level (6m) is top most, the intermediate level (18m) is next and the top level (30m) is at the bottom.

SIZE IN 0.3m BY 0.3m UNITS	NUGGET EFFECT	SILL	TOTAL SILL
1,1	67.05	291.32	358.37
3,3	7.55	290.99	298.54
7,7	1.45	289.70	291.15
11,11	0.62	287.90	288.52
17,17	0.28	284.57	284.85
33,33	0.09	273.66	273.75

Table 6.3: Semi-variogram parameters (spherical model) for the low nugget semi-variogram model

6.4 Results

The results of the experiment are presented in Tables 6.6 and 6.7 and Figures 6.1 and 6.2.

From the results of the experiment the following points are evident:

- Both the low nugget and high nugget semi-variograms show a rapid decrease in the variance of (Z*-Z) with increasing size.
- the rate of decrease becomes small after a sample size of approximately 1m by 1m.
- The variance of (Z*-Z) for the high nugget effect semi-variogram decreases more rapidly than the low nugget semi-variogram and attains a lower final variance.

No.	High nugget					
	1,1,40	3,3,40	7,7,40	11,11,40	17,17,40	33,33,40
1	0.0211	0.0061	0.0034	0.0027	0.0018	-0.0005
2	0.0364	0.0291	0.0246	0.0237	0.0235	0.0243
3	0.0211	0.0061	0.0034	0.0027	0.0018	-0.0005
4	0.0364	0.0291	0.0246	0.0237	0.0235	0.0243
5	0.1022	0.1868	0.2077	0.2088	0.2081	0.2048
6	0.0364	0.0291	0.0246	0.0237	0.0235	0.0243
7	0.0211	0.0061	0.0034	0.0027	0.0018	-0.0005
8	0.0364	0.0291	0.0246	0.0237	0.0235	0.0243
9	0.0211	0.0061	0.0034	0.0027	0.0018	-0.0005
10	0.0203	0.0051	0.0031	0.0028	0.0026	0.0022
11	0.0365	0.0290	0.0252	0.0252	0.0258	0.0280
12	0.0203	0.0051	0.0031	0.0028	0.0026	0.0022
13	0.0365	0.0290	0.0252	0.0252	0.0258	0.0280
14	0.1090	0.2091	0.2474	0.2596	0.2677	0.2791
15	0.0365	0.0290	0.0252	0.0252	0.0258	0.0280
16	0.0203	0.0051	0.0031	0.0028	0.0026	0.0022
17	0.0365	0.0290	0.0252	0.0252	0.0258	0.0280
18	0.0203	0.0051	0.0031	0.0028	0.0026	0.0022
19	0.0211	0.0061	0.0034	0.0027	0.0018	-0.0005
20	0.0364	0.0291	0.0246	0.0237	0.0235	0.0243
21	0.0211	0.0061	0.0034	0.0027	0.0018	-0.0005
22	0.0364	0.0291	0.0246	0.0237	0.0235	0.0243
23	0.1022	0.1868	0.2077	0.2088	0.2081	0.2048
24	0.0364	0.0291	0.0246	0.0237	0.0235	0.0243
25	0.0211	0.0061	0.0034	0.0027	0.0018	-0.0005
26	0.0364	0.0291	0.0246	0.0237	0.0235	0.0243
27	0.0211	0.0061	0.0034	0.0027	0.0018	-0.0005
	1.0006	1.0007	1.0000	1.0004	0.9999	0.9999

Table 6.4: Sample weights calculated for each sample size (high nugget effect semi-variogram model). The size is in unit samples of 0.3m by 0.3m by 0.3m. The sample number is given in the left hand column (see Figure 6.3).

No.	Low nugget					
	1,1,40	3,3,40	7,7,40	11,11,40	17,17,40	33,33,40
1	0.0050	0.0034	0.0030	0.0025	0.0018	-0.0006
2	0.0267	0.0233	0.0229	0.0229	0.0231	0.0242
3	0.0050	0.0034	0.0030	0.0025	0.0018	-0.0006
4	0.0267	0.0233	0.0229	0.0229	0.0231	0.0242
5	0.1994	0.2101	0.2103	0.2091	0.2081	0.2047
6	0.0267	0.0233	0.0229	0.0229	0.0231	0.0242
7	0.0050	0.0034	0.0030	0.0025	0.0018	-0.0006
8	0.0267	0.0233	0.0229	0.0229	0.0231	0.0242
9	0.0050	0.0034	0.0030	0.0025	0.0018	-0.0006
10	0.0041	0.0033	0.0031	0.0029	0.0027	0.0022
11	0.0263	0.0240	0.0241	0.0249	0.0257	0.0280
12	0.0041	0.0033	0.0031	0.0029	0.0027	0.0022
13	0.0263	0.0240	0.0241	0.0249	0.0257	0.0280
14	0.2253	0.2563	0.2631	0.2678	0.2717	0.2805
15	0.0263	0.0240	0.0241	0.0249	0.0257	0.0280
16	0.0041	0.0033	0.0031	0.0029	0.0027	0.0022
17	0.0263	0.0240	0.0241	0.0249	0.0257	0.0280
18	0.0041	0.0033	0.0031	0.0029	0.0027	0.0022
19	0.0050	0.0034	0.0030	0.0025	0.0018	-0.0006
20	0.0267	0.0233	0.0229	0.0229	0.0231	0.0242
21	0.0050	0.0034	0.0030	0.0025	0.0018	-0.0006
22	0.0267	0.0233	0.0229	0.0229	0.0231	0.0242
23	0.1994	0.2101	0.2103	0.2091	0.2081	0.2047
24	0.0267	0.0233	0.0229	0.0229	0.0231	0.0242
25	0.0050	0.0034	0.0030	0.0025	0.0018	-0.0006
26	0.0267	0.0233	0.0229	0.0229	0.0231	0.0242
27	0.0050	0.0034	0.0030	0.0025	0.0018	-0.0006
	0.9993	0.9993	0.9997	1.0004	1.0007	0.9995

Table 6.5: Sample weights calculated for each sample size (low nugget effect semi-variogram model). The size is in unit samples of 0.3m by 0.3m by 0.3m. The sample number is given in the left hand column (see Figure 6.3).

- The largest decrease occurs for the high nugget semi-variogram when moving from a unit size on 0.3m by 0.3m to a sample size of 0.9m by 0.9m.
- The "90th percentile of |Z*-Z|/Z" (see Table 6.8) indicates the relative difference below which 90% of the values lie. In other words, for the high nugget effect semi-variogram and a unit sized sample, 90% of the blocks estimated were within 25% of the true block value.
- The variance of (Z*-Z) for the high nugget semi-variogr decreases by approximately 86% on moving from a unit sized sample to a sample 10m by 10m. This compares to a drop of 50% for the low nugget semi-variogram model.

6.5 Discussion

The results show that, for the sample configuration chosen, 90% of the blocks differ from their true block values by less than 25% if a unit sized sample is used and a high nugget semi-variogram is expected (Table 6.8). This values improves to 9% if a 10m by 10m sample is adopted.

It has been suggested by some authors that the monthly or yearly variation in the expected mineral is the measure by which a mineral resource should be classified. For instance, for a measured resource, the level of confidence in the estimates should be such that the amount of mineral recovered over a month is known within 15%. If a global grade is known or local block estimates result in a variation in the mineral recovered in excess of 15% in one month, but less than 15% in one year, then the resource is classified as indicated. If the variation in mineral recovered is expected to be greater than 15% in a year then the resource is classified as inferred[2].

---

2 It is suggested that these error margins are taken at the 90% confidence interval.

SIZE IN 0.3m BY 0.3m UNITS	Mean of (Z*-Z)	VAR(Z*)	VAR(Z*-Z)	Kriging variance	Kriging VAR(Z*)	Slope Z/Z*
1,1	-0.290	35.5	29.5	28.3	30.3	0.688
3,3	-0.071	30.2	11.7	9.2	32.2	0.978
7,7	-0.093	33.9	8.7	5.6	34.5	1.002
11,11	0.121	30.2	7.3	4.9	35.1	1.005
17,17	0.195	29.8	7.7	4.6	35.4	1.007
33,33	0.133	32.8	4.1	4.1	35.7	1.007

Table 6.6: Simulated values compared to kriging values for the high nugget semi-variogram model.

SIZE IN 0.3m BY 0.3m UNITS	Mean of (Z*-Z)	VAR(Z*)	VAR(Z*-Z)	Kriging variance	Kriging VAR(Z*)	Slope Z/Z*
1,1	-0.180	125.7	25.3	28.9	130.6	0.991
3,3	0.030	139.8	21.6	19.8	137.1	1.005
7,7	0.040	139.9	19.7	18.6	138.9	1.007
11,11	0.120	121.8	18.1	18.1	139.8	1.007
17,17	0.190	133.8	18.1	17.5	140.8	1.007
33,33	-0.310	130.2	12.4	16.0	141.6	1.007

Table 6.7: Simulated values compared to kriging values for the low nugget semi-variogram model.

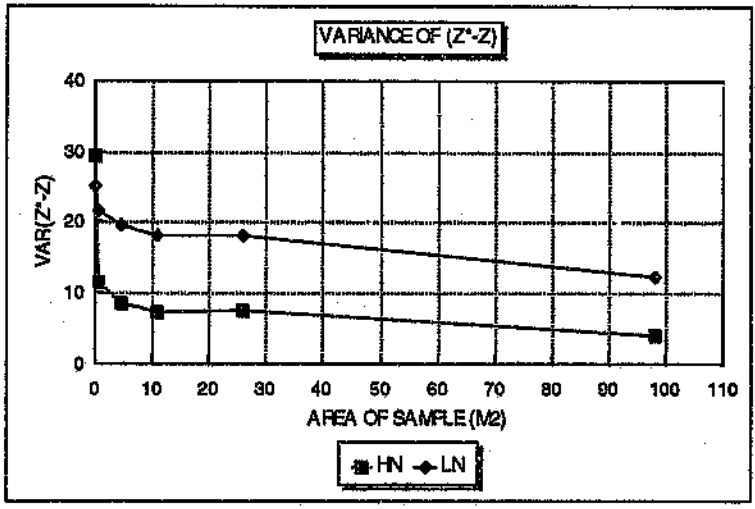


Figure 6.4: Variance of (Z*-Z) for the high and low nugget models against the area of the sample (0m^2 to 110m^2)

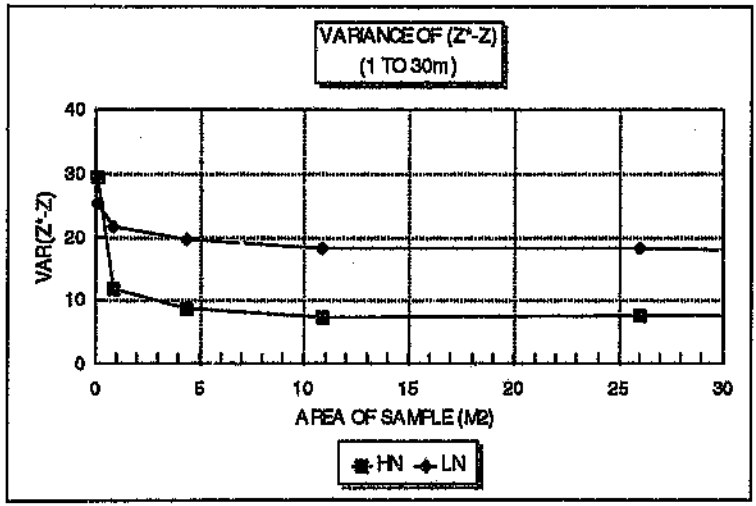


Figure 6.5: As for Figure 6.4 except the X axis has been limited to 0m^2 to 30m^2 to allow more detail.

SIZE IN 0.3m BY 0.3m UNITS	High nugget 90 th PERCENTILE IZ*-ZI/Z	Low nugget 90 th PERCENTILE IZ*-ZI/Z
1,1	0.246	0.220
3,3	0.157	0.220
7,7	0.130	0.190
11,11	0.122	0.200
17,17	0.122	0.190
33,33	0.095	0.170

Table 6.8: The "90th percentile of IZ*-ZI/Z indicates the relative difference below which 90% of the values lie. In other words, for the high nugget semi-variogram and a unit sized sample, 90% of the blocks estimated were within 25% of the true block value.

If 90% of individual blocks are to be estimated to within 15% of their true block value then a sample size of, at least 3 by 3 unit samples is required (0.9m by 0.9m) for the high nugget semi-variogram. With the low nugget semi-variogram a sample size larger than 10m by 10m is required.

Of course, in practice several blocks are mined together during one month. If we assume that six blocks are mined and they are, for illustration purposes, independent from one another then the mean of the six blocks would be $\sum Z_i/6$ and the 90% relative error of the combined blocks would be approximately 10%. If variation in the amount of predicted mineral was the only criteria considered then the data configuration chosen would suggest

that monthly production from the high nugget semi-variogram could be classified as measured.

6.6 "Cluster" sampling

The results in section 6.4 (Tables 6.6 and 6.7) indicated that a sample size of 9.9m by 9.9m by 12m (rounded for discussion to 10m by 10m by 12m) would reduce the variance of (Z^*-Z) by as much as one seventh for the high nugget semi-variogram and one half for the low nugget semi-variogram. In practice, we do not have a sample tool that can drill such a large sized sample. An alternative, suggested in Kleingeld 1992, is to replace the larger sample with a number of smaller, more practically sized samples, which are "clustered" within the larger sample area.

To test the number of 0.3m by 0.3m samples that would be required to represent a 10m square sample the following exercise was carried out. Samples (0.3m by 0.3m by 12m) were simulated on a regular grid within a 10m by 10m by 12m volume. After each simulation the grade of the block, in SPM3, was calculated and the simulation repeated. After 1000 simulations the variance of block estimates was measured and taken as an indication of the dispersion variance of the 10m block based on 2, 4, 9 or 16 samples (Journel and Huijbregts,1978, p.65).

The results for the low and high nugget semi-variogram models are shown in Figure 6.3.

Figure 6.3 suggests, for the low nugget semi-variogram model, that as few as 4, 0.3m by 0.3m samples are required to obtain the dispersion variance of the 10m by 10m sample.

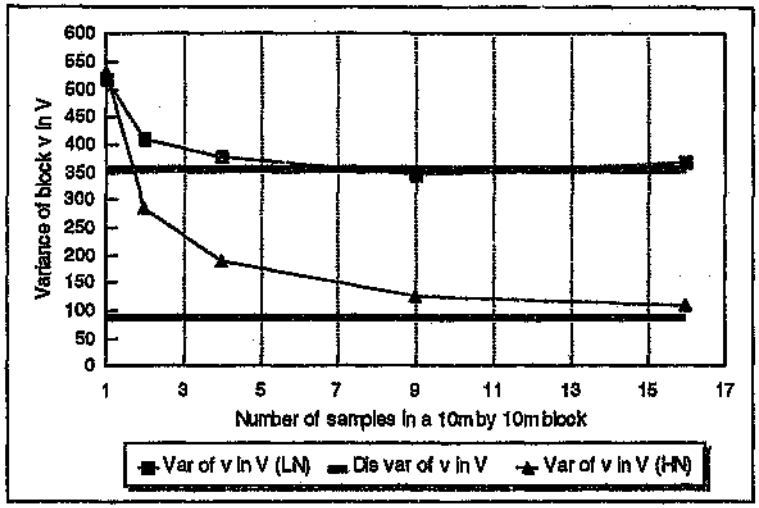


Figure 6.6: Variance of blocks based on 2, 4, 9 and 16 samples compared to the theoretical estimation variance of a 10m block for the high and low nugget semi-variogram models.

For the high nugget semi-variogram model the variance of Z* fails to reach the theoretical dispersion variance after 16 samples, although the variance has been reduced to less than half by 4 samples.

The results indicate, for the situation investigated, that benefit could be gained from the "clustering" of practically sized samples in order to achieve the variance reduction of a larger 10m sample. This is particularly the case if the spatial correlation is high.

It should be kept in mind that in practice it would be difficult to place more than 4 holes in a 10m by 10m area due to physical problems such as "blow back[3]".

---

3 "Blow back" refers to a loss of air pressure during drilling as air travelling through cracks in the rock is lost in adjacent drill holes.

6.7 Chapter conclusion

The results of this chapter indicate that, for local block estimates, and for the cases discussed, a benefit is gained in both the low and high nugget models by going to larger sample sizes. As for the global estimates, the benefit is greater for the high nugget model than for the low nugget model.

Table 6.8 indicates that, for the unit sample size, 90% of blocks estimated will be within 25% of the true value for both the low and high nugget models.

If it were possible to take a sample 9.9m by 9.9m (33 by 33 unit samples) then this could be improved to 17% for the high nugget model and 9% for the low nugget semi-variogram model.

The figure of 25% is wide if a single block is considered. However, if more than one block is mined (as is usually the case in a one month period) then this can be reduced. If six blocks are mined, and we assume independence between the blocks, then this figure can be reduced to 10%.

Finally, section 6.6 showed that a benefit could be gained from the "clustering" of 0.3m by 0.3m sized samples in order to achieve the variance reduction of a larger sample. This is particularly the case if the spatial correlation is high.

The previous two chapters have attempted to draw conclusions on how the sampling protocol can impact on global and local estimates. In the next chapter the Cox simulation is used to assess the impact of bottom cutoff on global and local estimates.

CHAPTER 7

THE EFFECT OF BOTTOM CUTOFF ON LOCAL AND GLOBAL ESTIMATION

In this chapter we :

- Examine the effect of the **bottom cutoff** on the confidence interval associated with global and local estimates
- We examine the viability of making a grade estimate using the grade over a **restricted part of the diamond size distribution**

7.1 Introduction

As mentioned in chapter 2 the bottom cutoff of the final production plant is often different from the bottom cutoff of the sampling plant. If the bottom cutoff of the production plant is known in advance an obvious question to ask is whether the sampling of the deposit should be carried out at the same bottom cutoff.

From an evaluation point of view the number of stones per sample is reduced if the bottom cut off is increased. In this chapter the Cox simulation is used to test the effect of change in the bottom cutoff on the confidence limits of global and local grade estimates.

The chapter begins with a description of the general approach, discusses an alterative method of estimating grade using a part of the complete diamond size distribution, outlines the experiment for global estimates, outlines the

experiment for local estimates and then concludes.

7.2 A general approach

The impact of the bottom cutoff was investigated from the following perspective:

The final estimate for the pipe is required at a 2mm bottom cutoff. Is it better to evaluate the pipe using sample data collected at a bottom cutoff of 1mm[1] or is it better to estimate the deposit directly at a 2mm bottom cutoff ?

From a mineral processing perspective the higher cutoff will result in cost savings relative to the plant at a 1mm cutoff. However, the advantage of estimating at a lower cutoff is that more stones per sample are collected.

To answer this question the Cox simulation was used to generate stones per sample for different sample grids where the original sampling had been carried out at a 1mm bottom cutoff.

The simulation parameters used are those of Deposit One described in chapters 4 and 5.

The samples generated using the Cox process were converted to carats per sample at a 1mm cutoff using the diamond size distribution for Deposit One. The samples were converted to grades, in carats per cubic metre, by dividing by a theoretical sample volume[2].

---

1 The estimate at 1mm is then adjusted to 2mm using the diamond size distribution.

2 We could have left the samples as carats per sample, however, it is easier to think in grade units.

The equivalent sample grades at a 2mm bottom cutoff were created by excluding stones (and therefore carats) below 2mm.

In addition to creating 1mm and 2mm grade estimates a third alternative was also considered. In the next section this additional option is motivated and discussed.

7.3 The creation of a sample grade between 1.5mm and 2.4mm

With the high cost of evaluating a kimberlite there is an ever increasing pressure "to do more with less". In its simplest terms this means evaluating a kimberlite with less sample information **while maintaining the same level of confidence in the final estimates.**

One way to reduce evaluation costs is to take smaller samples. Smaller samples are easier to take, quicker to extract and cheaper to treat. However, they contain fewer stones per sample and, particularly for local estimation, cannot give the same degree of local confidence as larger samples.

When sampling a kimberlite the usual objective is to obtain the grade of a sample above a specified bottom cutoff, for instance between 1mm and the maximum natural diamond size present in the deposit. An alternative approach is to sample for the grade of the deposit in a given size range, for instance between 1mm and 3mm. The proportion of stones that exist in this size range is usually high relative to the total size range. For Deposit One approximately 75% of the carats lie in this size range and 98% of the stones. The argument that follows is that less sample is required to estimate the grade in the 1mm to 3mm size range than is required to estimate the grade in the full size range.

The problem with the above approach is that we require the grade of the full size range above a given cutoff and not the grade of a restricted size range. However, if we know the diamond size distribution for the full size range we can correct the grade between 1mm and 3mm to the full size range in a similar way to adjusting the bottom cutoff from 1mm to 2mm.

The requirement to have the full diamond size distribution clearly limits the above approach to the situation where initial drilling has defined the full size range. Such a situation could arise in the phased approach to sampling when wide spaced sampling had established a global grade and diamond size distribution for each kimberlite facies. The drilling for local block estimates at the feasibility stage could then be carried out using smaller samples. Such smaller samples could also be used where an existing producer wishes to extend its reserves. In such a situation the diamond size distribution is known.

To experiment with the above concept a third grade was created along with the 1mm and 2mm grades. This was the grade of the sample between 1.5mm and 2.4mm.

It is widely observed that stones are lost prior to reaching the bottom cutoff of the sampling plant. This is reflected in the turning down of the diamond size distribution as it approaches the bottom cutoff. The reason for this, and the recovery of stones below the bottom cutoff, is the inefficient sieving of material in a production situation.

The bottom cutoff of 1.5mm was chosen as this is above the point at which stones are lost as the bottom cutoff is approached. The choice of the upper cutoff is more difficult. Essentially the interval chosen should ensure a representative number of stones are collected for the interval in each sample. It is therefore a function of sample size and the diamond size

distribution. If the interval is too wide the variability in the number of stones within the interval will be too high. If the interval is too small the number of stones collected will be too small. From a practical point of view, losing one stone in ten due to sampling efficiencies is far worse than losing 5 stones in 1000.

After consideration of the sample size and the diamond size distribution of the Deposit One, a size range between 1.5mm and 2.4mm was chosen.

7.4 The effect on global estimation

7.4.1 Method

To test the effect of bottom cutoff on global estimation five different sample grids were generated consisting of 2 by 2, 3 by 3, 4 by 4, 5 by 5 and 6 by 6 holes. Each hole consisted of 10, 12m samples with a diameter of 12.25". The grids were placed into an imaginary kimberlite measuring 300m by 300m giving a square grid spacing of 150m, 100m, 75m, 60m and 50m respectively.

The grids, with coordinates for each sample in three dimensional space, were used to simulate stones per sample using the Cox simulation. The statistical parameters used are those of Deposit One described in chapters 4 and 5. Each grid was simulated 500 times. The stones per sample in each realisation were converted to carats per cubic metre using the Deposit One diamond size distribution and by dividing each sample by a theoretical sample volume.

For each sample three grades were produced. These were the grade at 1mm, the grade at 2mm and the grade for the size range 1.5mm to 2.4mm.

For the 1mm samples the average 2mm sample grade was estimated for each grid by taking the arithmetic average of the 1mm sample grades and then adjusting the average grades to a 2mm cutoff using the diamond size distribution. The 500, 2mm grades produced were ranked from smallest to highest in value and the 10^{th}, 50^{th}, and 90^{th} percentiles found empirically.

For the 2mm cutoff samples the average grades were calculated by taking the arithmetic average of the 2mm sample grades for each grid. The 500 mean grades produced were ranked from smallest to highest in value and the 10^{th}, 50^{th}, and 90^{th}percentiles found empirically.

For the 1.5mm to 2.4mm samples the average 2mm sample grade was estimated for each grid by taking the arithmetic average of the 1.5mm to 2.4mm sample grades and then adjusting the average grades to a 2mm cutoff using the diamond size distribution. The 500 grades produced were ranked from smallest to highest in value and the 10^{th}, 50^{th}, and 90^{th} percentiles found empirically.

7.4.2 Results

The 10^{th}, 50^{th}, and 90^{th}percentiles were divided by the average of the 500 simulations and presented as a ratio. A value of one indicates that the estimate is equal to the simulation average. The ratios are shown as trumpet shaped lines in Figures 7.1 and 7.2.

The results indicate wider confidence limits for the 2mm grade information than for the adjusted 1mm or 1.5mm to 2.4mm estimates. However, the difference becomes less with increasing sample size. At 90 samples (9 drill holes in the configurations investigated) the lower confidence limit is 3% wider than the 1mm or 1.5 to 2.4mm confidence limits.

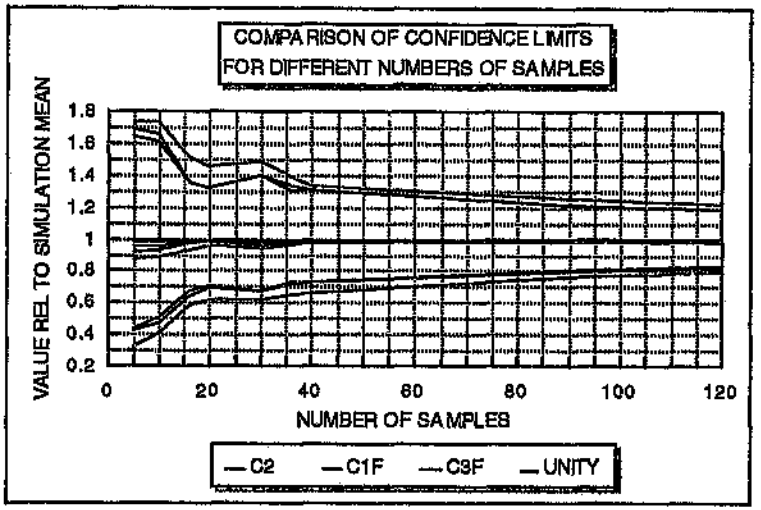


Figure 8.1: Comparison of the central 80% confidence limits for different numbers of samples. C2 is the 2mm grade, C1F is the 1mm grade factored to 2mm and C3F is the 1.5mm to 2.4mm grade factored to 2mm.

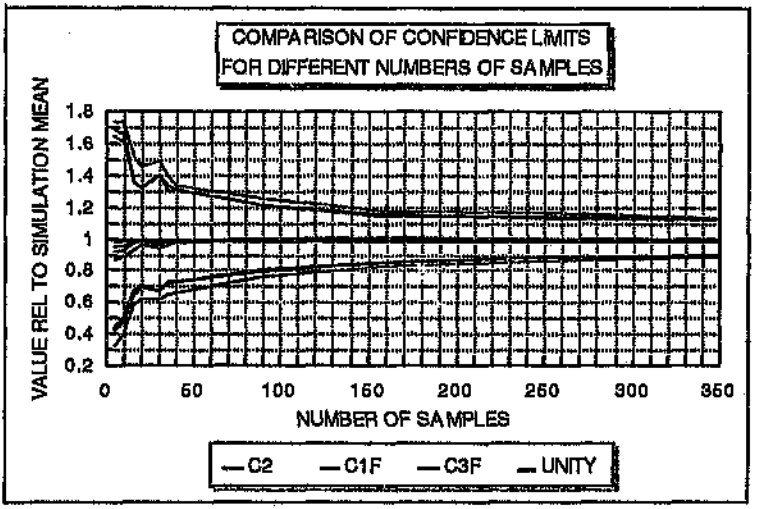


Figure 8.2: The same graph as Figure 8.1 except the X axis has been extended to 350 samples. C2 is the 2mm grade, C1F is the 1mm grade factored to 2mm and C3F is the 1.5mm to 2.4mm grade factored to 2mm.

The results for the adjusted 1mm and 1.5 to 2.4mm grades are very similar.

7.4.3 Discussion

The irregular shape of the confidence limits at small numbers of samples (less than 40) indicates that a larger number of simulations should be used. This was not done as the trend was indicated and, usually, more than 40 samples (4 drill holes) would be taken in each facies.

From a practical point of view the sample results are very similar. At 40 samples the lower 10% confidence limit of the 2mm grade is 6% wider than the 1mm factored grade or the 1.5 to 2.5mm factored grade. This reduces to 3% at 90 samples.

If we assume an estimated grade of 3.2 CPM3, then with 40 samples the lower 90% confidence limit (empirical) would be 2.1 CPM3 for the 2mm grades compared to 2.5 CPM3 for the 1mm factored grade. At 90 holes this difference has reduced to 2.5 CPM3 and 2.6 CPM3 respectively.

The differences are small and appear to indicate that the benefit is not large when dealing with a global estimate.

A likely reason for this is the number of stones used in the 2mm global estimate. Analysis indicates that the average number of stones per 1mm sample (no adjustments) is 41, the average number of stones for the 2mm sample is 4 and the average number of stones for the 1.5 to 2.4 mm sample is 10 stones (no adjustments). A global estimate based on 90 samples could contain 360 stones of 2mm or greater.

7.5 The effect on local estimates

7.5.1 Method

To test the effect of bottom cutoff on local estimation a single 50m grid was generated consisting of 16 by 16 holes. Each hole simulated 75, 12m samples.

This investigation is different in its approach to that used to investigate local block estimates in chapter seven. In chapter seven a number of realisations were created for a fixed block and sample configuration and used to empirically calculate the confidence limits for the configuration investigated.

In this method local block estimates are made from a single realisation of drill holes in a 50m grid. In addition a "true" value for each kriged block is created for comparison with the estimated value. To partially compensate for the use of only one simulation, the simulation area has been made very large. The area is approximately 10 times the range of the semi-variogram in the horizontal and vertical directions.

The grid, with coordinates for each sample in three dimensional space, was used to simulate stones per sample using the Cox simulation. Again, the statistical parameters used are those of Deposit One described in chapters 4 and 5. The stones per sample were converted to carats per cubic metre using the Deposit One diamond size distribution and by dividing each sample by a theoretical sample volume.

For each 50m by 50m by 12m block, 49 sample values were produced on a regular grid (7 by 7 by 1). The 49 values were used to estimate the "true" value of the 50m block. The centre position of the 49 values was used as the sample inside the block to be estimated.

For each sample three grades were produced. These were the grades at a bottom cutoff of 1mm and 2mm and a grade for the size range 1.5mm to 2.4mm. The number of samples and "true" block grades generated was 19 200. The histograms of the sample data in SPM3 are shown in Figures 7.3 to 7.5.

The sample data was used to estimate a semi-variogram for each sample grade. The semi-variograms are shown in figures 7.6 to 7.8.

The semi-variograms were then used, with their respective sample values, to estimate the 50m by 50m by 12m blocks. A rectangular search radius was selected measuring 100m by 100m by 30m allowing 125 samples in a complete kriging neighbourhood.

The results of each kriging is discussed below.

7.5.2 Results

The three means of the kriged data are all similar in value to the "true mean". The standard deviation of kriged data sets are 0.32 for the adjusted 1mm kriging, 0.30 for the 2mm kriging and 0.34 for the adjusted 1.5mm to 2.4mm kriging. This compares to a value of 0.41 for the standard deviation of the "true" block values. The lower standard deviations in the kriged data sets are expected and result from the smoothing action of kriging (Journel and Huijbregts 1978, p.479).

To indicate more clearly the differences between the three kriged data sets each was plotted against the "true" block values in an X Y plot. These plots are shown in Figures 7.9 to 7.11.

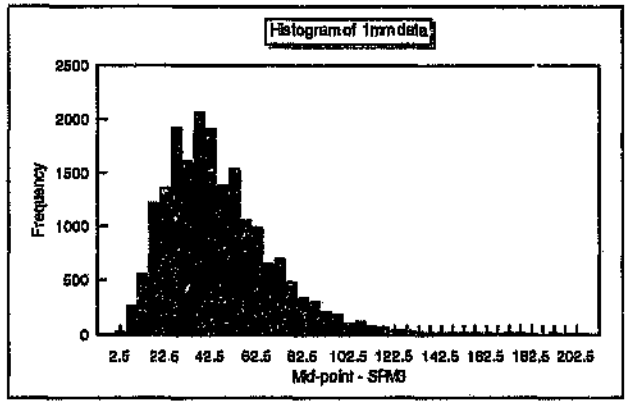


Figure 7.3 Simulated sample data at 1mm in SPM3

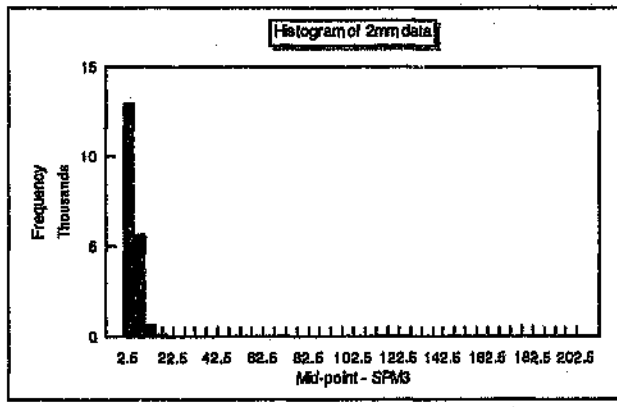


Figure 7.4 Simulated data at 2mm in SPM3

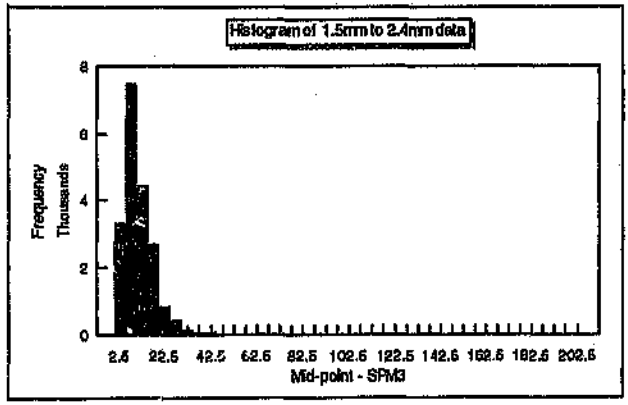


Figure 7.5 Simulated data at 1.5mm to 2.4mm in SPM3

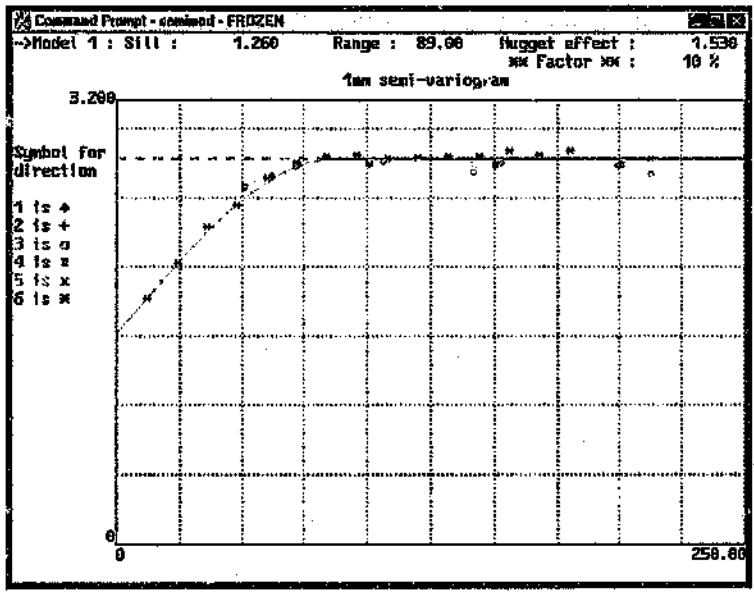


Figure 7.6: Semi-variogram of the 1mm data used for the kriging

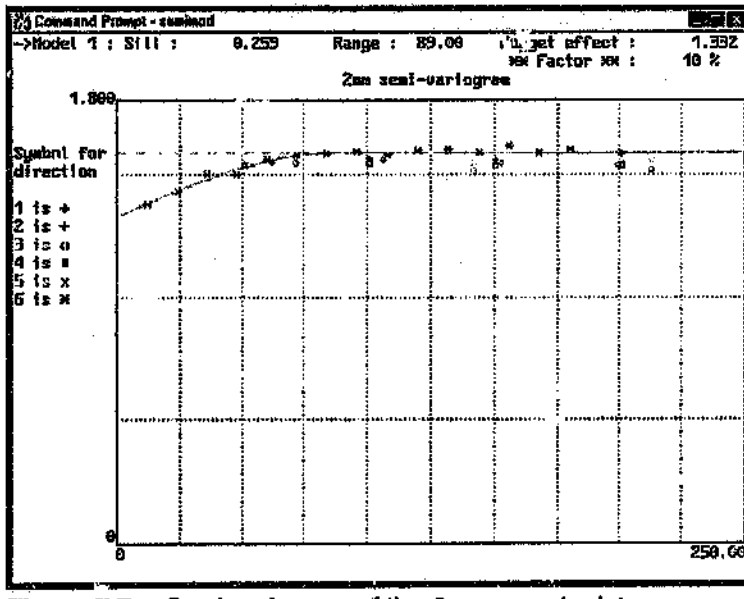


Figure 7.7: Semi-variogram of the 2mm sample data

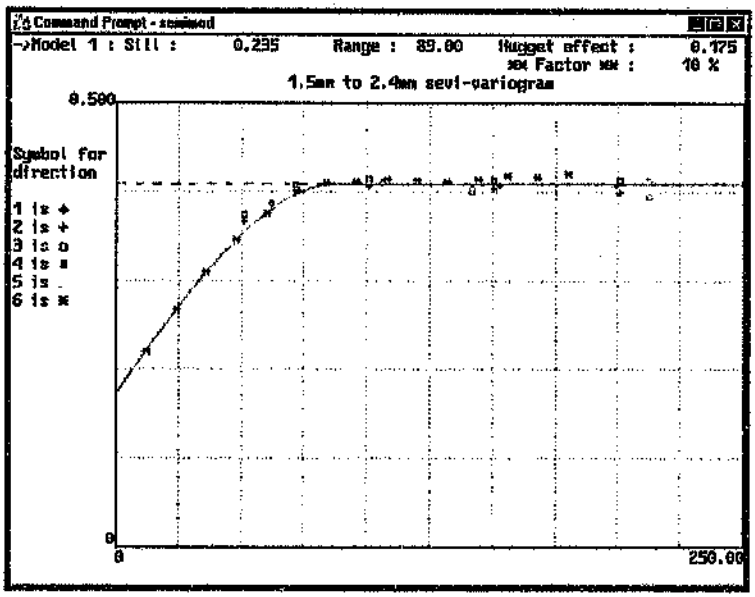


Figure 7.8: Semi-variogram of the 1.5mm to 2.4mm sample data

If the "true" and estimated values are normally distributed the scatter diagram takes the form of an ellipse. The pear shaped scatter plots in Figures 7.9 to 7.11 reflect the skew distributions in Figures 7.3 to 7.5.

A vertical line through the ellipse represents the dispersion of "true" grades for a given cutoff. Similarly, a horizontal cut through the ellipse represents the dispersion variance of estimated values for a given "true" grade.

In examining the three kriged data sets the following criteria were used to compare the performance of each estimation method.

- A factor, F, given by Z^*/Z, where Z^* is the estimated mean grade of the kriged data set and Z is the "true" mean grade. This was used to indicate the degree of global non-bias.
- The slope of the regression line of the "true" on estimated values was used to indicate the degree of conditional bias

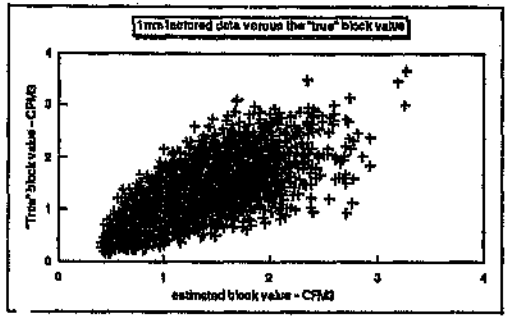


Figure 7.9 "True" estimates versus the 1mm adjusted block estimates

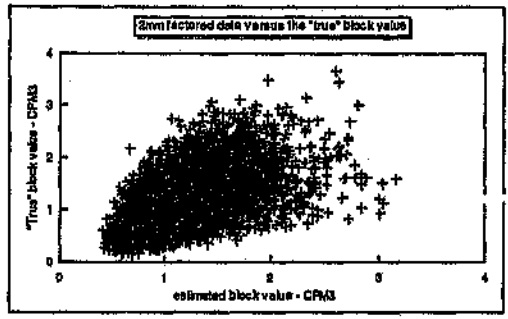


Figure 7.10 "True" block estimates versus the 2mm block estimates

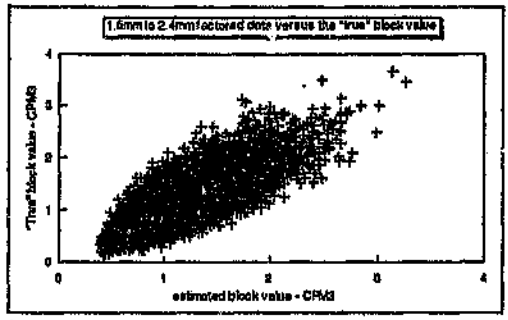


Figure 7.11 "True" block estimates versus the 1.5mm to 2.4mm adjusted block estimates

- The coefficient of correlation between the "true" and estimated values
- The variation in "true" values for all estimated grades given by the residual variance
- The distribution of the errors, Z-Z*, for each kriging set was examined and the mean and standard deviation of the distribution reported

The results are shown in Table 7.1.

KRIGING	BIAS(F)	SLOPE	RSQR	RES SD	MEAN OF (Z*-Z)	VAR OF (Z*-Z)
1mm	1.02	0.95	0.57	0.27	0.02	0.27
1.5-2.4mm	1.03	0.95	0.62	0.25	0.03	0.25
2mm	1.01	0.76	0.31	0.34	0.01	0.35

Table 7.1: Sample statistics for "true" on estimated block values

Table 7.1 shows that the global bias (F), the slope of regression (SLOPE), the coefficient of correlation (RSQR), the residual standard deviation (RES SD) and the variance of the errors are all better for the 1mm factored results and 1.5mm to 2.4mm adjusted data when compared to the 2mm kriged data. In addition, the results of the 1.5mm to 2.4mm kriged data is similar to the 1mm factored data.

7.5.3 Discussion

The results of this experiment demonstrated the advantage of using samples collected at a 1mm bottom cutoff to estimate the production grade at 2mm bottom cutoff.

The experiment also indicated that a restricted grade (1.5mm to 2.4mm) can be used to estimate the 2mm production grade with a similar degree of confidence to the adjusted 1mm grades.

As indicated in section 7.3.3 the average number of stones per 1mm sample (no adjustments) is 41 while the average number of stones for the 2mm samples is 4 stones.

In the kriging exercise the 1mm samples were used to estimate each mining block. The 2mm grades were then estimated by adjusting the 1mm block grades using the diamond size distribution.

The 1mm samples have produced a better defined spatial structure (compare Figures 7.6 with 7.7) than the 2mm samples and have resulted in a kriged result that is closer to the 2mm reality (compare Figures 7.9 and 7.10). This reflects the larger number of stones per sample in the 1mm samples (41 samples) versus the 2mm samples (4 samples).

The lack of spatial structure shown by the 2mm samples (see Figure 7.7) highlights the importance of obtaining a reasonable number of stones per sample. If this cannot be obtained by a single 12" hole per grid node then clusters of holes should be considered.

The use of the adjusted 1.5mm to 2.4mm samples gave similar results to the 1mm adjusted grades in terms of confidence limits. The average number of stones per sample was 10 versus the 41 stones per sample for the 1mm samples.

At first sight, it seems odd that the 1.5mm to 2.4mm size range, with only 10 stones per sample, should give similar confidence limits to the 1mm samples where the average number of stones per sample is 41.

A logical explanation is that only the grade of the size range 1.5mm to 2.4mm was estimated and not the grade between 1mm and the top natural diamond size. The penalty for estimating a smaller part of the size range is that the adjustment to move to a full grade above 2mm requires more information than that required to move the 1mm grade to a 2mm grade[3].

The experiment has shown that the grade of a restricted size range could be used to estimate the grade across the full size range provided the diamond size distribution is known. The implication of this is that smaller samples, that are easier and quicker to treat, could be used to estimate the grade of a mining block with the same degree of confidence that might be expected from a larger block.

7.6 Chapter conclusion

The objective of this chapter was two fold.

The first objective was to answer a question on evaluation approach. More precisely, if a grade estimate was required at a 2mm bottom cutoff, is it better to evaluate the pipe using sample data collected at a bottom cutoff of 1mm[4] or is it better to estimate the deposit directly at a 2mm bottom cutoff ?

The advantage of using samples collected at the higher cutoff is faster sample treatment and less concentrate to sort. Quicker treatment and less concentrate can result in cost savings. The disadvantage of a higher cutoff is that fewer stones are collected.

---

3 Knowledge of the diamond size distribution is required above and below the 1.5mm to 2.4mm size range rather than just between 1mm and 2mm as for the 1mm adjustment

4 The estimate at 1mm is then adjusted to 2mm using the diamond size distribution.

The results of the experiment to investigate the effect on global estimation show that the benefit is not large when dealing with a global estimate. However, the results from the experiment to investigate the effect on local estimates supports the approach of collecting sample data at a lower cutoff and then adjusting the grades to obtain the grade of the deposit at a higher cutoff rather than estimating the grade directly at the higher cutoff.

The second objective of this chapter was to estimate the grade at 2mm using the grade of a restricted size range (1.5mm to 2.4mm). This grade was adjusted to the 2mm grade using the diamond size distribution.

The advantage of this method is that the grade of the restricted size range can be estimated with a smaller sample.

The results of the exercise showed that the adjusted 1.5mm to 2.4mm grade had an equivalent confidence to the adjusted 1mm grade. This is despite having one quarter of the stones per sample.

CHAPTER 8

SUMMARY, CONCLUSIONS AND THE WAY FORWARD

Until the Urals there are roads and directions, beyond the Urals there are just directions - Old Russian saying

In this chapter we will:

- Summarise the objectives of the thesis
- Summarise the chapters
- Examine the sensitivity of the results to changes in simulation parameters
- Look at extensions to this research
- Conclude the thesis

8.1 Objectives of the thesis

The development of a newly discovered kimberlite into an operating mine involves a number of stages. At each stage sampling information is collected and analysed with a view to making a decision. In the early stages of prospect development the decision is whether continue spending money on a prospect or "walk away". At the feasibility stage of the project it may be whether to open a mine or not. The decisions made at each stage of development are based on the sample information available at the time and not on a complete knowledge of the deposit. The estimates made are therefore subject to uncertainty.

The objectives of this thesis were two fold. Firstly, to understand, **in a quantitative way**, how the uncertainty in the grade estimate changes with different sampling configurations, both in terms of **size of sample** and in terms of the **number of samples** taken.

The second objective, and necessary in order to achieve the first, was to **practically** apply a new simulation method that takes into account the statistical and spatial characteristics of the diamond distribution in the kimberlite. This new method of simulation (the Cox simulation) is applied to kimberlites for the first time in this thesis.

8.2 Summary of the previous chapters

The thesis consists of 8 chapters. Chapter one sets out the problem statement and aims of the thesis.

The objective of Chapter two was to provide the reader with a practical background to kimberlites. Chapter two discusses the formation of kimberlites, the sampling methods and philosophy of sampling, the grade units commonly associated with kimberlites, the stone density distribution and the diamond size distribution. The final section reviews the statistical and spatial models that are available for the modelling of diamond distributions. It is here that the beginnings of the Cox simulation are explained. In particular, the need for a simulation model that is consistent with the way the diamonds are concentrated and that is able to account for the diamonds in a "trap site" as well as the distribution of the "trap sites" themselves. The evolution of the Cox simulation from the Compound Poisson distribution (Sichel 1973) and the Neyman-Scott point process model (Kleingeld 1987) is explained.

In Chapter three a Poisson point process is used to simulate three different spatial patterns of stones in space. These patterns are sampled with the same sample configurations and produce different sample statistics. The results of the experiment are used to illustrate that the spatial distribution of diamonds in space is important and can lead to different statistical results from the sample campaign.

A serious draw back of the simulation method used in Chapter three is that only the mean is reproduced in the simulation. The histogram and semi-variogram of the deposit cannot be reproduced (at least not easily). To continue with the research it was necessary to use a simulation method that was capable of simulating diamonds in space with the correct histogram and semi-variogram.

In Chapter four the Cox simulation was presented and, importantly, how to estimate the simulation parameters from observed sample data. It was during the practical implementation of the simulation that the problem of sample shape was encountered. In particular, the problem of simulating pencil shaped samples. A solution was suggested in which anisotropy was introduced to compensate for the sample shape.

In Chapter five we use the Cox simulation method to draw conclusions about confidence limits around the global mean for different sample configurations. The discussions in Chapter five are limited to practical grids, sample sizes and sample numbers.

The work in Chapter five showed that, for a high nugget semi-variogram model and the grade variable SPM3, at least 8 holes are required to obtain

a global mean within 10% of the simulation mean value[1]. If the grade variable is CPM3 then the number of holes increases to 12. For the low nugget semi-variogram model the number of holes are 14 and 16 respectively.

Larger samples were tested by grouping unit samples together. The results showed very little improvement in the global confidence limits for the low nugget semi-variogram model while the high nugget semi-variogram model showed an improvement. At a sample size of 0.9m by 0.9m the number of holes required, for the same level of confidence, was reduced from 8 holes to 4.

The small improvement in the low nugget semi-variogram model is the result of the high correlation between samples at small distances and the sample shape (the sample has a width to length ratio of 1 to 40). In simple terms adding the unit samples together contributed very little additional information to the deposit. In the high nugget effect model the additional size of the sample benefited from the classical reduction in variance through increasing size.

The effect of decreasing the sample size was also tested. As might be expected, the smaller sample sizes resulted in wider confidence limits then for a unit sized sample.

The results of Chapter five indicated, for the first time, the sensitivity of the confidence interval around the global mean to the numbers and size of samples taken.

---

1 Central 80% confidence limits.

In Chapter six we examined the confidence limits around local block estimates and, in particular, the effect of sample size on these confidence limits.

Confidence limits were estimated for a 50m x 50m x 12m mining block surrounded by 27 samples located on a 50m x 50m x 12m grid. The block to be estimated was situated at the centre of the 27 samples and was estimated using ordinary kriging. For comparison with the kriged grade, a "true" grade for the block was calculated by averaging a grid of 10 by 10 simulated samples within the block. The block size and sample spacing investigated corresponds to the sample spacing and block size used on the mines familiar to the author.

The results of this chapter indicated that a benefit is gained in both the low and high nugget models by going to larger sample sizes. As for the global estimates, the benefit is greater for the high nugget model than for the low nugget model. For a unit sample size, 90% of the blocks estimated were shown to be within 25% of their true value for both the low and high nugget models.

In Chapter seven we use the Cox simulation to answer questions regarding the bottom cutoff of a sampling campaign. In particular, if the estimate for the pipe is required at a 2mm bottom cutoff, is it better to evaluate the pipe using sample data collected at a bottom cutoff of 1mm or is it better to estimate the deposit directly at a 2mm bottom cutoff ? The advantage of using samples collected at the higher cut offs faster sample treatment and less concentrate to sort.

The results indicated that the benefits for global estimation were minimal (for the sample configurations considered). However, for local estimation the

results showed less conditional bias, less variability in the error distribution and lesser tendency to mis-classify blocks if selective mining was present.

Also in Chapter seven, the concept of estimating diamond grade across part of the diamond size distribution was explored. The adjustment to a full diamond grade is carried out using knowledge of the diamond size distribution obtained from earlier sampling or production history. The advantage of this approach is that the grade of the restricted size range can be estimated with a smaller sample.

The results of this exercise showed that a 1mm grade, estimated from a restricted part of the diamond size distribution, had an equivalent confidence to the full 1mm grade.

8.3 Sensitivity of the results to changes in parameters

It is recognised that the results in Chapters five, six and seven need to be interpreted with respect to the geological, statistical and practical constraints of the experiments carried out. In the section that follows the results of the work presented in Chapters five to seven are discussed in terms of the various modifier variables.

The results of Chapter five indicate, for Deposit One and the low nugget semi-variogram model, that at least 16 holes are required to obtain a lower 90% confidence interval for CPM3 within 10% of the mean. If the spatial structure is more random, then the number of holes required, for the same degree of confidence, is reduced.

In this section we discuss how robust these results are to changes in the simulation parameters. For example, would the recommendation of 16 holes change if the range of the semi-variogram was increased or a coarser diamond size distribution used? To answer these questions, changes were made to the diamond size distribution, the range of the semi-variogram, the grid size and the mean number of stones per sample.

To allow comparisons to be made with the results in Chapters five, the changed simulation parameters were applied to 16 holes drilled on a regular grid inside a 300m x 300m simulation area. The sixteen holes were each drilled to a depth of 120m. Similarly, to allow a comparison with the results in Chapter six, the changed parameters were applied to the same local sampling configuration.

8.3.1 The diamond size distribution

The variability in the CPM3 results from the different exercises reflect the combined variability in the stone density distribution (the histogram of the stones per sample or, if normalised, the distribution of SPM3) and the diamond size distribution.

In the diamond size distribution for Deposit One 45% of the carats lie above 2mm and 9% of the stones. If other kimberlite diamond size distributions are compared, then this diamond size distribution has a small average stone size when compared to the others. For comparison, the coarsest diamond size distribution (observed by the author) would contain 65% of its carats above 2mm and 16% of its stones[2].

---

2 Both comparisons are made assuming a 1mm bottom cutoff

A coarser diamond size distribution could, intuitively, be expected to introduce more variability than a finer size distribution. To test this, and assess the additional variability added to the data by the diamond size distribution, two experiments were carried out.

In the first experiment the effect of the diamond size distribution on the global confidence limits associated with the 16 hole grid (75m x 75m) was tested. In the second experiment the effect of the diamond size distribution on local confidence limits associated with the estimation of a 50m x 50m x 12m mining block was tested.

In the first experiment 16 holes were simulated on a 75m square grid. Each hole consisted of ten 12m samples (the depth of kimberlite drilled would then be 120m). It was assumed that there would be one drill hole per grid node and that this sample would be taken with a 12" diameter bit. Diamonds would be recovered to a bottom cutoff of 1mm. In the authors opinion, such a situation would be quite realistic where a global estimate was required and the present sampling tools, familiar to the author, were used.

The sixteen holes were simulated 500 times using the Deposit One high and low nugget effect models (see Chapters four and five). The number of stones per sample generated for each sample was converted to carats per sample by allocating a carat weight to each stone based on the diamond size distribution for Deposit One (referred to as the fine diamond size distribution). The exercise was repeated, using the same stones per sample information, but replacing the fine diamond size distribution of Deposit One with a coarse diamond size distribution.

The results are shown in the first six lines of Table 8.1.

The results show that the central 80% confidence limits widen by 10% when the grade variable is expressed in CPM3 and not SPM3. There is no practical change in the width of the central 80% confidence limits if the fine diamond size distribution is replaced by the coarse diamond size distribution.

If the high nugget model is used then the relative increase in the width of the central 80% confidence limits is 23% (versus 10% for the low nugget model). This reflects the smaller relative width of the central 80% confidence limit in the case of the high nugget model (0.13 versus 0.19). As the variability added from the diamond size distribution is the same in both cases, the relative increase in variability is higher for the high nugget model.

The similarity of the fine and coarse diamond size distributions reflects the number of stones recovered in the exercise. In this case, assuming 41 stones per sample and 160 samples, we would have 6560 stones. This number of stones is sufficient, in both the fine and coarse diamond size distributions considered, to assess the average diamond size of the deposit to the same practical degree of confidence.

In the situation described above a coarser diamond size distribution does not have a practical effect on the results. **This result, however, is a function of the number of stones recovered and used for the global estimate.**

In the second experiment the effect of the diamond size distribution on the confidence limits associated with the estimation of a 50m x 50m x 12m mining block was tested.

In this experiment the mining block is assumed to be estimated with 27 samples situated on a 50m x 50m x 12m grid surrounding the block to be estimated. The samples are the result of drilling using a drill bit of 12"

diameter and where all diamonds above 1mm have been recovered. Again, in the author's opinion such a situation would be quite realistic where a local estimate was required and the present sampling tools, familiar to the author, were used.

The 27 samples surrounding the block were simulated 500 times using the high and low nugget effect models. The stones per sample generated for each sample was converted to carats per sample by allocating a carat weight to each stone based on the diamond size distribution for Deposit One. The exercise was repeated, using the same stones per sample information, but replacing the Deposit One diamond size distribution with the coarse diamond size distribution described above.

An estimate of the block value was generated by weighting the samples surrounding the block by the appropriate kriging weight. This method is similar to that used in Chapter six.

In addition, and in order to arrive at a "true" value of the block being estimated, 100 samples were simulated in the 50m by 50m by 12m block. These were averaged to give the "true" block value for comparison to the estimate.

The results are shown in the first six lines of Table 8.2.

The results show that the central 80% confidence limits widen by 55% when the grade variable is expressed in CPM3 and not SPM3. There is no practical change in the width of the central 80% confidence limits if the fine diamond size distribution is replaced by the coarse diamond size distribution.

If the variable is expressed in SPM3 then 50% of the blocks are within 9%

of the "true" block estimate. If the grade variable is expressed in CPM3 then this increases to 14%. There is no practical change in the width of the central 80% confidence limits if the fine diamond size distribution is replaced by the coarse diamond size distribution.

Again, this experiment (in this situation) shows that the coarser diamond size distribution does not have a practical effect on the results.

An interesting, but well known, observation is the high increase in variability when the grade variable is expressed in CPM3 and not SPM3. For the low nugget model the central 80% confidence limits increase by 53% and for the high nugget model by 19%. **Certainly, if possible, it is a better strategy to estimate the grade in SPM3 first and then adjust the grade to CPM3 using a global diamond size distribution.** The advantage of such a method is that the global diamond size distribution is estimated with more confidence than the local diamond size distribution.

In reality the success of such an approach is dependant on the ability to recognise zones of equal stone size and, more importantly, the ability to correct the actual stone counts per sample for diamond breakage that may result from the drilling process.

8.3.2 The Semi-variogram

To test the effect of range on **global** confidence limits two experiments were carried out. In the first experiment the 75m grid described above was simulated 500 times. In one case the range was increased to twice the actual range of Deposit One (178m) and in the second case it was halved (44.5m).

DESCRIPTION		MEAN	P10	P90	VAR	MED	rP10	rP90	C80/M
LN	S	44.92	40.72	49.16	10.63	45.09	0.91	1.09	0.19
LN	CF	2.48	2.23	2.75	0.04	2.48	0.90	1.11	0.21
LN	CC	3.81	3.43	4.22	0.09	3.80	0.90	1.11	0.21
HN	S	44.97	42.05	47.71	5.17	44.95	0.94	1.06	0.13
HN	CF	2.49	2.30	2.68	0.02	2.48	0.92	1.08	0.16
HN	CC	3.81	3.53	4.12	0.05	3.80	0.93	1.08	0.15
LN	SR	45.07	41.53	48.33	6.67	45.08	0.92	1.07	0.15
LN	-	44.92	40.72	49.16	10.63	45.09	0.91	1.09	0.19
LN	LR	44.74	37.00	53.32	37.56	44.71	0.83	1.19	0.36
HN	SR	44.96	42.27	47.56	4.09	44.88	0.94	1.06	0.12
HN	-	44.97	42.05	47.71	5.17	44.95	0.94	1.06	0.13
HN	LR	44.80	40.32	49.37	12.20	44.83	0.90	1.10	0.20
HN	-	44.97	42.05	47.71	5.17	44.95	0.94	1.06	0.13
HN-10	S	10.95	10.28	11.55	0.27	10.93	0.94	1.05	0.12
HN-10	CF	0.61	0.54	0.67	0.003	0.60	0.90	1.11	0.21

Table 8.1: Table of results for **global** estimation. LN is the low nugget effect model, HN is the high nugget effect model. S is the result for SPM3, CF is the result for CPM3 using the fine stone size distribution, CC is the result for CPM3 using the coarse stone size distribution. SR is the result using half the range, LR is the result using twice the range, "-" is the result using the actual range. HN-10 is the result where the mean number of stones has been reduced 10 SPS to create a lower grade. P10 is the 10^{th} percentile of the ranked results, P90 is the 90^{th} percentile of the ranked results, VAR is the variance of the results, MED is the median of the results, rP10 is the ratio of P10 to the mean, rP90 is the ratio of P90 to the MEAN and C80/M is the ratio of the central 80% confidence interval to the MEAN. The results of the experiment are shown in Table 8.1 for the high and low nugget effect models and for the effect of SPM3 only.

The results show that decreasing the range of the semi-variogram (all other variables remaining the same) narrows the central 80% confidence limits by 21% for the low nugget model and 8% for the high nugget model.

Increasing the range has the effect of widening the central 80% confidence limits by 89% for the low nugget effect model and 54% for the high nugget model.

The effect of the range on the sample data must be considered relative to the grid spacing. For the shorter range (the grid spacing is 1.7 times the range of the semi-variogram), the average grades, of each of the 500 simulations, are more similar in value than the 500 average grades calculated for the simulations with the larger range (the grid spacing is 0.42 of the range). The more similar average values for the short range leads to a tight confidence limit. Conversely, the more diverse average values of the longer range leads to a widening of the confidence limits.

The effect is more pronounced for the low nugget model. In the high nugget model the influence of the range is less as 80% of the variability is already in the nugget component.

The experiment shows, for the situation tested, that a strong correlation between samples leads to wider confidence limits for the global estimate. Put another way, for a deposit with a low nugget effect and a long range, more drill holes will be required to achieve the same degree of confidence as a deposit with a low degree of correlation.

To test the effect of different ranges on **local** confidence limits the 27 samples surrounding the block to be estimated were simulated 500 times. In one case the range was increased to twice the actual range of Deposit One

(178m) and in the second case it was halved (44.5m). The results of the experiment are shown in Table 8.2 for the high and low nugget effect models and for the effect of SPM3 only.

The results show that decreasing the range of the semi-variogram (all other variables remaining the same) widens the central 80% confidence limits by 33% for the low nugget model and 3% for the high nugget model. In a similar way it can be seen that 50% of the blocks have estimated within 12% of the "true" block value for the shortened range. This improves to 7% for the longer range.

Increasing the range has the effect of narrowing the central 80% confidence limits by 18% for the low nugget model and 14% for the high nugget model.

These results are the opposite to that seen for the global estimate. For a local estimate a high degree of correlation (for instance a low nugget and a long range) results in tighter confidence limits for the kriged estimate. Again, this result should be interpreted in terms of the ratio of the semi-variogram range to the sample grid. In the case of the local estimate the longer range results in the sample values around the block having similar values and therefore the confidence limit is narrowed.

The effect of changing the range is more pronounced for the low nugget model than for the high nugget model. In the high nugget model the influence of the range is less as 80% of the variability is already in the nugget component.

DESCRIPTION		M (Z*-Z)	VAR (Z*-Z)	P90 (Z*-Z)	P10 (Z*-Z)	P90 |Z*-Z|/Z	P50 |Z*-Z|/Z	M SPM3/ CPM3	rP90 (Z*-Z)	rP10 (Z*-Z)	C80 (Z*-Z)/M
LN	S	-0.118	35.71	7.00	-8.05	0.22	0.09	45.11	0.16	0.18	0.33
LN	CF	-0.002	0.34	0.66	-0.63	0.34	0.14	2.50	0.26	0.25	0.51
LN	CC	-0.003	0.73	0.96	-0.98	0.34	0.13	3.83	0.25	0.26	0.51
HN	S	-0.385	40.30	7.71	-8.22	0.24	0.09	44.63	0.17	0.18	0.36
HN	CF	0.001	0.20	0.56	-0.52	0.29	0.11	2.49	0.22	0.21	0.43
HN	CC	-0.006	0.44	0.84	-0.80	0.29	0.11	3.81	0.22	0.21	0.43
LN	SR	0.523	67.29	11.11	-8.71	0.32	0.12	45.17	0.25	0.19	0.44
LN	-	-0.118	35.71	7.00	-8.05	0.22	0.09	45.11	0.16	0.18	0.33
LN	LR	-0.362	27.64	5.72	-6.78	0.19	0.07	46.22	0.12	0.15	0.27
HN	SR	-0.233	37.64	7.38	-8.28	0.23	0.09	44.62	0.17	0.19	0.35
HN	-	-0.385	40.30	7.71	-8.22	0.24	0.09	44.63	0.17	0.18	0.36
HN	LR	-0.379	29.30	6.30	-8.00	0.19	0.09	45.52	0.14	0.18	0.31
HN	-	-0.385	40.30	7.71	-8.22	0.24	0.09	44.63	0.17	0.18	0.36
HN-10	S	-0.01	2.61	2.18	-2.06	0.25	0.10	11.02	0.20	0.19	0.38
HN-10	CF	-0.00	0.02	0.19	-0.18	0.40	0.17	0.61	0.32	0.29	0.61

Table 8.2: Table of results for local estimation. LN is the low nugget effect model, HN is the high nugget effect model. S is the result for SPM3, CF is the result for CPM3 using the fine stone size distribution, CC is the result for CPM3 using the coarse stone size distribution. SR is the results using half the range, LR is the result using twice the range, "-" is the result using the actual range. HN-10 is the result where the mean number of stones has been reduced to 10 SPS to create a lower grade. M is the mean of Z*-Z, VAR is the variance of Z*-Z, P10 is the 10th percentile of the ranked Z*-Z values, P90 is the 90th percentile of the ranked |Z*-Z|/Z values, P50 is the median of the |Z*-Z|/Z values, M SPM3/CPM3 is the mean grade value of the results in SPM3 or CPM3, rP10 is the ratio of P10(Z*-Z) to the mean, rP90 is the ratio of P90(Z-Z*) to the MEAN and C80/M is the ratio of the central 80% confidence interval of Z*-Z to the MEAN.

8.3.3 The effect of grid size

The grid size tested above is 75m x 75m. To test the impact of increasing the grid size, the simulation area was increased to 600m x 600m and again to 900m x 900m. In both cases the two areas were "drilled" with 16 holes giving a grid spacing of 150m x 150m and 225m x 225m respectively for the two areas. The depth of the drill holes was maintained at 120m.

The results of the exercise showed no practical difference in confidence limits for the two wider spaced grids, for both the low and the high nugget semi-variogram models.

8.3.4 The mean number of stones per sample

The effect of the mean number of stones per sample, on local and global confidence limits, can only really be tested by examining deposits with higher or lower mean values. Such a comparison is complicated due to the limited number of deposits sampled with 12" drilling and a single drill hole per grid node.

The mean number of stones per sample for Deposit One is 41 (an equivalent grade of approximately 90 CPHT if the diamond size distribution from Deposit One is used). To better understand the impact, on local and global confidence limits, of reducing the average number of stones per sample, two experiments were carried out.

In the first experiment the16 drill holes above were simulated 500 times using a mean value of 10 stones per sample (an equivalent grade of approximately 22 CPHT).

In the second experiment the local grid described in Chapter six was simulated 500 times using a the same mean value of 10 stones per sample.

In order to carry out the simulations two assumptions were necessary:

- That a linear relationship exists between the mean and standard deviation.
- That the nugget to sill ratio and range of the semi-variogram is unchanged at the lower mean number of stones per sample.

With respect to the first assumption, the lower number of stones per sample must result in a lower variance. As the relationship between the mean and standard deviation is unknown, a linear relationship was assumed.

Regarding the second assumption, the relationship (if any) between the mean grade of the deposit and its spatial statistics is unknown, the spatial relationship was therefore assumed unchanged.

A new stones per sample variance was calculated by scaling the Deposit One sample variance of 417 SPS^2.

$$\text{new SPS variance} = \frac{10^2}{41^2} * 417 = 24.81$$

This scaling was applied to the high nugget effect SPS semi-variogram giving a new SPS semi-variogram from which the semi-variogram of the potential and the multi-Gaussian semi-variogram was calculated (see section 4.5 of Chapter 4).

It should be noted that the low mean of 10 SPS and the spatial structure of the low nugget effect semi-variogram model, cannot be simulated using the Cox process. The experiment with a low mean of 10 SPS was therefore only carried out for the high nugget effect semi-variogram.

The results are shown in the last 3 lines of Table 8.1 and 8.2.

The results show that, for the sample configurations examined, the central 80% confidence limits for the global estimates are approximately the same if the variable considered is SPM3. If the variable considered is CPM3 (and the diamond size distribution from Deposit One is used) then the central 80% confidence limit increases by 62%.

For the local estimates the central 80% confidence limits are widened by 5% if the variable considered is SPM3. If the variable considered is CPM3 (and the diamond size distribution from Deposit One is used) then the central 80% confidence limit increases by 69%.

A more practical way to appreciate the difference is to consider the P50 (Z*-Z)/Z statistic in Table 8.2. For the high nugget model, with 41 stones per sample, 50% of the blocks are within 9% of the "true" block value if the variable considered is SPM3 and 11% if the variable is CPM3. At 10 stones per sample, 50% of the blocks are within 10% of the "true" block value if the variable considered is SPM3 and 17% if the variable is CPM3.

It is recognised that further research is required into very low grade deposits. It is possible that the results obtained in Chapters five to seven may not apply when stone counts are in the order of one or two stones per sample.

8.3.5 The large scale geological model

An important final point is that the experimental data has been taken from the **diatreme zone** of a kimberlite. The geological controls and concentrating mechanisms in the diatreme zone of a kimberlite pipe are different from those in the crater or root zones of the pipe. Given the method of formation and the concentrating mechanisms operating in the crater and root zones, it is likely that more drilling will be required than for the diatreme zone.

8.3.6 Conclusion

In examining the robustness of the results in Chapters five, six and seven to the assumptions made the following conclusions can be drawn:

- The effect of the diamond size distribution is small and will not adversely affect the results for the situations tested.
- For a global estimate, a range longer than the 89m of Deposit One widens the central 80% confidence limits. In practice this means that more drilling (or larger samples) may be required to achieve the same degree of confidence as indicated in Chapter five. The effect is more pronounced in the low nugget model and at the upper 90th percentile.
- For a global estimate a shorter range than Deposit One will narrow the 80% confidence limits. In practice this means that the drilling recommended in Chapter five is sufficient to achieve the confidence required. The effect is more pronounced in the low nugget model.
- A reverse of the above is noted for the local estimates. Where the range is increased beyond 89m the central 80% limits of a mining block are narrowed. In practice this means that the confidence in the local mining blocks is increased if the range is long relative to the drill hole spacing.

- If the range is shortened relative to the 89m of Deposit One then the central 80% confidence limits are widened. The effect is more pronounced in the low nugget model.
- For a global estimate, decreasing the average number of stones per sample widens the central 80% confidence limits although the increase is small if the variable observed is SPM3. If the variable is CPM3 then the increase is more significant.
- For a local estimate, decreasing the average number of stones per sample widens the central 80% confidence limits for both SPM3 and CPM3. The effect is more pronounced for the low nugget model.
- The experimental data is restricted to the diatreme zone of the kimberlite. Different concentrating mechanisms in the crater and root zones may lead to a different spatial character.

8.4 The way forward

This thesis has demonstrated the practical application of the Cox simulation to kimberlites. It has also shown the effect of sample size and the number of samples on the confidence interval around local and global estimates of grade for a number of practical sampling protocols.

It is clear that the Cox simulation work reported in this thesis can be expanded in several ways. In this section we look at some extensions to the work presented that would lead to a further understanding of the effects of sampling protocols in Kimberlites.

The extension to multiple geological facies

The simulation work presented so far has been restricted to a pipe consisting of one kimberlite facies. A kimberlite diatreme can consist of more than one

kimberlite type. During the early stages of the evaluation the composite nature of the pipe may not be known or, alternatively, the drilling budget may not allow the required minimum number of holes in each facies.

The effect on the confidence limits of a pipe containing more than one geology could be tested by sampling composite simulation models.

The extension to other geological units in a kimberlite pipe

The work carried out in this thesis has focussed on the diatreme facies of a Kimberlite pipe. Further work is required to quantify the risk associated with drilling campaigns in the crater and root zones of a kimberlite.

The extension of the study to very low grade deposits

As mentioned in section 8.3.4, the research should be extended to very low grade deposits.

Conditional simulation

The results presented in this thesis are based on non-conditional simulations (see Chapter two). The conditional simulation of the Cox process was presented in Kleingeld et al (1996), a paper co-written by the author. Although the conditioning algorithm has been applied to small data sets it has not yet been applied to large data sets similar to the ones used here.

A natural extension to the practical implementation of the non-conditional Cox simulation is to implement the conditioning of large simulations.

The further testing of grades estimated over a restricted diamond size distribution

A potentially useful tool is the idea of estimating grade across a limited range of the diamond size distribution and adjusting this grade using a global knowledge of the diamond size distribution obtained from earlier sampling. Although of limited use in green field projects, this idea could be applied to mineral reserve extensions on existing mines or to projects where early drilling had established a reasonable knowledge of the diamond size distribution[3].

Further testing of this method is required in a real situation which may well be more complex than the simulation example considered in Chapter seven. One suggestion would be to take historical sampling data, simulate a grade from part of the diamond size distribution, estimate block grades using this limited data, correct the estimated grades to the full diamond size distribution and, finally, draw conclusions on the success of the method by comparing the results to block grades generated using bulk samples.

Such an exercise should be repeated in a number of situations to ensure the method is robust. If the method is successful it has the potential to simplify and cheapen the later stages of evaluation in a kimberlite.

The simulation of other diamond attributes

The Cox simulation is used in this thesis to simulate stones in space. In the simulations described a stone size is added to the simulations allowing the

---

3 Consider, for instance, a project moving to a feasibility stage where local block estimates are required.

calculation of a carat weight per sample. In addition to stone size there are other attributes of the stone that would be useful to simulate. These include colour, quality and model (the shape of the stone). Size, colour, quality and model define the value of the stone. Simulation of these attributes in space would add a new dimension to the simulation allowing sensitivity to revenue to be added to the simulation output. It should be mentioned that such a simulation requires co-simulation of these attributes.

8.5 Chapter summary

In this thesis the Cox simulation was used to assess, in a quantitative way, how the uncertainty in the grade estimate changes with different sampling configurations, both in terms of size of sample and in terms of the number of samples taken. Two areas of original research are presented, firstly the quantification of uncertainty associated with local and global estimates in a kimberlite and secondly, the practical implementation of the Cox process.

The thesis consists of 8 chapters. The first chapter brought into focus the need for the thesis and emphasized the research elements. The second chapter provides some necessary background to the evaluation of kimberlites and sets the scene against which the research is carried out. Chapters 3 illustrates the need to understand the spatial distribution of stones in a kimberlite. Chapter four presents the Cox simulation used in this thesis while Chapters five and six apply the Cox simulation to the definition of uncertainty in a number of practical sampling protocols used to evaluate kimberlites. The results of Chapter five and section 8.3 of Chapter 8, suggest, for the sampling configurations tested, 16 holes will ensure that the lower 90% confidence limit of the global estimate is within 10% of the true mean. Chapter seven asks, and answers, some specific questions regarding the bottom cutoff in the evaluation process. Finally, in this chapter, the

results presented in the thesis are summarised and natural extensions to the thesis are discussed.

Four topics were of particular interest in the thesis.

Firstly, the impact of the spatial distribution of diamonds, on the confidence of local and global estimates, was clearly demonstrated. It was shown in Chapters five, six and eight, that a high degree of correlation in a kimberlite pipe improves the confidence in local estimates but widens the confidence limits around a global estimate.

Secondly, it is clear that the confidence in local and global estimates (but particularly local estimates) can be improved if estimation is carried out using SPM3 and a global diamond size distribution. Unfortunately, the breakage of stones during drilling limits this approach at present. Should a solution be found to correct for diamond breakage or, ideally, reduce it to an acceptable level, then a SPM3 approach to evaluation is the correct strategy.

Thirdly, a benefit is gained, in local estimation, if the bottom cutoff is kept as low as is practical. The bottom cutoff is less important for global estimation providing a large number of stones are available from each geological zone.

Lastly, and most exciting, is the possibility of estimating grade using a restricted part of the diamond size distribution. Although this approach cannot be used for "green field" projects, it could be used at the feasibility stage or for the extension of reserves at an existing mine, where the diamond size distribution is known from previous sampling or from production.

REFERENCES[1]

1 Aitchson,J., and Brown, J.A.C. *The Lognormal Distribution with Special Reference to its Uses in Economics*, Univ. Cambridge, Dept. Applied Economics, Monograph 5, London: Cambridge Univ. Press, 1966.

2 Alabert, A. The practice of fast conditional simulations through the LU decomposition of the covariance matrix, *Mathematical Geology*, vol. 19, No. 5, 1987, pp. 369-386.

3 Armstrong, M. and Dowd, P.A. (eds.), *Geostatistical Simulations*, Dordrecht: Kluwer Academic Publishers, 1994, pp. 37-42.

4 Armstrong, M. Course notes on the Truncated Plurigaussian simulation, Centre de Geostatistique, Fontainebleau, France, 1997.

5 Assibey-Bonsu, W. *New models for Borehole Evaluation of New Mining Operations and Routine Valuation of Ore Reserve Blocks*, Ph.D. (Eng) Thesis, University of the Witwatersrand, Johannesburg, 1991.

6 Caers, J. *Statistical and geostatistical valuation of diamond deposits*, Ph.D. Thesis, Katholieke Universiteit te Leuven, 1996.

7 Clement, C.R. *Some Geological Implications arising from "Kimberlite pipes - Information Requirements and Ore Reserve management"*, Johannesburg: Anglo Corporation of South Africa, August 1988, Consulting Geologists Department.

8 Clark, I. *Practical Geostatistics*, London: Applied Science Publishers, 1982.

9 Cox, D. R. Some statistical methods connected with series of events, *Journal of the Royal Statistical Society*, Series B (methodological), Vol. 17, No. 2, 1955, pp. 129-157.

10 Cressie, N.A.C. *Statistics for Spatial Data*, New York: John Wiley and Sons, inc., 1991.

---

1 References 32, 33 and 49 are recommended as essential reading for an understanding of the Cox simulation presented in this thesis.

11 David, M. *Geostatistical Ore Reserve Estimation*, Amsterdam: Elsevier Scientific Publishing Company, 1982.

12 Deutsch, C.V. and Journel, A.G. *Geostatistical Software Library and User's Guide (GSLIB)*, Oxford: Oxford University Press, 1992.

13 Dohm, C.E. *Improvement of Ore Evaluation through the Identification of Homogeneous Areas using Geological, Statistical and Geostatistical Analyses*, Ph.D. (Eng) Thesis, University of the Witwatersrand, Johannesburg, 1995.

14 Dowd, P.A. A review of recent developments in geostatistics, *Computers and Geosciences*, vol. 17, No, 10, 1992, pp. 1481-1500.

15 Dowd, P.A. and Sarac, C. An extension of the LU decomposition method of simulation, in: Armstrong, M. and Dowd, P.A. (eds.), *Geostatistical Simulations*, Dordrecht: Kluwer Academic Publishers, 1994, pp. 23-36.

16 Duval, D., Green, T., Louthean, R. *The Mining Revolution*, London: Rosendale Press, 1996, p.20.

17 Feller, W. *An Introduction to Probability Theory and its Applications*, New York: Wiley, 1968.

18 François-Bongarçon, D. Geostatistical determination of sample variances in the sampling of broken gold ores, *CIM Bulletin*, vol. 84, No. 950, June 1991, pp. 46-57.

19 Freulon, X., and de Fouquet, *C. Remarques sur la Practique des Bandes Tournantes à Trois Dimensions*, Centre de Geostatistique, Fontainebleau, France, 1991, Cahiers de Geostatistique No. 1, pp.101-117.

20 Freulon, X. *Conditionnement du modèle gaussien par des inégalitiés ou des randomisées*, Ph.D. Thesis, Centre de Geostatistique, Fontainebleau, France, 1992.

21 Galli, A., Beucher, H., Le Loc'h, G., and Doligez, B. The pros and cons of the Truncated Gaussian method, in: Armstrong, M. and Dowd, P.A. (eds.), *Geostatistical Simulations*, Dordrecht: Kluwer Academic Publishers, 1994, pp. 217-233.

22 Gómez-Hernández, J.J. and Cassiraga, E.F. Theory and practice of sequential simulation, in: Armstrong, M. and Dowd, P.A. (eds.), *Geostatistical Simulations*, Dordrecht: Kluwer Academic Publishers, 1994, pp. 23-36.

23 Gotway, C. A. Stochastic simulation for imaging spatial uncertainty: Comparison and evaluation of available algorithms, in: Armstrong, M. and Dowd, P.A. (eds.), *Geostatistic Simulations*, Dordrecht: Kluwer Academic Publishers, 1994, pp. 1-21.

24 Gy, P.M. *Sampling of Particulate Materials Theory and Practice*, New York: Elselver Science Publishing, 1979.

25 Hawthorne, J.B. Model of a kimberlite pipe, in: Ahrens, L.H. et al, (eds.), *Physics and chemistry of the earth*, Vol 9, Oxford: Pergamon Press Limited, 1975, pp. 1-20.

26 Journel, A.G. *Simulations Conditionnelles - Théorie et Practique*, Ph.D. Thesis, Centre de Geostatistique, Fontainebleau, France, 1974.

27 Journel, A.G., and Huijbregts, Ch. J. *Mining Geostatistics*, London: Academic Press, 1978.

28 Journel, A.G. and Alabert, F. Non-Gaussian data expansion in the earth sciences, *Terra Nova*, vol. 1, 1989, pp. 123-134.

29 Kapteyn, J.C. *Skew Frequency Curves in Biology and Statistics*, Astronomical Laboratory, Groiningen: Noordhoff, 1903.

30 King, H.F., McMahon, D.W., Bujtor, G.J. A Guide to the Understanding of Ore Reserve Estimation, *Supplement to the proceedings of the Australian Institute of Mining and Metallurgy*, No. 281, March 1982.

31 Kleingeld, W.J. *La Géostatistique pour des Variables Discretes*, Ph.D. Thesis, L'Ecole Nationale supérieure des mines de Paris, 1987.

32 Kleingeld, W.J., Lantuéjoul, C. Sampling of ore bodies with a highly dispersed mineralisation, in: Soares, P. (ed.), *Geostatistics Tróia '92*, Dordrecht: Kluwer Academic Publishers, 1993, vol. 2, pp. 953-964.

33 Kleingeld, W.J., Lantuejoul, C., Prins, C.F., Thurston, M.L. The non-conditional simulation of a Cox process with application to a sampling problem, *Proceedings of the Conference on Mining Geostatistics held at Berg-en-Dal*, September 1994, pp. 26-38. Published by the Geostatistical Association of South Africa, July 1996.

34 Kleingeld, W.J., Lantuejoul, C., Prins, C.F., Thurston, M.L. The conditional simulation of a Cox process with application to deposits with discrete particles, in: Baafi, E.Y., Schofield, N.A. (eds.), *Geostatistics Wollongong '96*, Dordrecht: Kluwer Academic Publishers, 1997, vol. 2, pp. 683-694.

35 Lantuéjoul, C. Non-conditional simulation of stationary isotropic multigaussian random functions, in: Armstrong, M. and Dowd, P.A. (eds.), *Geostatistical Simulations*, Dordrecht: Kluwer Academic Publishers, 1994, pp. 147-167.

36 Lassonde, P. *The Gold Book - The Complete Investment Guide to Precious Metals*, Toronto: Penguin Books, 1990.

37 Le Loc'h, G. and Galli, A. Truncated Plurigaussian method: Theoretical and practical points of view, in: Baafi, E.Y. and Schofield, N.A. (eds.), *Geostatistics Wollongong '96*, Dordrecht: Kluwer Academic Publishers, 1997, pp. 211-222.

38 Mantoglou, A. and Wilson, J.L. The turning bands method for simulation of random fields using line generation by a spectral method, *Water Resources Research*, vol.18, No.5, October 1992, pp. 1379-1394.

39 Mantoglou, A. Digital simulation of multivariate two- and three dimensional stochastic processes with a spectral turning bands method, *Mathematical Geology*, vol. 19, No. 2, 1987, pp. 129-149.

40 Matheron,G. The intrinsic Random Functions and their applications, *Advances in Applied Probability*, No.5, pp. 439-468, 1973.

41 Matheron,G *Quatre familles discrètes*, Fontainebleau: research report, N-7032, Centre de Géostatistique, 1981.

42 Mitchell, R.H. *Kimberlites: Mineralogy, Geochemistry and Petrology*. New York: Plenum Publishing Corporation, 1986.

43 Neyman, J. On a new class of "contagious" distributions, applicable in entomology and bacteriology, *Annals of Mathematical Statistics*,

vol. 10, 1939, pp.35-57.

44 Rombouts, L. Evaluation of low grade/high value diamond deposits, *Mining Magazine*, September 1987, pp. 217-220.

45 Rombouts, L. Sampling and statistical evaluation of diamond deposits, *Journal of Geochemical Exploration*, vol. 53, nos 1-3, March 1995, pp. 351-367.

46 Rombouts, L. Statistical Distributions for Diamonds, in: Proceedings of the Fifth International Kimberlite Conference, 1995, pp. 202-214.

47 Rombouts, L. A year of overfeed, *Diamond International*, Jan/Feb 1996, pp.62-68.

48 Sichel, H.S. On a family of discrete distributions particularly suited to represent long tailed frequency data, in: Laubscher, N.F. (ed.), *Proceedings of the third symposium on Mathematical statistics*, Pretoria, 1971, pp. 51-97.

49 Sichel, H.S. Statistical Valuation of Diamond Deposits, in: Salamon M.D.G. and Lancaster F.H. (eds.), *Application of Computer Methods in the Mineral Industry*, Johannesburg, 1973, pp.17-25.

50 Zimmerman, D.A., and Wilson, J.L. *Description of and user's manual for TUBA: a computer code for generating two-dimensional random fields via the Turning Bands method*, SeaSoft, 1990, Albuquerque, New Mexico.

Author:Thurston, Malcolm Lawrence.
Name of thesis:The quantification of uncertainty attached to selected sampling protocols in a kimberlite using a discrete simulation method / Malcolm Lawrence

PUBLISHER:
University of the Witwatersrand, Johannesburg
©2015

LEGALNOTICES:

Copyright Notice: All materials on the University of the Witwatersrand, Johannesburg Library website are protected by South African copyright law and may not be distributed, transmitted, displayed or otherwise published in any format, without the prior written permission of the copyright owner.

Disclaimer and Terms of Use: Provided that you maintain all copyright and other notices contained therein, you may download material (one machine readable copy and one print copy per page)for your personal and/or educational non-commercial use only.

The University of the Witwatersrand, Johannesburg, is not responsible for any errors or omissions and excludes any and all liability for any errors in or omissions from the information on the Library website.